JIMMA UNIVERSITY

SCHOOL OF GRADUATE STUDIES

JIMMA INSTITUTE OF TECHNOLOGY

FACULTY OF CIVIL AND ENVIRONMENTAL ENGINEERING

HYDROLOGY AND HYDRAULIC ENGINEERING CHAIR

MASTERS OF SCIENCE PROGRAM IN HYDRAULIC ENGINEERING

ASSESSING THE IMPACT OF CLIMATE CHANGE ON STREAMFLOW OF THE RIBB WATERSHED, ABAY BASIN, ETHIOPIA

BY

ANDUALEM MITIKU

A Thesis Submitted to the School of Graduate Studies of Jimma University, Jimma Institute of Technology in Partial Fulfillment of the Requirements for the Degree of Masters of Science in Hydraulic Engineering

JANUARY, 2022

JIMMA, ETHIOPIA

JIMMA UNIVERSITY

JIMMA INSTITUTE OF TECHNOLOGY

SCHOOL OF GRADUATE STUDIES

FACULTY OF CIVIL AND ENVIRONMENTAL ENGINEERING

HYDROLOGY AND HYDRAULIC ENGINEERING CHAIR

MASTERS OF SCIENCE PROGRAM IN HYDRAULIC ENGINEERING

ASSESSING THE IMPACT OF CLIMATE CHANGE ON STREAMFLOW OF THE RIBB WATERSHED, ABAY BASIN, ETHIOPIA

BY

ANDUALEM MITIKU

A Thesis Submitted to the School of Graduate Studies of Jimma University, Jimma Institute of Technology in Partial Fulfillment of the Requirements for the Degree of Masters of Science in Hydraulic Engineering

Main Advisor: Mr. Mamuye B. (Assistant Professor)

Co-Advisor: Mr. Abebe C. (MSc.)

JANUARY, 2022

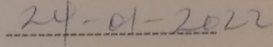JIMMA, ETHIOPIA

DECLARATION

DECLARATION

I Andualem Mitiku declares that the thesis entitled "**ASSESSING THE IMPACT OF CLIMATE CHANGE ON STREAMFLOW OF THE RIBB WATERSHED, ABAY BASIN, ETHIOPIA**" is my original work and has not been presented by me for a degree in any other University.

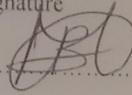| Andualem Mitiku		24-01-2022
(MSc.) Candidate	Signature	Date

We, the undersigned, certify that a thesis entitled "**ASSESSING THE IMPACT OF CLIMATE CHANGE ON STREAMFLOW OF THE RIBB WATERSHED, ABAY BASIN, ETHIOPIA**" is the original work of Mr. Andualem Mitiku and has been submitted for examination with our approval as university advisors.
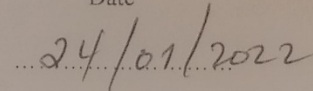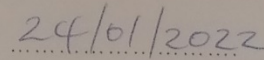
Name	Signature	Date
Mr. Mamuye Busier (Assist. Prof.)		24/01/2022
(Main advisor)		
Mr. Abebe Chala (MSc.)		24/01/2022
(Co-Advisor)		

APPROVAL PAGE

APPROVAL PAGE

This is to certify that the thesis prepared by Mr. Andualem Mitiku entitled "ASSESSING THE IMPACT OF CLIMATE CHANGE ON STREAMFLOW IN THE RIBB WATERSHED, ABAY BASIN, ETHIOPIA." and submitted as partial fulfillment for the award of the Degree of Master of Science in Hydraulic Engineering complies with the regulations of the University and meets the acceptance standards concerning originality, content, and quality.

Signed by Examining board:

	Signature	Date
External Examiner: Acie Abebe (PhD)		24/01/2022
Internal Examiner: Abdata Wakjira		24/01/2022
Chairperson: Nasir Gebi		24/01/2022

ii

ABSTRACT

Among many challenges, climate change is one of the world's most pressing issues today. Changing climate may have a major effect on water availability. It would have an adverse effect on food productivity, socio-economic processes, and environmental sustainability. These effects can put their main influence, especially over developing countries whose economies rely heavily on agricultural production. By considering those occurring issues, this study intended to assess the impact of climate change on the streamflow of the Ribb Watershed. Hydrological data have taken from 1990-2017, and meteorological data (Rainfall and Temperature) was from 1990-2019. Spatial data used were Soil, Land use, and digital elevation model of the Ribb watershed. The performance of three regional climate models (KNMI-RACMO22T, SMHI-RCA4, and CLMcom-CCLM4-8-17) from GCM MOHC-HadGEM2-ES with their ENSEMBLE model checked and by comparing their performance, KNMI-RACMO22T was the one which performing best and selected for further simulation and impact assessment. Rainfall and Temperature data of KNMI-RACMO22T RCM for RCP4.5 and RCP8.5 were bias-corrected by power transformation and linear transformation techniques respectively. Trend analysis was analyzed for two-time horizons, near-term from 2025-2054 and long-term 2055-2084 by using Mann-Kendal trend test. The result shows that in the future, for both near-term and long-term, mean month rainfall is increased on December to April and decreasing from May-September. Summer and autumn show rainfall decrease while spring and winter are increasing on both RCP4.5 and RCP8.5. Annual rainfall shows decreasing trend on both RCP4.5 and RCP8.5 for near and long term. Near and long term, mean month maximum and minimum temperature show mostly an increasing trend on both scenarios. Annual temperature tends increasing on both scenarios in near and long term. HEC-HMS version 4.7.1 calibration (1990-2010) and validation (2011-2017) result of the model shows satisfactory agreement between observed and simulated streamflow in which coefficient of determination (R^2) and Nash-Sutcliffe Efficiency (NSE) was 0.89 and 0.86 for calibration and 0.87 and 0.84 for validation respectively. The near-term RCP4.5 and RCP8.5 show the highest decrease in streamflow in August ($-46.52m^3/s$ and $-49.43m^3/s$), respectively. Long-term streamflow also shows the highest decrease in August ($-42.85m^3/s$ and $-43.86m^3/s$), respectively. On seasonal time-step, summer shows a decrease in streamflow; the winter season tends to increase on both RCP4.5 and RCP8.5 over near-term and long-term time horizons. Annually the stream flows appear decreased on RCP4.5 and RCP8.5 in near-term and long-term time horizons. Flow Duration curve used to examine the mean monthly extreme flows, and the result was increasing in low flow and decreasing in high flow. Future streamflow of the Ribb watershed have decreased compared to the base period. This will occur because of decrease in rainfall and increase in temperature. Therefore, there should be proper water resource planning and management in the area for the better operation and usage of stream water of the Ribb watershed.

Key Words: Climate change, HEC-HMS, Hydrology, Streamflow, Ribb Watershed

ACKNOWLEDGMENT

Table of Contents

List of Tables

List of Figures

APPENDIXES

ACRONYMS AND ABBREVIATIONS

AOGCM	Atmospheric-Ocean General Circulation Model
ASF	Alaska Satellite Facility
CORDEX	Coordinated Regional Downscaling Experiment
CMIP5	Coupled Model Inter-comparison Project Phase 5
DEM	Digital Elevation Method
EMA	Ethiopian Mapping Authority
FDC	Flow Duration Curve
HEC-HMS	Hydrologic Engineering Center Hydrologic Modeling System
GCM	Global Circulation Models
GHG	Green House Gas
GIS	Geographic Information System
HadCM3	Hadley Center for Climate Prediction, version 3
HadGEM2-ES	Hadley Centre Global Environmental Model, version 2, Earth System
IPCC	Intergovernmental Panel on Climate Change
MoWIE	Ministry of water and irrigation engineering
NMSA	National Meteorological Services Agency, Ethiopia
RCM	Regional Climate Model
RCP	Representative Concentration Pathways
SDSM	Statistical Downscaling Model
SRES	Special Report on Emission Scenarios
SRTM	Shuttle Radar Topography Mission
UNFCCC	United Nations Framework Convention on Climate Change.
WCRP	World Climate Research Program

1. INTRODUCTION

1.1 Background

One of the world's most pressing issues today is climate change; it is one of the notable changes experienced around the world today. Changes in average climatic conditions and natural events have expected to major impact human and ecological processes. One of the most vulnerable to climate change is the water supply. Climate change is predicted to impact water sources by influencing hydrological variables such as precipitation and temperature, which determine the hydrological cycle (Mengistu *et al*., 2021).

Changing climate because of changes in the hydrological cycle may have a major effect on water availability. Temperature and precipitation shifts, for example, may significantly influence runoff part. As a result, major shifts in the geographical and temporal supply of water resources will affect agriculture, manufacturing, and economic growth (Gebre and Ludwig, 2015).

When the occurrence of climatic extremes such as heatwaves, droughts, and changes in rainfall patterns rises because of global warming, climate change will have a significant effect on the supply and variability of freshwater. As a result, water availability would affect food productivity, socio-economic processes, and environmental sustainability; climate change would significantly affect developing countries whose economies rely heavily on agricultural production. Africa is one of the regions most vulnerable to climate change and variability (Worqlul *et al*., 2018).

Changes in water supplies, natural weather, drought, reduced growing season indicated climate change impacts. Today, climate change for natural habitats and basins is becoming a severe phenomenon, and the increasing tempers of the upcoming decade, the decline in precipitation, and the rise in temperature are among those most important consequences of climate change. Water services are one of the most significant sectors impacted by climate change (Ahmadi and Azizzadeh, 2020).

Because of the worst droughts in decades Ethiopia has experienced, it is vulnerable to climate change. Many studies, therefore, have focused on the possible effect on future stream volumes of certain rivers in Ethiopia of climate change. Despite the recent drying trends and

recurring droughts, some of these studies have projected that the flow of Ethiopian fluvial will rise by the mid and late 21st centuries (Gizaw *et al.*, 2017).

Research has been conducted investigations in the upper Blue Nile basin to explain climate change's current and future effects. The HEC-HMS Soil Moisture Accounting (Habibu et al., 2020) algorithm was used to examine the long-term effects of climate change on the Blue Nile's water resources availability. As a reason, a thorough understanding of the rainfall-runoff relationship at various small-scale watershed levels in the upper Blue Nile River basin aids in the analysis of the basin's water quality, water resources management, and flood control. For runoff simulations assessment, the simple, sensitive parameters and good modeling methods for each process component were defined (Gebre and Ludwig, 2015). HEC-HMS will explore the differences in hypothetical stream flows and water equilibrium in the research area between present and future scenarios (Meenu, 2013). Hydrological models always forecast variable status and, therefore, need further models to make the management of the water resources more real. Analysis and execution of the watershed model are essential to conducting a valid assessment of water resources (Aawar and Khare, 2020).

Using the HEC-HMS version 4.7.1 model simulation, this study investigated and analyzed the impact of climate change on the Ribb watershed. It focuses on determining how climate change would affect the availability of water resources in the Ribb River basin in north-eastern Ethiopia, utilizing the RCP's climate scenario and future temperature forecasts. Furthermore, evaluations of the influence of climate change on the watershed's water supplies will give useful data for future water resource management in the area. Bias corrected precipitation and temperature RCM data were used as model input for assessing the future streamflow of Ribb watershed in two-time horizons near term and long term.

1.2 Statement of the Problem

Climate change has a significant effect on water supply worldwide, altering their availability and have an effect on rainfall and temperature, significant impact on runoff (Gebre and Ludwig, 2015). Changes influence the state of the hydrological cycle in both air temperature and rainfall. Scarcity of water, caused by reduced river flow and groundwater recharge due to climate change, affects the number and distribution of people. As a result, over one-third of the world's population lives in countries with water scarcity (Chakilu *et al.*, 2020).

Ethiopia's economy is heavily reliant on agriculture, as in many African countries. As a result, climate change has a significant effect on the country's economy. A substantial majority of Ethiopia's land is arid or semi-arid, home to impoverished and marginalized people that are completely reliant on rainfall. Furthermore, inadequate land management and rising temperature extremes are impacting these peoples' livelihoods. To incorporate effective climate change adaptation and mitigation plans, it is important to consider the effect of climate change on water supplies (Worqlul *et al*., 2018).

Lake Tana's sub-basin water resource is expected to be highly vulnerable to climate change. The investigation by (Setegn *et al*., 2011) showed that changes in hydrologic cycles and water supply are expected to be a significant consequence of climate change in this sub-basin. In this sub-basin, the risk of reduced water supply is a significant threat. It will have a commutative effect on the surrounding catchments. Runoff can have become more and more seasonal, causing small streams to dry up entirely. For a portion of the year, this will result in drying wetlands, small springs, and other water sources (Tarekegn and Tadege, 2006). Investigation by (Nurelegn and Amare, 2014) proposes that there is a decrease in water availability of Ribb watershed due to climate change.

Climate change impact on streamflow studies were made from a basin to watershed scale including (Soliman *et al*., 2009, Abdulahi *et al*., 2021, Ayalew *et al*., 2021, Negewo and Sarma, 2021, Deressa *et al*., 2022), and these studies are mainly based on a single RCM. However, each RCM models have their own strength and weakness (Endris *et al*., 2013). Thus, instead of directly using a single RCM for impact assessment, it is acceptable to check the performance of different RCMs over a study area.

Previous investigations in Abay basin on impact of climate change on streamflow have mainly based on SWAT simulations while HEC-HMS is preferable for rainfall-runoff simulations. Hence, by filling the abovementioned gaps, this study focuses on assessing the impact of climate change on streamflow of the Ribb watershed, which would be a preparation to cover these problems by contributing scientific information for water resource management of the area.

1.3 Objectives

1.3.1 General objective

The general objective of this study is to assess the effect of climate change on streamflow of the Ribb watershed.

1.3.2 Specific objectives

   i. To analysis the trend of future precipitation and Temperature over Ribb watershed

  ii. To evaluate the future impact of climate change on streamflow of the Ribb watershed on monthly, seasonally and annually time scales

 iii. To assess the effect of climate change on high and low flows

1.4 Research Questions

1. What will be the trend of Precipitation and Temperature of the Ribb watershed in the future?
2. What will be the impact of climate change on stream flow of the Ribb watershed on mean monthly, seasonal and annual time scales?
3. What will be the effect of climate change on high flow and low flow?

1.5 Significance of the Study

By researching the effects of climate change on hydrology and water quality, it can enhance food productivity, exploit water reserves, conserve natural resources, and manage water resources well. The study's key importance is to have a clear explanation for planners, policymakers, stakeholders, and anybody else who is interested in the effects of climate change on hydrological variables (such as precipitation, temperature, and streamflow) and the influence these have on the rainfall-runoff capacity of the Ribb watershed. As a result, this research provides insight into the changing trends of future precipitation and temperature and their possible impacts on the streamflow of the Ribb watershed.

1.6 Scope of study

This study is, principally a watershed level study, focuses on the performance evaluation of three RCMs, trend analysis on Rainfall and Temperature and climate change impact on the streamflow of the Ribb watershed. Climate change impact assessment was achieved by the use of Regional Climate Model (RCM) CORDEX Africa. The RCM was downscaled for future time horizon under RCP4.5 and RCP8.5 divided in two future periods: 2025-2054 as a

near-term and 2055-2084 as a long-term to generate the future impact climate change on streamflow with baseline period 1990 to 2019 based on IPCC, 2014 most common to use 30 years for climate change assessment.

1.7 Limitation of the study

The land use/cover soil data were assuming it would remain the same at future time horizons. However, in the real world, the land covers and soil type change. DEM has downloaded from Alaska Satellite Facility at a website of https://www.asf.alaska.edu and CORDEX data has downloaded from website https://www.esgf-node.llnl.gov/search/esgf-llnl/ that needs a strong connection, which may not be available in this case.

2. LITERATURE REVIEW

2.1 Climate Change

As per the Intergovernmental Panel on Climate Change's Fifth Assessment Report, GHG emissions are expected to increase due to global population and economic activities unless additional measures are taken to reduce GHG emissions. In 2100, compared to preindustrial levels, baseline scenarios result in global mean surface temperature increases of 3.7°C to 4.8°C(Stocker, 2014). Climate change is the most critical concern affecting the whole world today. It is already generally accepted that climate change is now underway. An additional change is unavoidable; the average global temperature increased by 0.74 degrees Celsius over the last century (1906 and 2005). It happened in two stages: from the 1910s to the 1940s, and then again from the 1970s to the present.

Notwithstanding continued temperature increases and increased depletion of mass from glaciers and ice sheets, the world average sea level will begin to rise in the 21st century under all RCP scenarios. Hydrological processes affect water supplies in quantities and consistency due to changing precipitation or snow and ice melting (IPCC, 2014). The IPCC also states that measurements over the past century indicate international variations in the number, severity, frequency, and precipitation types. Atmospheric and ocean temperatures have warmed, the volume of snow and ice has declined, the sea level has risen, and greenhouse gas emissions have intensified (IPCC, 2013).

Nowadays, solid empirical evidence indicates that the global temperature of the Earth's surface is rising due to greenhouse gas emissions. Global warming and precipitation are predicted to differ considerably from region to region. Average climate change, changes in the frequency and severity of extreme weather conditions are expected to substantially impact natural and human environments (Aerts and Droogers, 2004).

These days, understanding the consequences of climate change on human activities has escalated. The impact of climate change has several major impacts on the hydrological cycle and thus, therefore, on the framework of hydrology and water supply. The Intergovernmental Commission discussed this implementation on Climate Change (Solomon *et al*., 2007).

Different institutions have also run such simulations using temperature or circulation models. Outcomes from these models provide unclear signs of transition. Another very recent

scientific report by the Intergovernmental Panel on Climate Change (Iturbide *et al.,* 2020) Confirms that human-induced emissions of gasses such as carbon dioxide (CO_2) have occurred in the late 19th century. Catch heat in the atmosphere as a greenhouse has led to a rise of around 0.3 to 0.7 $^{\circ}$C in global mean surface air temperatures. Based on the IPCC mid-range scenario of potential greenhouse gas and aerosol emissions, their best estimate of Climate intensity is expected to increase by two degrees centigrade by 2100 (IPCC, 2013).

2.2 Indication on the Presence of Change in Climate

The primary proof that suggests global climate change in the past, current, and future is given by IPCC studies over various periods. These reports draw on the researchers' observations working on them based on tangible facts. The IPCC AR5 stresses that potential GHG emissions and climate change are still a source of great confusion. The IPCC introduced four scenarios to characterize alternative climate futures in the AR5 to reflect this ambiguity. For their relative impact on the global environment, this current set of scenarios is referred to as representative concentration pathways (RCPs) (Scott *et al.*, 2016). Prior to IPPC, forecasts on changing climate variables such as CO_2 concentration, global average temperature, and sea-level rise are pretty well expected. However, estimations of increased CH4 and N2O concentrations are not in the correct ranges, which are lower than expected/projected (IPCC, 2013).

After seven years of near-zero development, the methane volume in the atmosphere (CH4) increased in 2007. According to recent studies, a second phase transition happened in 2014. Between 2014 and at least the end of 2018, the volume of CH4 in the atmosphere nearly doubled the levels seen since 2007. Since CH4 is a powerful greenhouse gas, increasing ambient CH4 poses a significant obstacle to meeting the Paris Agreement's limiting temperature rise to 2°C or, if necessary, 1.5°c over preindustrial levels (Fletcher and Schaefer, 2019).

The study by (Bartolini *et al*. 2019) showed an observable change in climate since the 1990s; there have been significant trends in the warming of autumn-winter monthly minimum and average temperatures. The mean maximum temperature has risen by 0.5%, while the mean minimum temperature has dropped by 1.1°C. However, total rainfall (monsoon from June to

October + local rains from November to May) has decreased by 17% over the last seventy years, while local rains have increased by 27% since 1981 (Negi *et al.*, 2003).

According to findings in the context of Ethiopia, the country's mean annual temperature has increased by almost 1.3°C since 1960, at an average rate of 0.28°C per decade, and spatial and temporal rainfall variability has increased. As a result, Ethiopia has affected by both climate variability and change. Drought conditions and mass starvation have become more widespread because of climate change. Flood damage and the spread of disease, desertification, loss of wetlands, loss of biodiversity, water scarcity, and rising prevalence of pests and diseases, such as the spread of cereal stem borers and malaria to higher elevation areas, are all contributing to the decline in agricultural production and productivity. On the other hand, Ethiopia has asserted environmental and policy responses to climate change (Zegeye, 2018).

The impacts of climate change on lake volume depletion in the Central Rift Valley Basin, Ethiopia, were investigated (Behulu *et al.*, 2018). According to the findings, under RCP4.5 and RCP8.5, annual predicted precipitation would decline by 7.97% and 2.55 percent, respectively. In addition, under RCP4.5 and RCP8.5, the highest temperature will rise 1.73 °C and 2.36 °C, respectively, whereas the minimum temperature will increase 2.16 °C and 3.07 °C.

2.3 Climate change studies and its impact on stream flows in Ethiopia

Ethiopia has made only a tiny contribution to global greenhouse gas (GHG) emissions. The average Ethiopian is responsible for an estimated one metric ton of CO_2 per year. As per the country's normal scenario, GHG emissions in Ethiopia have projected to grow from around 150 metric tons CO_2 to somewhere around 400 metric tons CO_2 in the coming decades (FDRE, 2011). It would primarily become the consequence of agricultural development, mainly commercial cultivation and farming, and deforestation, which has affected by the extension of cropland and population development. Nevertheless, there would still be Ethiopia in this projected doubling in pollution.

Compared to the 1961-1990 average, the world's temperature could increase by 2.7-3.4 °C by 2080. The temperature rise was highest from July to September (0.32°C per decade). According to reports, between 1960 and 2006, the total number of hot days a year rose by 73 (an additional 20% of days), and the number of hot nights increased by 137 (an additional 37.5 percent of nights). In June, July, and August, the growth rate was the highest. Conversely, the overall number of chilly days and nights declined by 21 (5.8% of days) and 41 (11.2%), respectively, during the same period. September and November have had the most declines (Adem and Bewket, 2011).

The Effect of Climate Change on Hydrological Drought in the Lake Tana Catchment was analyzed (Enyew *et al*., 2014). According to the study, CNCM3 suggests the lowest rise in mean temperature about 1.7°C, and the highest about 8.9°C during this time frame. For the summer period (JJAS), as the basin experiences more than 70-90 percent of overall rainfall, precipitation varies by around 2.6 and 5.7 percent for CNCM3 and IPSL, respectively. In contrast, ECHAM expects a 5.8 percent decrease in precipitation for the intermediate future. Both ECHAM and IPSL forecast a 3.5 percent rise in precipitation at the end of the century, while CNCM3 predicts a 0.3 percent decrease.

However, according to (Houghton *et al*., 2001) rising greenhouse gas levels in the atmosphere cause increases in minimum and maximum temperatures and changes in rainfall distribution and volume. Climate change affects aspects of the water cycle, such as precipitation and drainage, and even the timing, spatial distribution, and amount of water. Temperature and precipitation, in particular, are signs of climate change. As the temperature rises, so does evaporation, resulting in water disequilibrium between the surface and the atmosphere. Ground hydrology and water resources are adversely affected by variations in precipitation. Flooding and droughts are caused by temperature and precipitation changes, affecting a region's hydrology and water supply. As a result, river discharge is influenced by climate change. Climatic variables, particularly precipitation, are one of several variables that impact water flows.

In contrast to a minimum and maximum temperature and associated evaporation, the outcome of downscaled precipitation demonstrates that precipitation does not show a comprehensive increment in all future time horizons for both A2 and B2 scenarios.

Considerable shifts and fluctuations in seasonal and monthly flows are anticipated in the future. In the 2080s, the rainy season's runoff volume will indeed be decreased by about 116% and 101% for the A2 and B2 cases, respectively. The results of synthetic exponential scenarios often show climate change sensitivities. When the temperature rises by 2 degrees Celsius and rainfall declines by around 20%, up to 33% of seasonal and annual runoff is predicted to decrease (Abdo *et al*., 2009).

When the RC of river flows is greatly affected by both PET and precipitation over the observation period, panel data analysis suggests that precipitation can contribute more to the RC of streamflow. As a result, this research adds to our understanding of measuring and comparing the interaction between streamflow and the future environment at the basin scale (Wang *et al*., 2020).

The Impacts of Climate Change on the Water Resources of the Guder Catchment, Upper Blue Nile, is studied by (Fentaw *et al*., 2018). To examine the hydrological effects of potential future climate change in the Guder catchment, Upper Blue Nile Basin, this analysis uses Climate Model outputs from HadCM3A2a and HadCM3B2a SRES climate scenarios and downscales the prediction models into smaller scale resolution through Statistical Downscaling Model (SDSM) (Tigabu *et al*., 2020). The climate model's findings were compared to observation-based datasets for precipitation and temperature from 1990 to 2008. Climate change forecasts for precipitation and temperature were split into 30-year timeframes from 2011 to 2100 to predict the magnitude of the effects of climate change. In all future periods in the research catchment, the downscaled A2a and B2a pollution scenarios reveal a major growing pattern in mean temperature and precipitation. Temperature projections showed a growing trend varying from 0.13°C/decade to 5°C/decade for all parts of the Guder drainage basin, with a high degree of trust. Meanwhile, predicted precipitation patterns revealed a growing pattern across the entire sample region, varying from 11.5 to 25% across all cycles.

Dile *et al*., 2013 evaluated the hydrological response to climate change for the Gilgal Abay River in the Tana Lake Basin, Upper Blue Nile Basin of Ethiopia. The Mathematical Downscaling Tool (SDSM) was being used to minimize the HadCM3 (Hadley Center Climate Model 3) Global Circulation Model (Reshmidevi *et al*., 2018) Scenario data to a

more excellent resolution. The outcome forecast the dependent effect of rainfall and temperature changes on the Lake Tana Basin's hydrology using the HadCM3 GCM A2a and B2a climate scenarios for the 2010-2100 period. The research used the SDSM predictive downscaling method to test GCM outputs. The climate projections' findings (mean monthly temperature rise to +2.5 °C in the 2020s, +3.1 °C in the 2050s, +5 °C in the 2080s) are consistent with the results of many other recent surveys.

The Future Impacts of Climate Change on the Hydrology and Water Resources Security of the Didessa Catchment, Blue Nile River basin is studied (Legesse *et al*., 2015). This investigation established future climate change scenarios for precipitation, temperature, and potential evaporation, using the output from dynamically downscaled data from the ECHAM5 50 KM resolution under the A1B emission scenario 2030s (2031-2040) and 2090s (2091-2100). In contrast to the baseline period, the GCM model's future forecasts of climatic parameters highlighted the growing pattern (1991-2000). Over through the Didessa catchment, average annual precipitation will increase by +33.22 percent and +8.40 percent in the 2030s and 2090s, respectively. Hydrologic modeling was used to assess the impacts of climate anomalies on the Upper Blue Nile Basin (BNB) in Ethiopia, a large basin with limited hydro-climatic data (Elsanabary and Gan, 2015). The findings shed light on the impact of global oceanic anomalies on the hydrology of UBNB.

Melkamu *et al*., 2018 used greenhouse gas (GHG) emission scenarios RCP2.6, RCP 4.5, and RCP8.5 from the CORDEX database to produce potential climate variables to determine the impacts of climate change on the Gibe-III Reservoir. In addition, the water equilibrium was simulated using the HBV hydrological model. In both cases, the outcome shows a 9.8% decline on average.

Woldeselassie, 2015 examined the effect of climate change on runoff capacity in the upper awash basin. The effect of climate change will contribute to a rise in annual runoff over future periods, which will rise to 14.3 percent in Legedadi and 17 percent in Dire by the 2050s. Substantial Seasonal mean runoff have observed during the Kiremt season, and greater radiation have observed during the Bulge season. It varies (+20 percent and-32 percent of Legedadi) (+23.9 percent and-51.9 percent of Dire). Susceptibility analyses

showed that both catchments are much more vulnerable to rainfall. The rise in runoff magnitude could positively affect the water supply needs of Addis Ababa's city.

Nigatu *et al*., 2016 measured the hydrological effect of climate change on the water balance of Lake Tana, Ethiopia. Impact analyses are carried out using the downscaled General Circulation Model (GCM) performance and hydrological modeling. Precipitation, maximum, and minimum temperature predictions from the HadCM3 GCM were used for A2 and B2 pollution scenarios. Effect studies were performed for three-time spans in the future: the early, mid, and late twenty-first centuries. The prediction of mean annual over lake precipitation for both A2 and B2 pollution scenarios indicates an increasing trend for the twenty-first century about the baseline age. Abdella, (2013) examined climate change's effect on the Omo gibe basin's water resources capacity.

Beyene *et al*., 2010 investigation shows that, due to significantly lowering of precipitation, the Nile River have predicted to undergo a decrease in streamflow late in the study period (2010–2039), as summed overall 11 GCMs. Because of both precipitation decreases and enhanced evaporative demand, streamflow is projected to decrease during the mid- (2040–2069) and late-century (2070–2099).

2.4 Global Climate Models (GCMs)

Global models of the Earth's system are the primary tools scientists use to understand the Earth's climate system. The critical insights into the Earth's climate system components include the atmosphere, land, oceans, and biosphere, the processes at work within and between them, and how natural factors and human activities affect regional to global scale. Scenarios of human greenhouse gas and aerosol emissions provide probable future climatic trajectories and consequences that the Intergovernmental Panel on Climate Change (IPCC) may examine and utilize to influence policy and governance compel them. However, long-term GCM forecasts are fraught with uncertainty due to parameterizations and absent or insufficient limitations on feedback mechanisms and interactions between the geosphere and biosphere (Steffen *et al*., 2020).

In essence, climate models are an expansion of weather forecasting. However, while weather models forecast small regions and short timeframes, climate models are wider and evaluate long timeframes. They forecast how the average conditions in the area would change over the

coming decades. Climate models include more atmospheric, oceanic, and land cycles than weather models such as ocean currents and melting glaciers. Usually, these models are developed from mathematical equations that use thousands of data points to simulate energy and water transitions in climate systems. GCMs (Global Circulation Models) are numerical models that depict physical processes in the atmosphere, seas, cryosphere, and land surface. Climate forecasts are made using GCMs. Temperature, precipitation, and other climatic components may all be measured using GCMs, which come in various models (Ertuğrul, 2019).

Climate models are based on well-established physical assumptions that reliably reproduce current and historical climate changes. AOGCMs (Atmosphere-Ocean General Circulation Models) provide accurate computational forecasts of potential climate change, particularly at continental and larger scales, and there is considerable confidence in them. Some climate variables (for example, temperature) have greater confidence in these projections than others (e.g., precipitation). Climate simulations are being put to more rigorous assessments, such as prediction evaluations on time scales ranging from days to years. This broader range of tests boosts confidence in the model's ability to accurately reflect processes that influence climate forecasts (Randall *et al*., 2007).

Since the AR4, climate models have continued to be developed and improved, and many of them have been extended into Earth System models by including biogeochemical cycles that are important to climate change. These models can be used to make policy-relevant calculations, such as the amount of carbon dioxide (CO2) emissions compatible with a given climate stabilization target (Flato *et al*., 2014).

Scientists and engineers often use computational models to understand complex systems and understand the processes, interactions, and associated physics, chemistry, and biology affecting the world around us. In the case of the Earth's climate, such models are particularly important, as they allow scientists to construct a visual "lab" where they can run experiments on an entire planet, whether studying the circulation of Jupiter's atmosphere, paleoclimate in the Earth's distant past, or how the climate today responds to the choices that humans make now and the future.

The complex global climate models (GCMs) that simulate the Earth's climate have a variety of uses. Including comparing them against observations to evaluate the scientific understanding of individual components of the system and its processes; examining how these components respond to changes in both internal and external factors; determining how well we understand past and current changes in climate, and projecting how climate could change in the future. These models can incorporate both theoretical understanding and direct observations (e.g., observed changes in the output from the sun and documented changes in the emissions from human activities) to study the past and the present response of the climate system to such changes, as well as to provide the basis for projecting climate into the future (Council, 2011).

Because of their unique ability to simulate the response of the Earth's climate system to human choices, and because their output takes the recognized shape of maps, which enables scientists and decision-makers to connect human choices to their resulting impacts at the regional scale, these models provide an essential foundation for action on climate change. As a result, they often form the basis for analyses that range from understanding the science of climate change to setting local, regional, national, or even international targets to examining and comparing potential options for adaptation and mitigation.

Climate simulations expand weather forecasting. However, unlike weather models, which make forecasts about short and brief periods, climate models are more comprehensive and look long. They forecast how average conditions in an area would change over the next few decades. Modeling climate change involves developing computational statistical models of climate to understand better the phenomena and, finally, predictability (Schneider and Dickinson 1974). For example, based on climate change models, the individual effects of temperature and precipitation on peak flow revealed that peak flow changes were primarily due to increased precipitation (Jiang *et al*., 2020).

2. 10 Coordinated Regional Climate Downscaling Experiment (CORDEX)

The World Climate Research Program (WCRP) sponsored an international program, Coordinated Regional Downscaling Experiment (CORDEX), to develop a coordinated ensemble of high-resolution, regional climate projections for the majority of land regions of the world. CORDEX involves more than 20 regional climate modeling and statistical

downscaling groups. Providing regionally downscaled climate projections for most land regions of the Globe, complementing the global climate model projections performed within the fifth Coupled Model Intercomparison Project (CMIP5), is the initiative's objective. The WCRP task force on Regional Climate Downscaling (RCD) launched CORDEX with the goal of creating downscaled regional climate change estimates for all terrestrial regions utilizing both dynamical and statistical methodologies (Hewitson, *et al*., 2012).

The World Climate Research Programme (WCRP) supports the Coordinated Regional Climate Downscaling Experiment, an international endeavor (CORDEX). The initiative's purpose is to produce regionally downscaled climate forecasts for the majority of the world's land areas as a supplement to the global climate model estimates made as part of the fifth Coupled Model Intercomparison Project (CMIP5). Data from both dynamical and statistical downscaling are included in CORDEX. Because of its higher resolution and regional focus, the CORDEX dataset is expected to link to the impacts and adaptation community (Evans, 2011).

2.7 Representative concentration pathways (RCPs) and emission scenarios

In climate research, different emission scenarios are used to assess the long-term impact of atmospheric greenhouse gases and pollutants based on assumptions of population growth, economic development level, etc. RCPs are called pathways to highlight that their primary goal is to offer time-dependent estimates of greenhouse gas (GHG) concentrations in the atmosphere (Bjørnæs, 2013). RCPs are a set of four new pathways developed for the climate modeling community as a foundation for long-term and near-term modeling experiments. The four RCPs cover the range of radiative forcing values found in the open literature for 2100, ranging from 2.6 to 8.5 W/m^2. The RCPs result from a collaborative effort between integrated assessment modelers, climate modelers, terrestrial ecosystem modelers, and emission inventory experts. The RCPs are a significant step forward in climate science, as they pave the foundations for further research and development, including pollution reduction and impact analysis (Van Vuuren *et al*., 2011). These new scenarios, known as Representative Concentration Pathways (RCPs), have being used for new climate model simulations under the World Climate Research Program's Coupled Model Intercomparison Project Phase 5 (CMIP5).

The Future greenhouse gas (GHG) emissions are the product of very complex dynamic systems determined by driving forces such as; demographic development, socio-economic development, and technological change. Consequently, their future evolution is highly uncertain. Therefore, the development of climate change scenarios is an essential step in the hydrological impact of climate change study.

According to IPCC (2001a), for explicit use in investigating the potential impacts of anthropogenic climate change of a future climate constructed from reliable assumptions about future emission of greenhouse gases (GHGs) and other pollutants, the climate change scenario is a possible representation. It also states that Scenarios are not forecasts of future climate but are proposed to provide suitable quantitative measures of uncertainty that are represented with a range of plausible future paths. For example, future greenhouse gas concentrations are unknown because we cannot predict what activities humans will use to reduce or increase them.

RCP 8.5 – High emissions

This RCP is consistent with a future with no policy changes to reduce emissions. It was developed by the International Institute for Applied System Analysis in Austria and is characterized by increasing greenhouse gas emissions that lead to high greenhouse gas concentrations over time. This scenario is highly energy-intensive, with total consumption continuing to grow throughout the century reaching well over three times current levels. Oil use grows rapidly until 2070, after which it drops even quickly.

Land use continues current trends with crop and grass areas increasing and forest areas decreasing. A critical difference between the new RCPs and the previous scenarios is that there are no fixed sets of assumptions related to population growth, economic development, or technology associated with RCP. Another key difference is that the RCPs are spatially explicit and provide information on a global grid at a resolution of approximately 60 kilometers gives spatial and temporal information about the location of various emissions and land-use changes. It is an important improvement as the location of some emissions affects their warming potential.

RCP 6 – High emissions

The National Institute develops this RCP for Environmental Studies in Japan. Radioactive forcing has stabilized shortly after the year 2100, which is consistent with applying various technologies and strategies for reducing greenhouse gas emissions. Oil consumption remains high, during biofuel and nuclear play a minor role than in the other three scenarios. Cropping area continues to change on the current trend, while grassland area has rapidly reduced. Natural vegetation is similar to RCP4.5.

RCP 4.5 – Intermediate emissions

The RCP 4.5 scenario is a stabilization scenario, which ensures the radiative forcing level stabilizes at 4.5 W/m^2 until 2100 by employing various technologies and techniques for lowering greenhouse gas emissions. Employment of a range of technologies and strategies for reducing greenhouse gas emissions has assumed in this stabilization scenario.

RCP 2.6 – Low emissions

This RCP has developed by PBL Netherlands Environmental Assessment Agency. Here radioactive forcing reaches 3.1 W/m^2 before it returns to 2.6 W/m^2 by 2100. To reach such forcing levels, ambitious greenhouse gas emissions reductions would be required over time. Cropping area increases faster than current trends, while grassland area remains constant. Forest vegetation continues to decline at current trends.

2.8 Bias Correction

The core concept behind bias correction identifies potential biases between observed and virtual climate variables, which serves as the foundation for using a transformation algorithm to correct control and scenario RCM runs (Ehret *et al*., 2012). Adjusting modeled values to match the observed distribution and statistics is bias correction. Bias associated with climate model data may be described roughly but safely as the time-independent component of model error or the component of model error that remains constant throughout datasets when conducting climate change impact studies.

Despite significant progress in recent years, the output of global and regional circulation models is still plagued by biases to the point where it cannot be used directly, particularly in climate change impact studies. It is well understood, and bias correction (BC; i.e., the

correction of model output towards observations in a post-processing step) has become a standard. A protocol in climate change impact studies is used to fix the question. This article contends that bias correction is often misused: it is applied to the GCM/RCM model chain without adequate evidence that the latter's accuracy (i.e., consensus between model dynamics/model performance and our judgment) and generality of applicability improve. By altering spatiotemporal field consistency, relationships among variables, and violating conservation principles, BC methods frequently detract from circulation models' benefits (Ehret *et al*., 2012).

Global Climate Models (GCMs) have been the main source of evidence for designing climate simulations, and they serve as the framework for evaluating climate change impacts at all scales, from local to global. However, climate models experience systematic error (biases) due to restricted spatial resolution, simplistic physics, thermodynamic systems, computational schemes, or inadequate knowledge of climate system processes, so impact studies seldom explicitly use GCM outputs. In addition, GCM simulations have many errors compared to historical data (Ramirez-Villegas *et al*.. 2013). As a result, bias correcting the raw climate model outputs is critical for producing climate forecasts essential for sustainable modeling.

2.11 Hydrological Models

A hydrologic model is a simplified representation of a real-world system (for example, surface water, soil water, wetland, groundwater, or estuary) that aids in interpreting, predicting, and managing water supplies. Hydrologic simulations are widely used to analyze both the flow and the consistency of water. Hydrological models are mathematical representations of a portion of the hydrologic cycle that is condensed. Where data is unavailable, hydrological models are used to define baseline characteristics and measure difficult-to-calculate long-term impacts (Lenhart *et al*., 2003).

2.11.1 Lumped models

The lumped-element model (also known as the lumped-parameter model or lumped-component model) reduces the definition of spatially distributed physical systems' behavior to discrete topology entities that approximate the distributed system's behavior under certain assumptions. Since lumped hydrologic models' parameters do not differ spatially within the

lake, basin response is assessed only at the outlet, leaving individual sub-basin responses unaccounted for. The parameters often do not reflect the physical characteristics of hydrologic processes and are primarily based on empiricism. These models will provide just as effective simulations as sophisticated biologically dependent models if the primary interest is discharge estimation.

2.11.2 Distributed Models

The distributed model describes the interaction between the system's components and how resources are shared and operated on multiple platforms to increase the mission's efficiency and success. Parameters of distributed models are fully allowed to vary in space at a resolution usually chosen by the user. Distributed modeling approach attempts to incorporate data concerning the particular distribution of parameter variations together with computational algorithms to evaluate the influence of this distribution on simulated precipitation-runoff behavior. Distributed models generally require large amounts of (often-unavailable) Data for parametrization in each grid cell. However, the governing physical processes are modeled in detail, and if correctly applied, they can provide the highest degree of accuracy.

2.11.3 Semi-Distributed Models

 Parameters of semi-distributed (simplified distributed) models are partially allowed to vary in space by dividing the basin into a number of sub-basins. The main advantage of these models is that their structure is more physically based than the lumped models, and they are less demanding on input data than fully distributed models. There are two types of semi-distributed models:

1) Kinematic wave theory models (KW models, such as HEC-HMS)

2) Probability distributed models (PD models, such as TOPMODEL)

The KW models are simplified versions of the surface and subsurface flows of equations of physically-based models (Bevin, 2000). In the PD models, spatial resolution is accounted for using probability distributions of input parameters across the basin.

2.12 Hydrological Model Selection

Selecting a model necessitates deciding on a perceptual and logical model. The results of hydrological simulation experiments differ depending on the model used. Even though selecting a hydrological model is a significant move, experience shows that hydrologists prefer to stick with the model they are familiar with and seldom turn to compete models, even though they are more appropriate for the research objectives (Addor and Melsen, 2019).

(Nguyen, 2015) studied the calibration and validation results using two hydrological models indicate that both models could adequately simulate streamflow for the specific study areas. In his investigation, the SWAT hydrological model offers better-simulated streamflow than the HEC-HMS hydrological model. On the other hand, the other research, which was considered by (Habibu *et al*., 2020), compares these two hydrological models' efficiency when used to evaluate the effects of climate change on streamflow at the basin scale HEC-HMS outperforms ArcSWAT. These ideas indicate a better performing hydrological model for a particular watershed. Another performance evaluation of HEC-HMS and SWAT on run-off-rainfall was investigated (Aliye *et al*., 2020). They found that the simulated streamflow given by the HEC-HMS model is more satisfactory than that provided by the SWAT model.

2.13 HEC-HMS Model

The Hydrologic Engineering Center of the US Army Corps of Engineers developed the HEC-HMS hydrologic modeling program to predict precipitation runoff in catchments. Programming software contains a number of different versions. The Hydrologic Engineering Center (HEC) of the United States Army Corps of Engineers (USACE, 2013) was founded in 1964 to institutionalize the technological knowledge known as hydrologic engineering. Many well-known and widely used hydrologic approaches for simulating rainfall-runoff processes in river basins are included.

Compared to the lumped conceptual model, which requires minimal input data, it is a semi-distributed model that requires physical data to anticipate hydrologic simulations, comprehensive data, and more detailed parameterization. The key reasons for using the HEC-HMS model are its loose coupling with GIS software (Geo-HMS extension), simplicity,

availability, and general acceptance, as well as the fact that it is a well-known Rainfall-Runoff simulation model.

The HEC-HMS rainfall-runoff model is one of the most useful. The peak discharge has estimated using rainfall-runoff models with rainfall data as input. When longer precipitation records are available than runoff, or when precipitation can be more reliably estimated from nearby stations, their use can be advantageous. We examine the differences between these interpretations while assessing model performance in peak flow magnitude and runoff volumes. The Hydrologic Modeling System (HEC-HMS) model, developed by the Hydrologic Engineering Center, has many parameters that can then adjusted.

The goal of this Hydrologic system is to simulate the precipitation-runoff processes in a dendritic watershed. It has made to work in various settings and solve a wide range of problems. Examples are small urban or natural watershed runoff, ample river basin water supply, and flood hydrology. The program's hydrographs have used in water availability studies, urban drainage, flow forecasting, future urbanization impact, reservoir spillway design, flood damage reduction, floodplain regulation, and system operation, either on their own or in conjunction with other software.

3. METHODOLOGY

3.1 Study area description

3.1.1 Location and Topography

The Ribb River is 130 kilometers long and drains roughly 1790 square kilometers, with an annual average discharge of about 18.88m^3/s. The research area is located in Ethiopia's northwestern upper Abay basin. It is situated between 11°40'0"- 12° 10'0" N latitude and 37°40'0''- 38°15'0" E longitude. This catchment is a member of the Tana sub-basin. The Blue Nile Basin is Ethiopia's largest basin, increasing population growth.
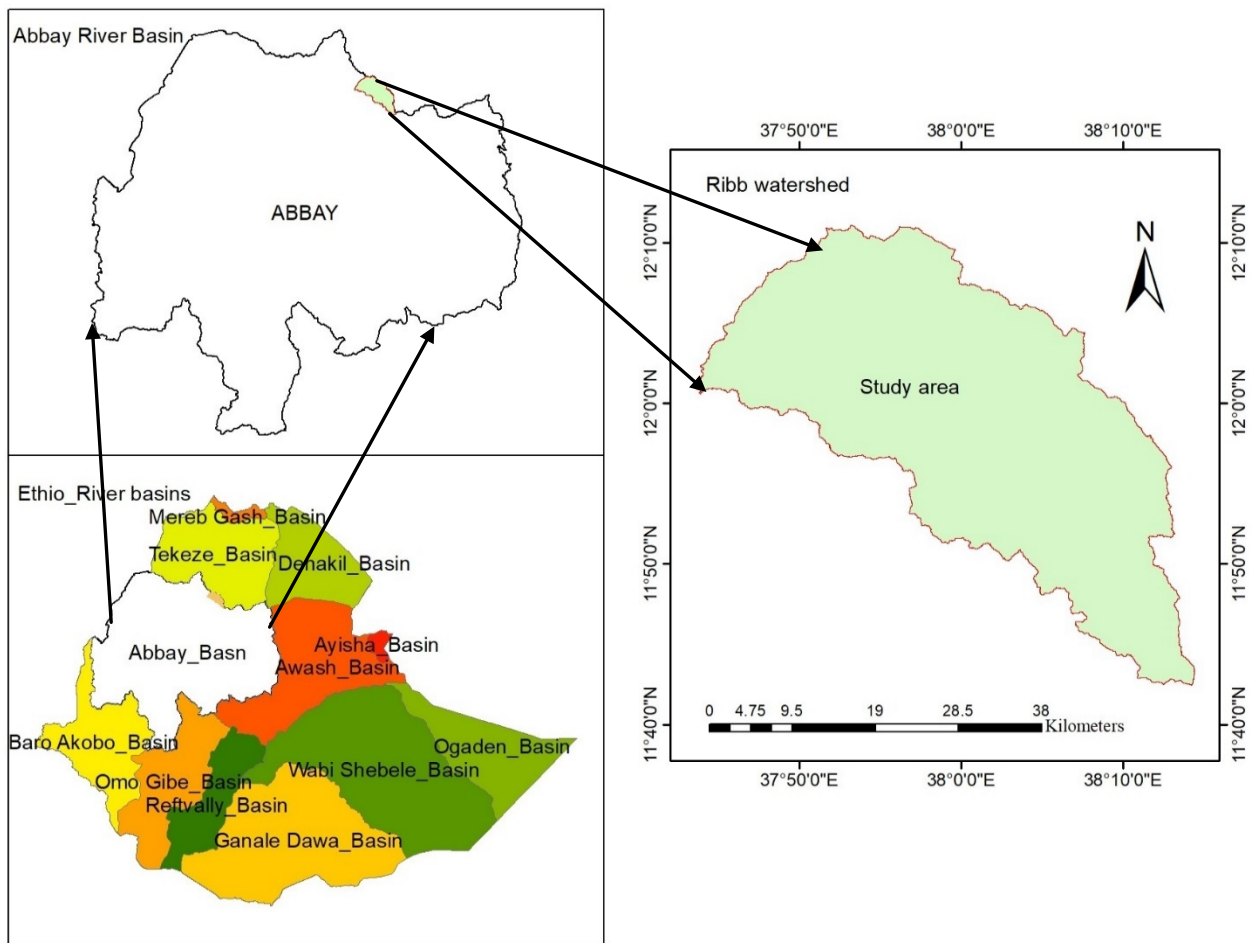
Figure 3. 1 Study Area Map

3.1.2 Slope map of Ribb watershed f

The slope is one of the watershed characteristics that affect the volume and velocity of surface runoff at the watershed level, and the Ribb watershed contains a variety of slope characteristics. Therefore, a Digital Elevation Model with a resolution of 12.5x12.5m was processed to estimate the slope of the watershed pixel by pixel, and the average slope was calculated. In the northern and northeastern regions of the watershed, the study area is relatively steep (Figure 3.2).
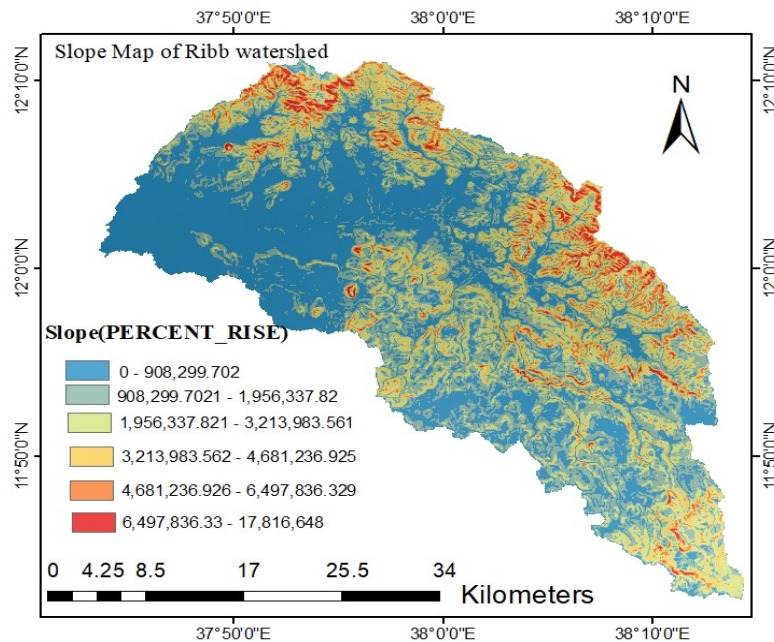
Figure 3. 2 Slope Map of Ribb Watershed

3.1.3 Elevation map of Ribb watershed

The area's topographic characteristics influence runoff formation, velocity and rainfall patterns, and temperature. By raising the water table and increasing the prevalence of saturated soil conditions in low-lying places, rising sea levels can increase surface runoff from coastal areas. As surface runoff rises, less rainwater infiltrates the Earth, reducing groundwater discharge to the shore. The watershed elevation was created using ArcGIS10.4 software and a DEM at a resolution of 12.5m X 12.5m.
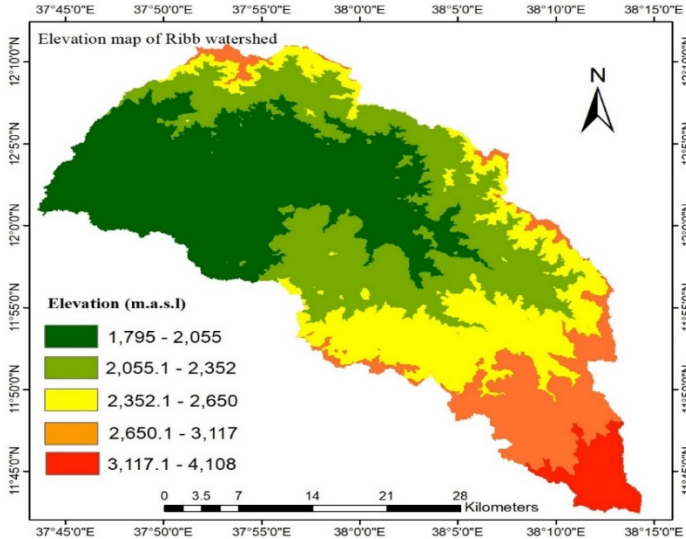
Figure 3. 3 Elevation map of Ribb Watershed

3.1.4 Land Use/ Land Cover

At local, regional, and global stages, land use and land cover have important environmental repercussions. Global loss of biodiversity, disturbances in hydrological cycles, increased soil erosion, and sediment loads are consequences of these changes at the regional and global levels. Ribb watershed is dominated by cultivated land (Figure 3.4). As stated by (Asitatikie and Tabor, 2020), bush/shrub areas were considerably converted to cultivated and grazing pastures throughout the research period, with a decline in forest cover. According to their findings, the magnitudes of cultivated land grew by 29.947 percent, whereas the magnitudes of bush/shrublands declined by 34.195 percent.
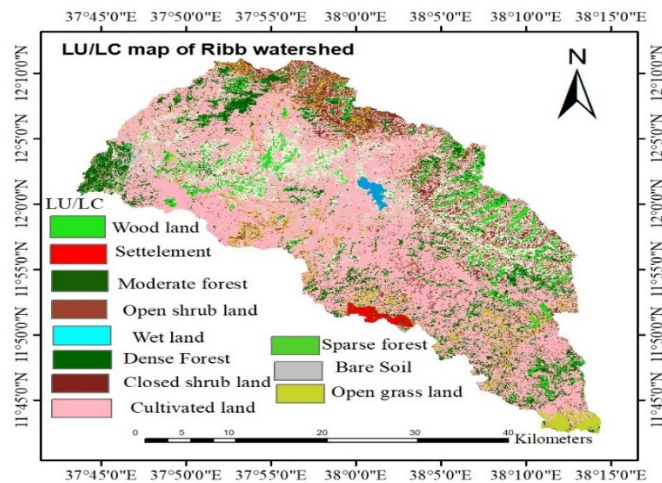
Figure 3. 4 Land use/Land cover map of Ribb watershed

24

3.1.5 Soil Type

Another aspect that influences runoff production and velocity is soil type. The soil was used as an input to an HEC-HMS model curve number grid preparation to know the loss in a given catchment. Chromic Luvisols, Humic Nitosols, Eutric Vertisols, Hepatic Luvisols, and Lithic Leptosols were among the major soil types identified in the watershed (Figure 3.5).
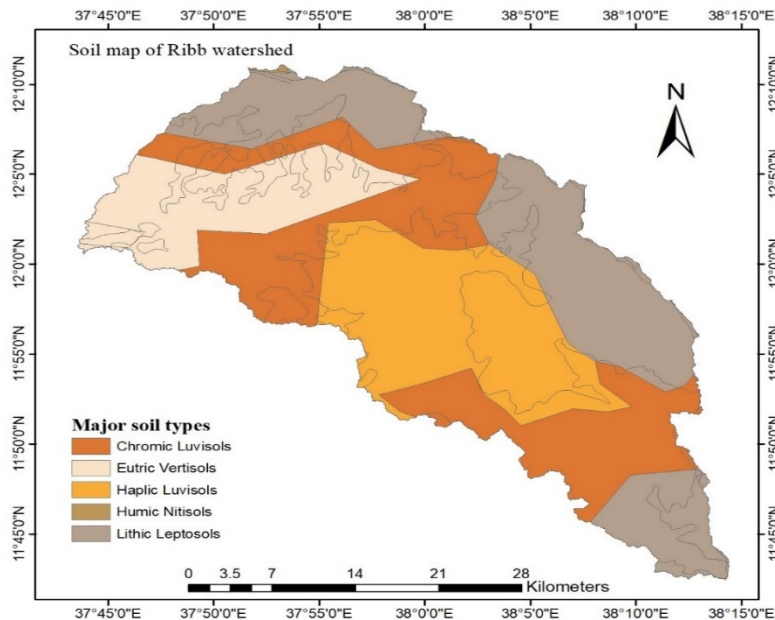
Figure 3. 5 Major Soil types in Ribb Watershed

3.1.6 Climate

Climate refers to the condition of the atmosphere over extended periods, such as decades. It is a collection of daily weather conditions collected over a lengthy period of time. Climate also considers extremes or changes that may occur outside of normal settings. As a vast country in the Horn of Africa, Ethiopia has a broad range of altitudes and meteorological conditions. Furthermore, the country is prone to substantial temporal and geographical weather fluctuations due to its proximity to the equator and the Indian Ocean. The seasonal migration of the Intertropical Convergence Zone (ITCZ), related atmospheric circulations, and Ethiopia's complicated terrain are thus the primary determinants of the country's climate. The climate ranges from tropical in the north-eastern and south-eastern lowlands to temperate and cold in the highlands due to its location and varying topography (Fazzini *et al*., 2015).

3.1.7 Stations Rainfall pattern over Ribb Watershed

Rainfall varies spatially, temporally, and seasonally. Four near stations were under consideration in the Ribb catchment, mean monthly, seasonally, and annually. The monthly rainfall is highest from June-September for all stations, and from those, Debre-Tabor station records the highest monthly rainfall. This is why the Debre-Tabor station is at the highest elevation from others (Figure 3.7). The seasonal rainfall is highest in summer (June-August) for all stations (Appendix A 1). According to research findings obtained at Lake Tana subbasin and the Blue Nile basins by (Conway, 2000); (Tarekegn and Tadege, 2006), (Kebede *et al*., 2006); the hydrological year of the areas of study is best described by one main rainy season (summer) between Junes to September, in which 70% to 90% of the annual total rainfall occurs (Appendix A 2).
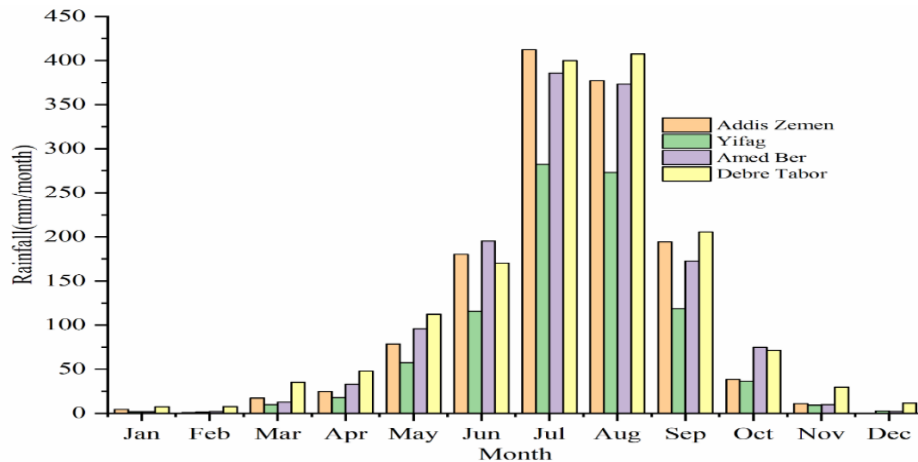
Figure 3. 6 Monthly Rainfall distribution of stations

3.1.8 Maximum and minimum observed Temperature of Stations over Ribb Watershed

The month of March saw all stations reach a record high for temperature. High-Temperature records were also set in February, April, October, November, and December. Conversely, the coldest months were August and July. In terms of minimum temperature, the highest temperatures were recorded in May and July, while the lowest temperatures were recorded in December, November, and January. On a Seasonal basis, the warmest Seasons are spring and winter throughout all locations, and in summer, the lowest maximum Temperature record was detected. The same holds for minimum temperature as maximum temperature. Spring and winter have the highest minimum temperature, and summer has the lowest minimum temperature (Appendix A 3-5).
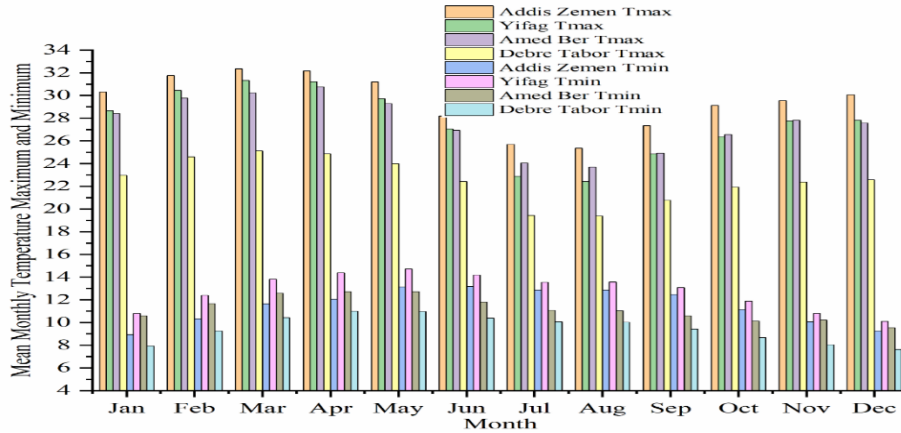
Figure 3. 7 Mean Monthly Maximum Temperature of stations

3.2 Materials

3.2.1 Spatial Data

The spatial data used are Land use/land cover data, Soil data & DEM. Land use land cover data were obtained from the FAO Geo-hydro database http://www.fao.org/news/story/ en/item/216144/icode/ or http://www.fao.org/geonetwork. Parameters derived from the land-use map are used in runoff estimation and hydrodynamic flow routing. Soil data has obtained from the FAO Soil database www.fao.org/soils-portal/soil- survey/soil, and it is one of the physical catchment characters that affect the runoff coefficient. The main input of different soil data for topographic parameter extraction and other related spatial data would be processed and delineated.

Spatial data, or geospatial data, is knowledge about a geographical object that can interpreted numerically in a geographic coordinate system. Spatial data, in general, refers to the position, scale, and form of an entity on Earth, such as a house, a lake, a mountain, or a township. DEMs are sequences of uniformly spaced elevation values horizontally referenced to a Universal Transverse Mercator (UTM) projection or a spatial coordinate system. A Digital Elevation Model (DEM) provides elevation, slope, and the location of a basin's stream network. Digital elevation model data was downloaded from https: www.asf.alaska.edu website.

3.2.2 Time Series Data

Two types of time series data are available. These are Hydrological data (observed stream discharge) & Meteorological data (observed daily rainfall, temperature (minimum &

maximum), and evaporation data). Observed stream discharge/flow was obtained from MoWR from 1990-2017. It has utilized for hydrologic model data assimilation and error corrections. Observed daily Rainfall and Temperature (maximum and minimum) were obtained from NMSA from 1990-2019. Daily observed rainfall is an input for the hydrological model for operational and real-time data for simulation model and forecasting model for calibration and validation. Maximum & minimum temperature have obtained at NMSA from 1990- 2019. The primary data required for this research is hydrological and meteorological data, including streamflow data, Rainfall, Temperature, land use/land cover data, DEM, soil data and climate scenario data. Historical data was selected from 1990 to 2019, and two future time horizons were identified, the 2040s (2025-2054) and 2070s (2055-2084).
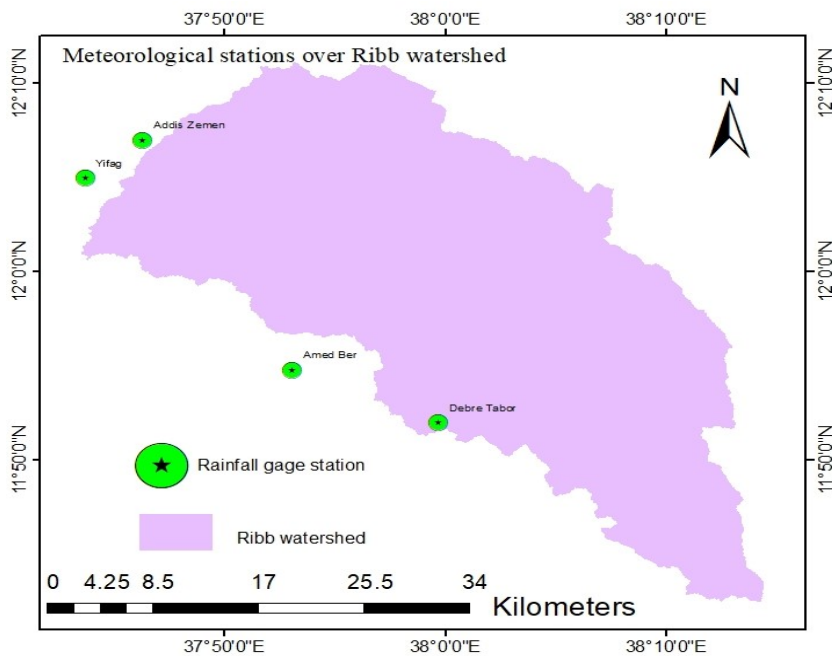
Figure 3. 8 Meteorological Stations on Ribb Watershed

Table 3. 1 Data Availability

No.	Type of Data	Temporal scale	Duration	Description	Source
1	Hydrological and meteorological data	Daily		Streamflow, Rainfall, Temperature maximum and Minimum	MoWIE & NMSA
2	DEM	-	-	Digital Elevation Model	ASF
3	Climate scenario data /RCM data	Daily	1990-1984	Precipitation data and Maximum and Minimum Temperature	ESGF
4	LU/LC map	-		LULC	FAO
5	Soil Data	-		Soil Type	FAO

Table 3. 2 Tools Used

No.	Tool	Purposes
1	ArcGIS 10.4	Geo-referencing, climate data extraction, and other various spatial analysis
2	HEC-HMS 4.7.1	For Calibration, Validation, flow simulation and forecasting
3	Origin pro-2018	For Graph sketching
4	XLSTAT2021	For data quality assessment (Data filling and trend analysis) of meteorological and flow data
	Rainbow	For Homogeneity test
5	UTM converter	used to convert the coordinates of the stations and gauge station from latitude and longitude to UTM and UTM to latitude and longitude
6	Google Earth pro	Helps to cross-check the recorded coordinates of the metrological and gauge stations, to cross-check the land use features of the study area
7	EndNote	used to insert bibliography and references

3.2.3 CORDEX Data

Climate modeling data has often needed for a small geographic area with a finer resolution than Global Climate Models (GCM) can offer. CORDEX makes a concerted effort to close the gap. Regional Climate Models (RCM) and a technique called dynamical downscaling have used to measure CORDEX results. The domain has embedded in a simulated global environment using a GCM or data from a global climate simulation has used as feedback for an RCM. Climate scenario data (precipitation, maximum and minimum air temperature) has downloaded from https://esgf-node.llnl.gov/search/esgf-llnl/ to calculate the abrupt changes in climatic variables the present and potential time horizons and used as inputs to hydrological simulations to determine rainfall-runoff impacts. RCM simulated variables' biases will result in unrealistic hydrological simulations; RCM outputs must be modified to account for biases (Bürger *et al*., 2007).

A climate scenario is a realistic depiction of future climate conditions (temperature, precipitation, and other climatological phenomena) that has been developed for practical use in studying the likely impacts of anthropogenic climate change (Houghton and Organization, 2002). Climate change simulations are created to provide coherent, internally reliable, and realistic explanations of the world's future situation. Climate change models should be evaluated based on their compliance with global forecasts, physical plausibility, the applicability of impact evaluations, and representativeness (Fentaw, 2010).

The RCPs cover a wide range of potential future improvements in anthropogenic (i.e., human) Greenhouse Gases (GHG) emissions (Ebi *et al*., 2014). The RCP2.6 predicts that global annual GHG emissions will plateau between 2010 and 2020 (in CO_2-equivalents), accompanied by a noticeable decrease (IPCC, 2014). In the RCP 4.5 scenario, emissions plateau around 2040 and decrease (IPCC, 2014). In RCP6.0, emissions plateau about 2080 and then decrease, while in RCP8.5, emissions begin to increase throughout the twenty-first century (IPCC, 2014). The mid-and late-twentieth-century averages and forecasts based on the RCPs are 2046-2065 and 2081-2100, respectively. The IPCC AR5 estimates for global mean sea level rise and global warming in relation to sea levels and temperatures in the late 20th and early 21st centuries are below. Two driving models (GCMs) with their corresponding four downscaled (RCMs) was used in this study.

RCM output bias-corrected was used as input for hydrological models in this study analysis to reflect the future climate change on the hydrology of the catchment. Daily climate variables (precipitation, maximum and minimum air temperature) from the RCA5 regional climate model for RCP4.5 and RCP 8.5 scenarios are bias-corrected using Power transformation and linear regression bias correction approaches, respectively, and then fed into the HEC-HMS hydrological model to determine possible climate change effects on catchment streamflow potential.

3.3 Methods

3.3.1 Data quality assurance

Data Quality Assurance is a method for determining relevant data quality dimensions and requirements and processes for ensuring that data quality criteria are met over time. It entails a data profiling method to uncover contradictions, outliers, incomplete data interpolation, and other data anomalies. Data quality assurance is the practice of profiling data to detect discrepancies and other irregularities and aiding in data cleansing operations (e.g., outlier exclusion, incomplete data interpolation) to enhance data quality. Both data quality auditing software intended for use by external audit teams and routine data quality evaluation tools designed for capability building and self-assessment are used in the data quality assurance package of tools and methods, which helps curriculum implementers to make appropriate improvements to the program's configuration and how they can better carry out the whole exercise.

Missing data and data identified as erroneous by validation can be substituted by interpolation from neighboring stations. These procedures are widely applied to daily rainfall. Estimated rainfall values using such interpolation methods are obtained for as many data points as required. However, in practice, usually, only a limited number of data values will require to be estimated at a stretch.

3.3.2 Filling of missed data

The first stage estimates the missing data in most climatological, environmental, and hydrological research. Data acquisition system reports often blame several factors such as lack of an analyst, instrument errors, and contact line loss. Leakages in the acquisition system report that emerging economies also have an impact. The estimated missing data is

particularly significant in mountain and forest locations, where the weather stations are few and observational data are influenced by terrain and forest microclimate(Kashani and Dinpashoh, 2012). These time-series data are used in many model implementations and mathematical studies (for example, extreme value evaluation). Accordingly, these time series' stability and appropriateness are important. As a result, filling data gaps in raw data collections is essential (Gao *et a*l., 2018).

Due to socioeconomic, structural, technical, and technological issues, missing data in historical hydrological datasets is frequent in developing nations. Multiple imputations is a technique for filling in gaps in data when virtual altimetry stations are unavailable, and it has been widely utilized in hydrological research. Multiple imputations fill in data gaps by simulating the required number of values by fitting real data to a distribution based on statistical characteristics such as the dataset's mean and standard deviation while considering the uncertainty regarding the presumed true meaning. The expression "multiple imputations" refers to the process of simulating missing data multiple times, in this case, five times with the XLSTAT2021 program, which is appropriate in previous studies (Ekeu-wei *et al*., 2018). Because of its interoperability with the Microsoft Excel data format, XLSTAT has gained popularity as a statistical software tool of choice for everyday multivariate statistics(Vidal *et al*., 2020). Also, (Demissie and Sime, 2021) used XLSTAT to fill missing data.

3.3.2.1 Arithmetic Average Method

If the average annual rainfall at the station in question is within 10% of the average annual rainfall at the neighboring stations, this method is used. The simple average of nearby stations is used to estimate the erroneous or missing rainfall at the station under consideration. Thus, if the estimate for the erroneous or missing rainfall at the station under consideration is Ptest and the rainfall at M adjoining stations is Pbase, i (i = 1 to M), then:

$$\boldsymbol{Ptest = \frac{1}{M}(Pbase, 1 + Pbase, 2 + Pbase, 3+ \ldots +Pbase, M)} \ldots \ldots \ldots \ldots \ldots \ldots (3.1)$$

3.3.2.2 Normal Ratio Method

If the average (or normal) annual rainfall at the station in question differs by more than 10 percent from the average annual rainfall at nearby stations, this technique can chose. For estimating the erroneous or missing precipitation at a station under consideration, the weighted average of neighboring stations. The ratio between the average annual precipitation

at the station considering and the average annual precipitation at each of the neighboring stations is used to weigh the precipitation. The rainfall for the erroneous or missing value at the station under consideration can estimated as:

$$Ptest = \frac{1}{M}\left(\frac{Ntest}{Nbase,1} * Pbase, 1 + \frac{Ntest}{Nbase,2} * Pbase, 2 + \dots + \frac{Ntest}{Nbase,M} * Pbase, M\right)\dots\dots\dots (3.2)$$

3.3.3 Consistency of Rainfall Data

Understanding precipitation dissipations is critical, recognizing that observational data sets are prone to substantial variation. Observational precipitation reports are being investigated in environmental and hydrological modeling, climate change, and resource and risk management (Timmermans *et al*., 2019). When assessing rainfall statistics, it is important to double-check the veracity of the rainfall station reports. After computing missing data from the watershed, the double mass curve approach is utilized in this study to check the accuracy of the stations in the catchment. Successful data administration and handling are essential for meteorological and hydro-climatological science. This demands data quality and consistency assurance solutions for data collection, delivery, storage, and processing. Data inconsistencies will be corrected, additional stations will be added, and the model will be enlarged to handle varied dimension sizes to achieve more accurate results(Duque-Méndez e*t al*., 2014)
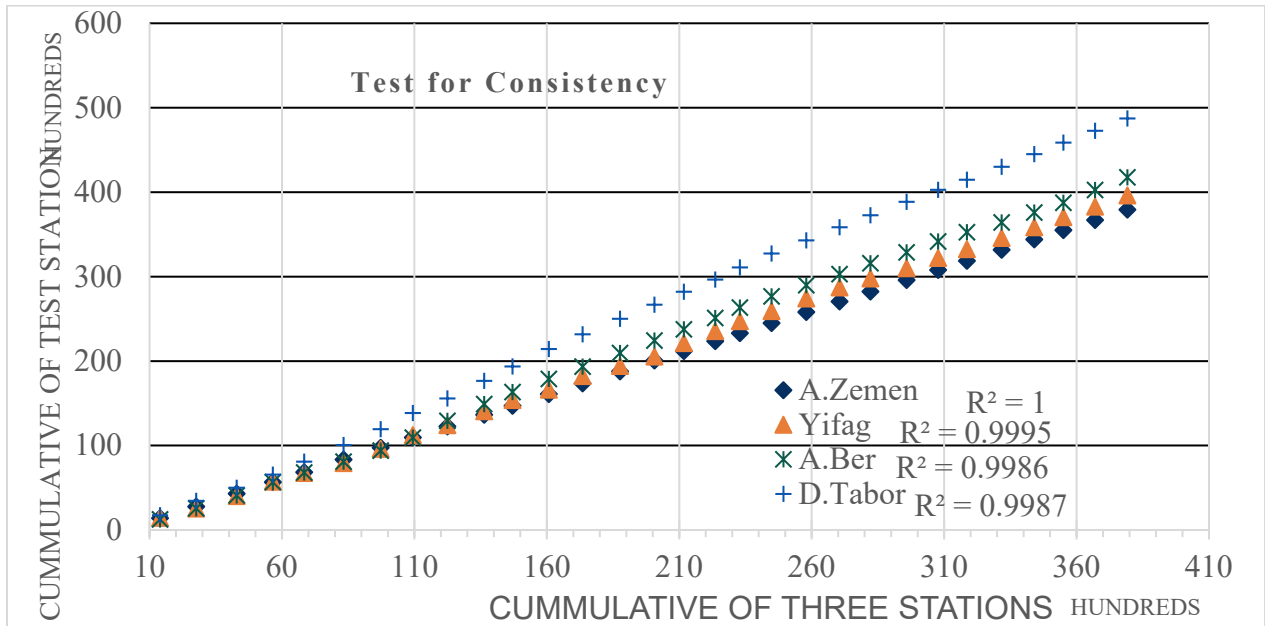
Figure 3. 9 Rainfall Consistency test Stations

3.3.4 Homogeneity

Various factors influence the precision and dependability of data gathered at meteorological stations. Rainfall records have influenced by the location of the gauging station, the instrument, and the method of data collection and processing, and the observation quality and time series might be inhomogeneous. As a result, the data utilized in hydrology and water supply system modeling should scientifically validated for correctness and dependability. The normal structure of the observation values does not decrease when the precipitation time series is homogenous in content. Several techniques have been proposed and utilized for determining the homogeneity of meteorological sequences. There are two methods for assessing sequence homogeneity: the "absolute approach" and the "relative technique." In the first phase, the test is carried out individually for each station. The verification phase in the second technique frequently involves nearby reference stations (Firat *et al*., 2010). The homogeneity test for other stations is involved in Appendix B 1-3.
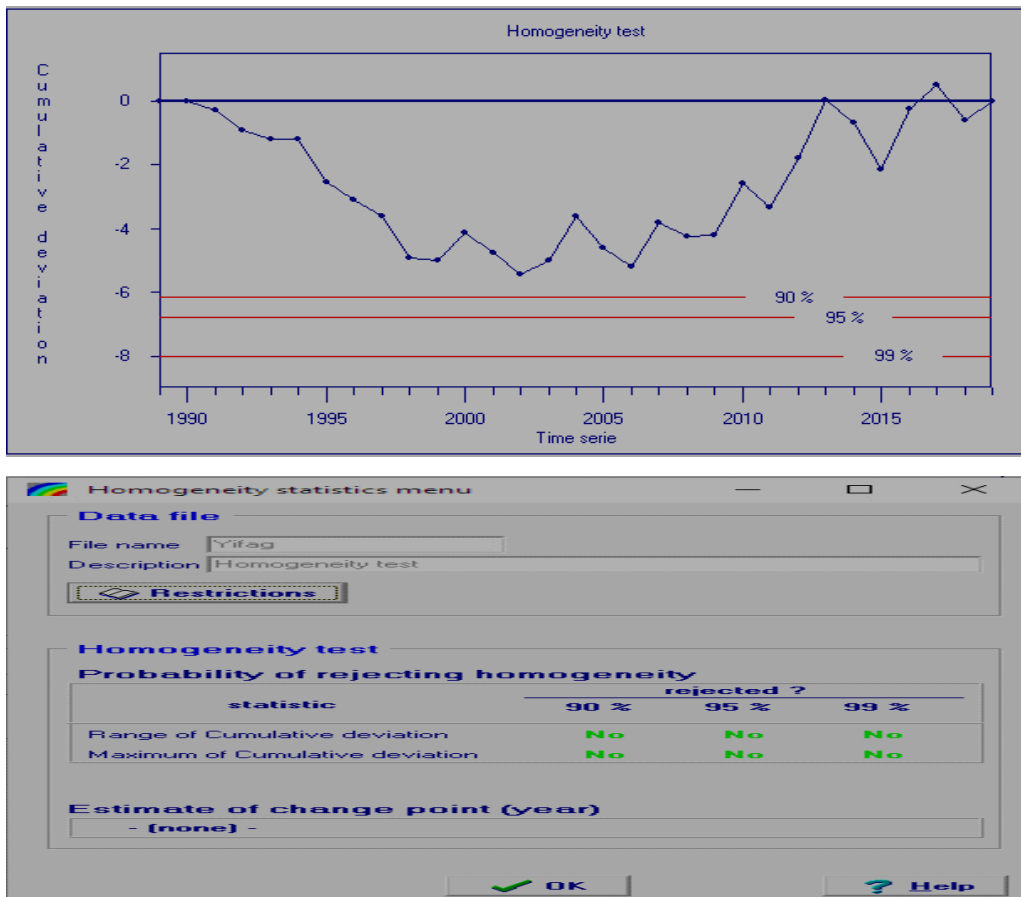
Figure 3. 10 Homogeneity test for Yifag station

3.3.5 Areal Rainfall

For areal Rainfall estimation, the Theissen polygon method has used. The Thiessen polygon technique has commonly used because of its great calculation accuracy and speed. The Thiessen polygon technique is straightforward to calculate since just the area data of the sample point is required (Zhou *et al*., 2009). If there are, x gages on the watershed, the area assigned to each is A_x, and P_x is the rainfall measured at the xth gage. The watershed's average rainfall is as follows:

$$Pareal = \frac{1}{A}\sum_{x=1}^{x} AxPx \dots\dots\dots\dots\dots\dots\dots\dots\dots\dots\dots\dots\dots\dots\dots\dots\dots\dots (3.4)$$
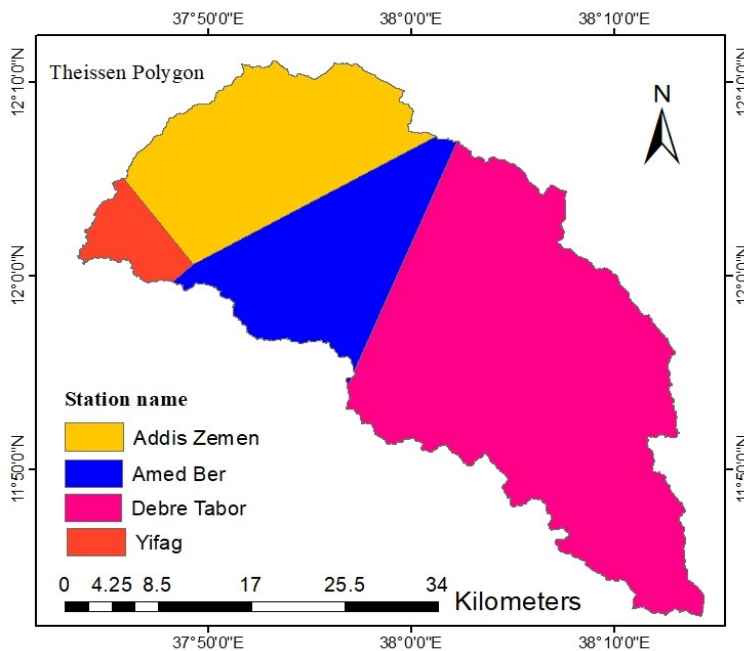
Figure 3. 11 Thiessen polygon developed for Ribb watershed rainfall stations

3.4 Performance evaluation of the RCM models

The catchment, hydrological model, climate models (GCM/RCM), climate change scenarios utilized, and the flow index analyzed all influence the size and direction of the climate change effect(Zhang *et al*., 2016). Furthermore, the performance of climate models have been established and is now accessible in terms of modeling precipitation, temperatures, and other climatic variables. To put it another way, climate models with the requisite resolution do not consistently forecast and simulate the climate variables that are supposed to drive climate change. Criteria for RCMs performance efficiency include the Pearson correlation

(r), Root means square error (RMSE), and Pearson bias (BIAS) has used to evaluate the model performance of RCM model (Dibaba *et al.*, 2019). The smaller BIAS and RMSE indicates the better performing ability of RCM over a specific area. The value of r ranges from (-1 to 1) in which values close to zero are considered as poor correlation. BIAS, RMSE and r can calculated as follows:

$$BIAS = \frac{\sum_{k=1}^{n}(simu,k - obs,k)}{n} \dots\dots\dots\dots\dots\dots\dots\dots\dots\dots\dots\dots\dots\dots\dots\dots\dots\dots\dots\dots\dots \text{(3.5)}$$

$$RMSE = \sqrt{\frac{1}{n}\left[\sum_{i=1}^{n}(simu - obs)^2\right]} \dots\dots\dots\dots\dots\dots\dots\dots\dots\dots\dots\dots\dots\dots\dots \text{(3.6)}$$

$$r = \frac{\sum_{i}^{n}(simu - Simu,mean)*(obs - obs,mean)}{\sqrt{\sum_{i=1}^{n}(simu - simu,mean)^2}*\sqrt{\sum_{i=1}^{n}(obs - obs,mean)^2}} \dots\dots\dots\dots\dots\dots\dots\dots\dots\dots\dots\dots\dots \text{(3.7)}$$

3.5 Bias Correction

Bias correction is the method of scaling outputs from the climate model for their systemic mistakes to increase the fitness of observations. Bias errors across climate models and measurements can be due to improper conceptualization, discretization, and spatial averaging inside grid cells. For instance, biases normally arise with limited precipitation intensities or high temperatures on extremely wet days. Unrealistic fluvial flux simulations can result from biases in the outputs of RCMs. Climate model estimates of precipitation and temperature in the control cycle seldom match measurements in the same period. Such errors can affect potential virtual flow performance. In order to increase the reliability of climate model effects in the future, bias correction approaches try to achieve the fitting of climate model models to observations in the control period (Soriano *et al.*, 2019). There are some ways of bias adjustment, including linear scaling and Power Transformation. For this investigation, the power transformation bias correction approach have used for raw precipitation, and the linear scaling method was used for temperature. Five bias correction methods, performance was cheeked by (Berhanu 2018) on Lake Tana sub-basin and concluded that the five bias correction procedures utilized could improve the RCM-simulated precipitation and temperature.

a. Linear Scaling

Teutschbein (2012) adopted the Linear-scaling approach for this study due to its suitability for bias correction daily. The linear correction applies a scaling factor to transform raw precipitation to corrected precipitation magnitude. The climate time series, RCM simulation will be adapted with an estimated daily mean for each future time horizon. Observational data has calculated on a daily mean basis. The future daily bias-corrected temperature (T*) and daily precipitation (daily RCM P *) time series will be built using equations 3.21 and 3.22, respectively.

$$TRCM, daily* = TRCM, daily((Tobs, daily)mean - (TRCM, daily)mean) \quad (3.8)$$

$$PRCM* = PRCM, daily \times \frac{(Pobs, daily)mean}{(PRCM, daily)mean} \ldots\ldots\ldots\ldots\ldots\ldots\ldots\ldots\ldots\ldots\ldots \quad (3.9)$$

Where: $TRCM$, is the daily RCM simulated temperature data, $(TRCM, daily)$mean is the mean daily RCM simulated temperature for respective time horizons

$(Tobs, daily)$mean is the mean daily observed temperature for the given period; $PRCM, daily$ is the daily RCM simulated precipitation; $(Pobs, daily)$mean is the mean daily observed precipitation for the given period; $(PRCM, daily)$mean is the mean daily RCM simulated precipitation for respective future forecasted time horizons.

b. Power transformation

The Coefficient of Variation (CV) as well as the mean are corrected using a power transformation (Leander, Buishand et al. 2008). Each daily precipitation quantity P has turned into a corrected P* using the following nonlinear correction:

$$Ptest = aP\text{\textasciicircum}b \ldots\ldots\ldots\ldots\ldots\ldots\ldots\ldots\ldots\ldots\ldots\ldots\ldots\ldots\ldots\ldots\ldots\ldots\ldots\ldots\ldots \quad (3.10)$$

P_{test} represents bias-adjusted daily precipitation, P represents uncorrected daily precipitation, and a and b represent transformation coefficients. The b parameter is determined repeatedly until the coefficient of variation of the corrected RCM daily precipitation time series equals that of the observed precipitation time series for each grid box in each month. The parameter a is then chosen so that the mean of the modified daily data matches the observed mean. Finally, to construct the corrected daily time series, monthly constants a and b are applied to

each uncorrected daily observation corresponding to that month. Because temperature is known essentially as normally distributed, a related power-law like the one used to correct precipitation cannot be used to correct temperature.

3.6 Mann-Kendall Trend test of Hydrological and Meteorological data

This method is non-parametric (they are generally distribution-free tests, and they detect trend/change and quantify the size of the trend/change using Sen's slope. They are very useful because most hydrologic time series data are not normally distributed. The presence of outliers less influences them). This method tests whether there is a trend in the time series data, increasing or decreasing. Mann-Kendall trend analysis is widely used to test increasing or decreasing trends in precipitation and Temperature*(Yadav et al*., 2014). The mathematical equations for calculating Mann-Kendall Statistics S and V(S) can calculated as:

$$S = \sum_{i=1}^{n-1}\left[\sum_{j=k+1}^{n} Sign(Rj - Ri)\right] \dots\dots\dots\dots\dots\dots\dots\dots\dots\dots \text{(3.11)}$$

$$Sign(Rj - Ri) = \begin{cases} 1 \ if \ Rj - Ri > 1 \\ 0 \ if \ Rj - Ri = 1 \\ -1 \ if \ Rj - Ri < 1 \end{cases} \dots\dots\dots\dots\dots\dots\dots\dots \text{(3.12)}$$

Where Rj and Ri represents n data points at times j and i respectively.

$$V(S) = \frac{n(n-1)(2n+5) - \sum_{i=1}^{m} ti(ti-1)(2ti+5)}{18} \dots\dots\dots\dots\dots\dots\dots\dots \text{(3.13)}$$

Where t_i has considered as the number of ties up to sample i.

Software used for performing statistical Mann-Kendall test was Addinsoft XLSTAT2021. It was tested at 95% confidence level for precipitation, both maximum and minimum temperature and stream flow data.

3.7 Flow Duration Curve (Discharge Frequency Curve)

The flow-duration curve is a cumulative frequency curve that show the percent of time specified discharges have equaled or exceeded during a given period. The FDC is a stochastic representation of the variability of runoff, which arises from the transformation, by the catchment, of within-year variability of precipitation that can itself be characterized by a corresponding duration curve for precipitation (PDC) (Yokoo, Y. and Sivapalan, M., 2011).

Variability in precipitation and temperature will influence both high and low flows resulting from climate change. The fact that streamflow changes throughout a water year are widely recognized. Flow-duration curves are one of the most used ways to investigate streamflow variability (Discharge Frequency Curve) (Subramanya, 2013). To examine extreme flows (high flow and low flow) on the future, Flow Duration Curve has used. This curve has drawn from mean monthly stream flow and percent exceedance. By using this curve, the extent of future high flow and low flow relative to the observed stream flow have easily be estimated.

3.8 Hydrological Modeling

3.8.1 Model Setup

This study used HEC-HMS version 4.7.1 software, a conceptual semi-distributed model designed to simulate the rainfall-runoff processes. This model is selected based on the applicability and limitations of each model, availability of data, suitability for the same hydrologic condition, well establishment, stability, wide acceptability, researcher recommendations, etc. The model will be found to be accurate in spatially and temporally predicting watershed response in event-based and continuous simulation and simulating various scenarios in flood forecasting and early warning.

For the loss method, SCS Curve Number was selected. It is superior to other approaches in the following ways: It is a basic conceptual technique for estimating the direct runoff quantity that is well supported by actual evidence; it simply uses the curve number, which is a function of the key runoff-producing watershed features of soil type and land use/cover. Comparing to the initial and constant loss rate methods, it is widely employed in many situations and produces superior results. Just a few variables must be calculated based on hydrologic soil type and land use, making it easy to calculate (Tassew *et al*., 2019). SCS-CN, as (Kaffas and Hrissanthou, 2014) confirms, it is frequently used in hydrology, particularly in precipitation-runoff computer software packages, and it is an excellent means of estimating surface runoff. SCS Unit Hydrograph, Constant monthly, and Muskingum were selected as transform, base flow, and routing methods.

3.8.2 HEC-HMS Input Terrain Processing

The land surface elevation is required for identifying a watershed and developing a basin model based on that delineation. Terrain data are utilized in the delineation process and may also be used as a base map to display the relief of a watershed. Each terrain data component has a single continuous digital elevation model (DEM) connected to numerous basin models. In this study, HEC-HMS 4.7.1 has used for terrain processing. The latest version of HEC-HMS 4.7.1 can delineate a watershed, and the delineated basin model for the Ribb watershed has shown in the Figure 3.12.
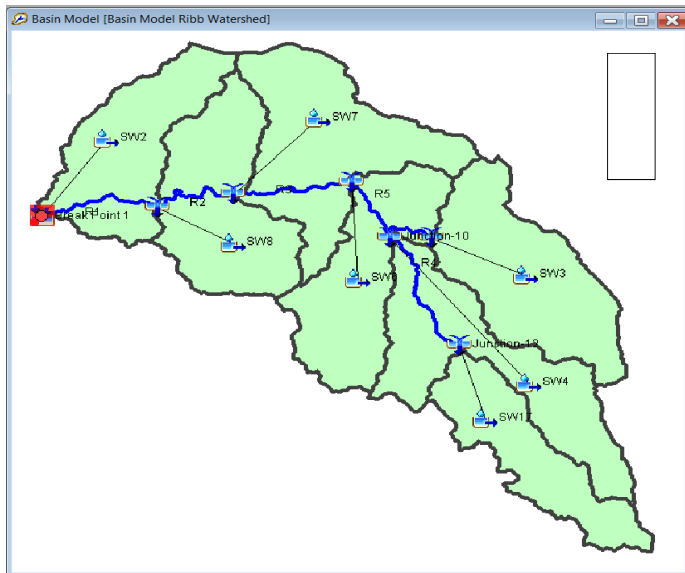

Figure 3. 12 Basin development and Ribb watershed delineation using HEC-HMS 4.7.1

3.8.3 HEC-HMS Model Sensitivity Analysis, Calibration and Validation

The Hydrologic Modeling System (HEC-HMS) developed by the Hydrologic Engineering Center in the United States has been calibrated and verified for the Ribb watershed to forecast its hydrologic performance. Calibration and validation are the first hydrological modeling (Cunderlik and Simonovic, 2004). The calibration technique determines the best parameter values for minimizing the objective functions. Modifying model parameters until the model's simulated outputs match the historical data is known as model calibration. The HEC-HMS model has a set of parameters that grow in number as additional system components are included and manual or automatic calibration should be used. The parameters of this calibration model are modified until the value of the specified goal function is optimal. Model validation is a technique for determining if a model can put on

data other than those used for calibration with acceptable accuracy. The values of calibrated model parameters are unchanged during this procedure; instead, they maintained unchanged. Two deterministic search strategies are offered to maximize the goal function and return optimal parameter values.

The univariate technique assesses and modifies one parameter throughout the optimization simulation; when the univariate method is used, the user can choose just one parameter for the software to alter. The Simplex approach uses a downhill simplex to examine all parameters concurrently and determine which one should be adjusted. The simplex approach is the default method; however, at least two parameters must be set (HEC-HMS user's manual, 2021). For this study, rather than using the univarient technique, the Nelder and Mead optimization method was applied. The reason for this is is the Nelder and Mead technique employs downhill simplex to analyze all parameters at the same time and determine which ones should be adjusted. This automated calibration procedure is used to reduce the sum of absolute errors, sum of squared errors, percent error in peak, and peak weighted root mean square error as stated by (Gebre S.L, 2015). Sensitivity analysis finds the factors that have the greatest impact on the model's performance in the case study. Although sensitivity analysis minimizes the number of factors to be improved, it necessitates an excessive amount of trial and error (Dariane *et al*., 2020).
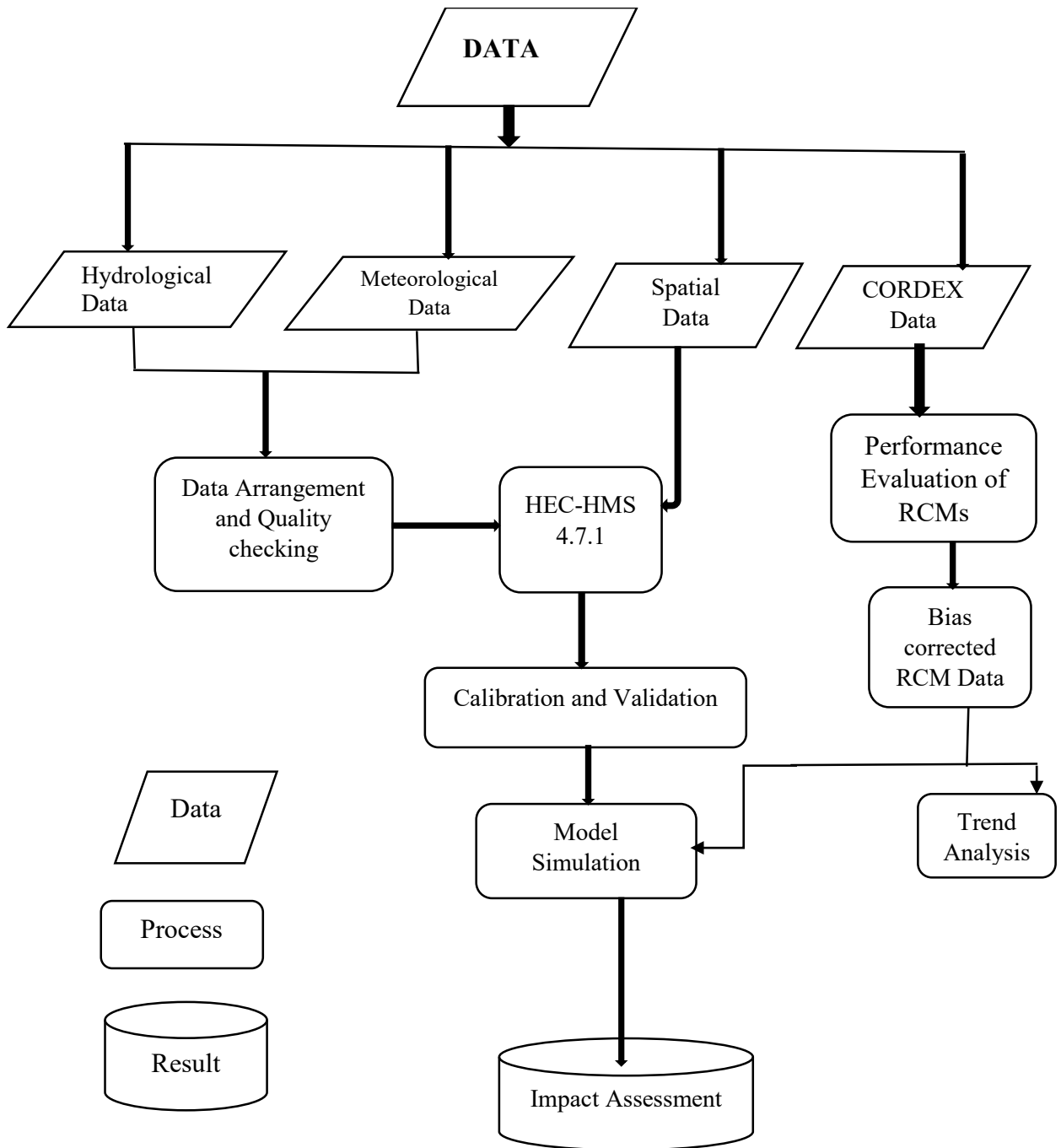
.

Figure 3. 13 Conceptual Frame Work of the Study

4. RESULTS AND DISCUSSIONS

4.1 HEC-HMS Model Sensitivity Analysis, Calibration and Validation

4.1.1 Sensitivity Analysis

Sensitivity analysis has executed on HEC-HMS parameters on a daily time step using observed streamflow. There are various factors that impact a complicated hydrological simulation, according to (Song, X *et al*., 2015). Because to regional variability, measurement inaccuracy, and insufficient descriptions of both the constituents and processes present in the system, the majority of these parameters' values are unknown. As a result, adjusting a model's internal parameters is critical for achieving a well-representative hydrological model. Sensitivity analysis aids in the selection of significant and influential parameters for model calibration by identifying parameters with higher output sensitivity owing to input variability.

An observed stream flow data from 01 January 1990 to 31 December 2017, of gage station near Addis Zemen has used. The result shows that Muskingum-K and Muskingum-X were sensitive parameters during HEC-HMS model optimization.

4.1.2 Calibration Result

The HEC-HMS handled automated calibration to lower a specific objective function, such as the sum of absolute errors, the sum of squared errors, percent error in peak, and peak-weighted root mean square error. The coefficient of determination (R^2) and Nash-Sutcliffe Efficiency (NSE) during calibration were 0.89 and 0.86, respectively, indicating that the observed data and the model strongly agree.

Table 4. 1 Reach (R) Parameter values before optimization (BOP) and after optimization (AOP)

Element	Parameter	BOP	AOP	Element	Parameter	BOP	AOP
R1	Muskingum K(HR)	55.801	62.907	R3	Muskingum K(HR)	73.815	76.373
	Muskingum X	0.0843	0.1667		Muskingum X	0.4564	0.256
R13	Muskingum K(HR)	88.937	93.964	R4	Muskingum K(HR)	92.582	114.19
	Muskingum X	0.0954	0.2744		Muskingum X	0.0962	0.1872
R2	Muskingum K(HR)	69.749	74.896	R5	Muskingum K(HR)	65.239	72.841
	Muskingum X	0.3654	0.2359		Muskingum X	0.2459	0.1151

Table 4. 2 Loss and Transform parameter values of HEC-HMS model for Ribb watershed

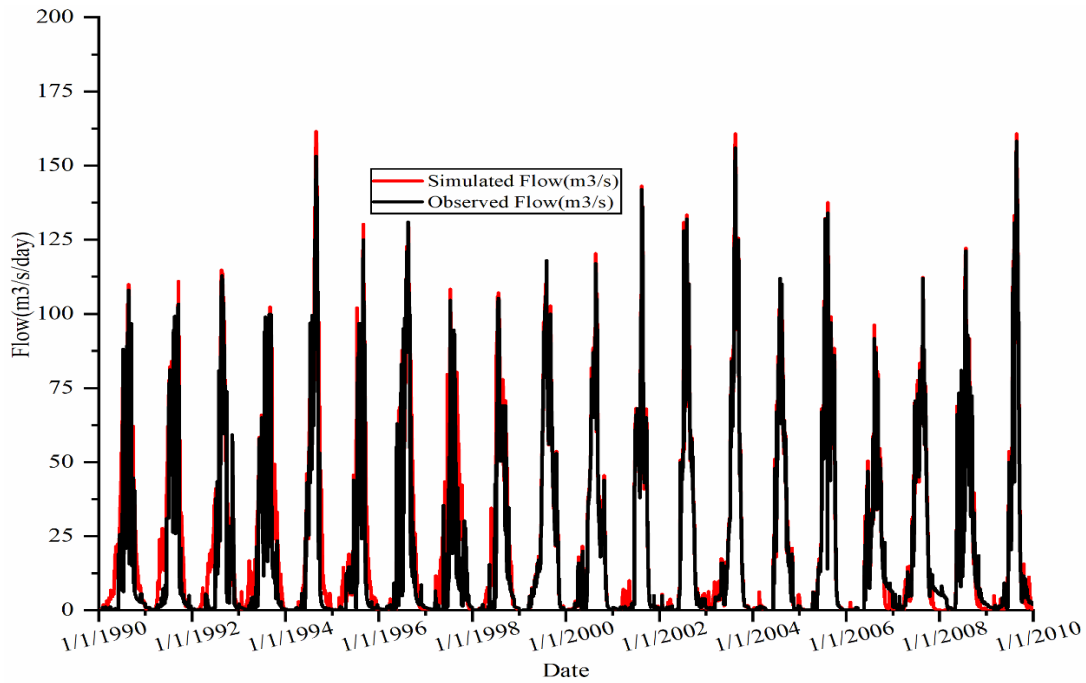| Subbasin	Area (km^2)	Initial Abstraction (mm)	Curve Number	Impervious (%)	Lag(min)
SW17	131.06	0.43919	82.10	0.00	190.5023
SW2	162.82	0.10806	92.69	0.00	136.4019
SW3	198.94	0.25779	88.58	0.00	90.2042
SW4	194.60	0.15774	94.87	0.00	173.5587
SW6	166.79	0.22457	91.11	0.00	121.5167
SW7	218.84	0.19806	89.91	0.00	101.8495
SW8	187.90	0.19516	90.99	0.00	117.1226

Figure 4. 1 Daily Observed and Simulated Flow during Calibration

4.1.3 Validation Result

Validation verifies the model's performance for simulated flows throughout periods other than the calibration period, with no additional adjustments to the calibrated parameters. It is the act of confirming something as true or correct. The validation process entailed using the optimized parameters of a different period and confirming the goodness of fit for the observed and simulated streamflow confirming the goodness of fit for the observed and simulated streamflow. The optimized values gave the Coefficient of determination (R^2) and Nash-Sutcliffe (NSE) 0.87 and 0.84, respectively, for validation.
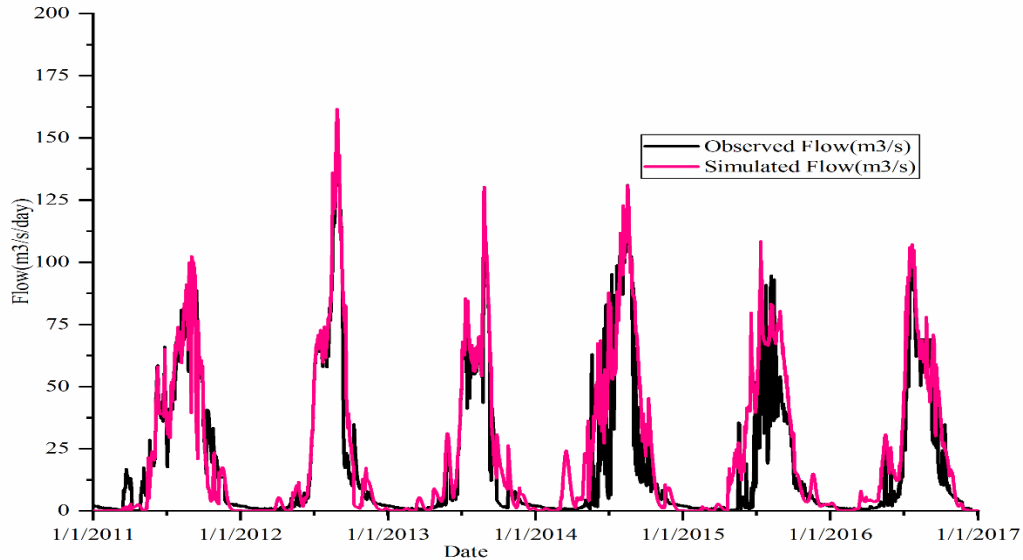
Figure 4. 2 The Validation result of HEC-HMS model

4.2 Performance Evaluation of regional climate models (RCMs) for simulating Rainfall

The performance of three regional climate models (RCMs), KNMI-RACMO22T, SMHI-RCA4, and CLMcom-CCLM4-8-17, and their ENSEMBLE was checked by solving for PBIAS, RMSE (Root mean square error), and r (Pearson's correlation) for each station. To determine the best performance of the model, it was necessary to evaluate their comparison of historical and observational data. This was important because the best model of evaluation results was use as input in the impact assessment model. As shown in on Table 4.3, KNMI-RACMO22T shows the lowest BIAS, lowest RMSE, and greatest Pearson correlation, r for all stations as compared to others (Figure 4.3). In addition to having the best parameter values, it clearly shows that KNMI-RACMO22T data goes on the graph with the observed data of all stations (Figure 4.4 - 4.7). By comparing PBIAS, RMSE, and r of each RCM with that of the ENSEMBLE, the KNMI-RACMO22T regional climate model has the best performance on each station and it can concluded that this RCM can perform best for Ribb watershed and it was selected as impact assessment RCM model for this study. This study supports the investigation on RCM models' performance on the upper blue Nile basin, Fincha and Didessa catchments by (Dibaba *et al*., 2019) as they concluded CRCM5 and RACMO22T both best simulate rainfall.

46

Table 4. 3 Performance evaluation on statistics parameters of RCMs and their ENSEMBLE

Station	BIAS			
	CLMcom-CCLM4-8-17,	SMHI-RCA4	KNMI-RACMO22T	ENSEMBLE
Addis Zemen	4.763	1.844	1.515	1.660
Yifag	2.767	-1.474	1.296	1.354
Amed Ber	2.936	1.532	1.141	1.258
Debre Tabor	2.027	0.658	1.456	1.546
	Root mean Square Error, RMSE			
	CLMcom-CCLM4-8-17,	SMHI-RCA4	KNMI-RACMO22T	ENSEMBLE
Addis Zemen	1.103	-0.374	-0.260	0.265
Yifag	0.754	-0.334	0.428	0.543
Amed Ber	0.756	-0.384	-0.272	0.333
Debre Tabor	0.176	0.036	-0.313	-0.362
	Pearson Correlation, r			
	CLMcom-CCLM4-8-17,	SMHI-RCA4	KNMI-RACMO22T	ENSEMBLE
Addis Zemen	0.362	-0.262	0.887	0.644
Yifag	-0.705	-0.742	0.753	-0.725
Amed Ber	0.034	-0.028	0.949	0.593
Debre Tabor	-0.209	0.275	-0.818	-0.683

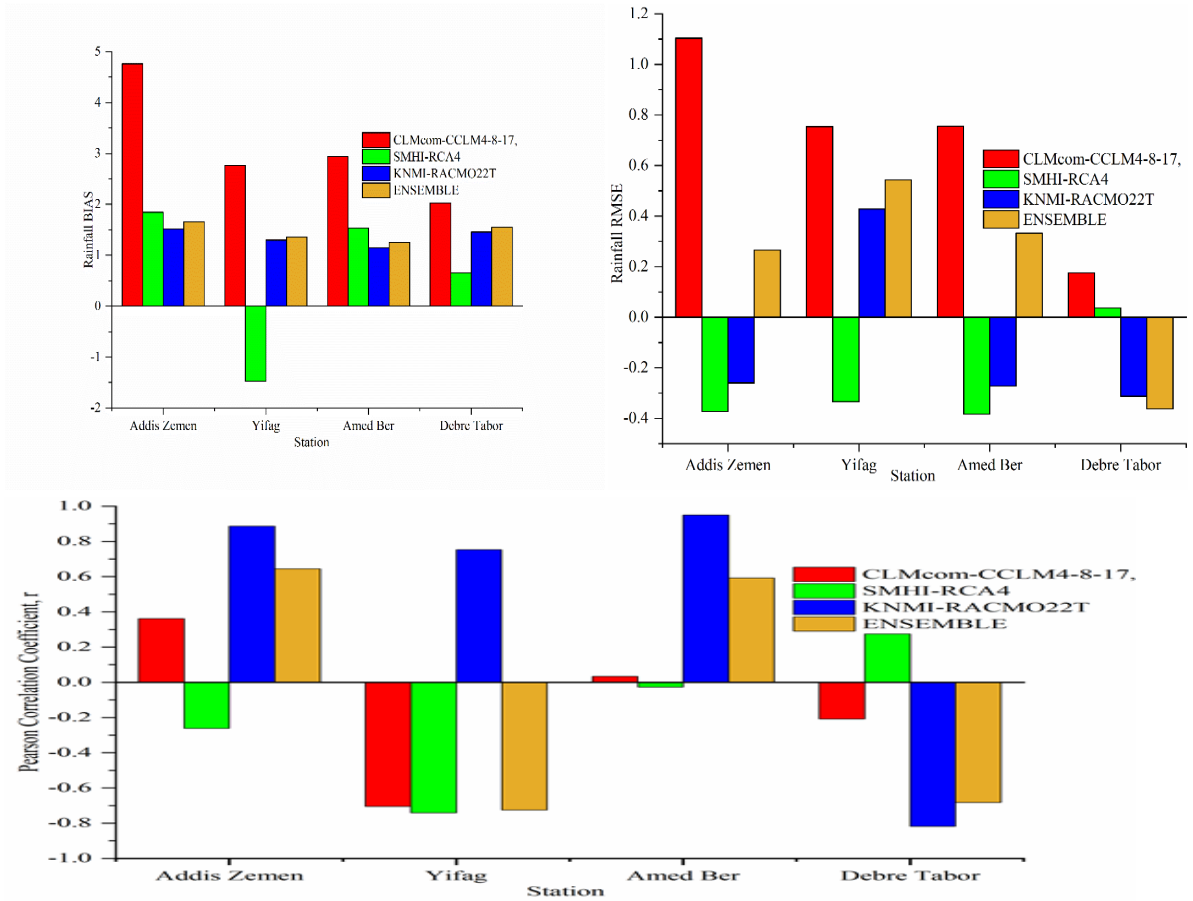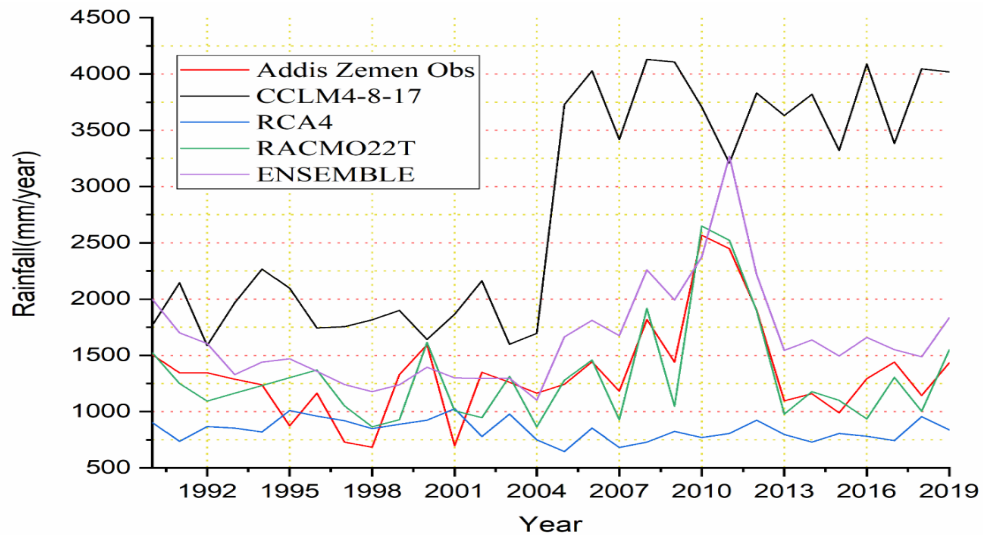Figure 4. 3 Performance statistics of RCMs and their ENSEMBLE over stations

Figure 4. 4 Annual observed and Historical Rainfall at Addis Zemen station
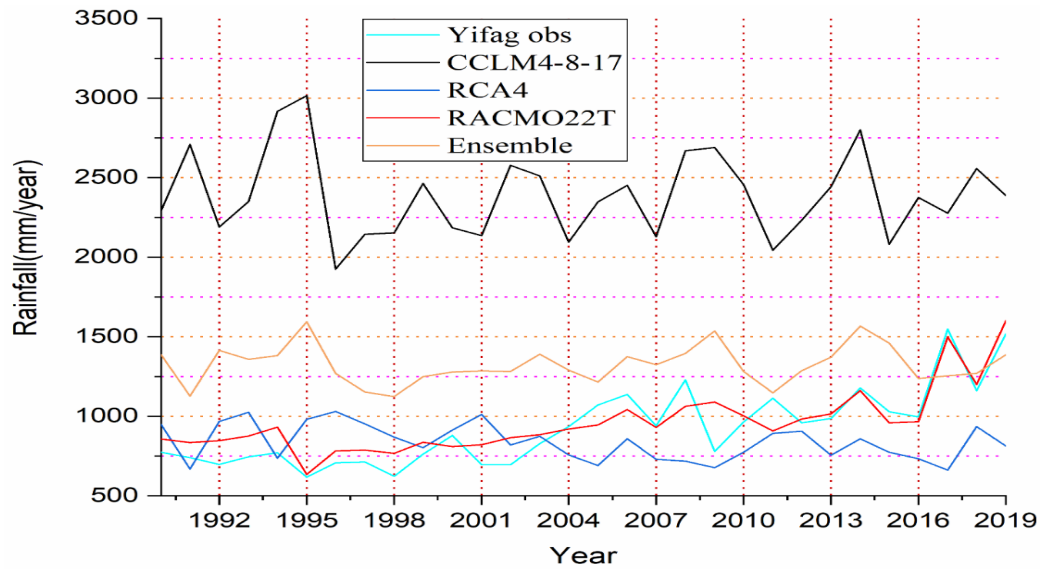
48

Figure 4.5 Annual observed and simulated Rainfall at Yifag station for Performance evaluation of different RCMs and their ENSEMBLE
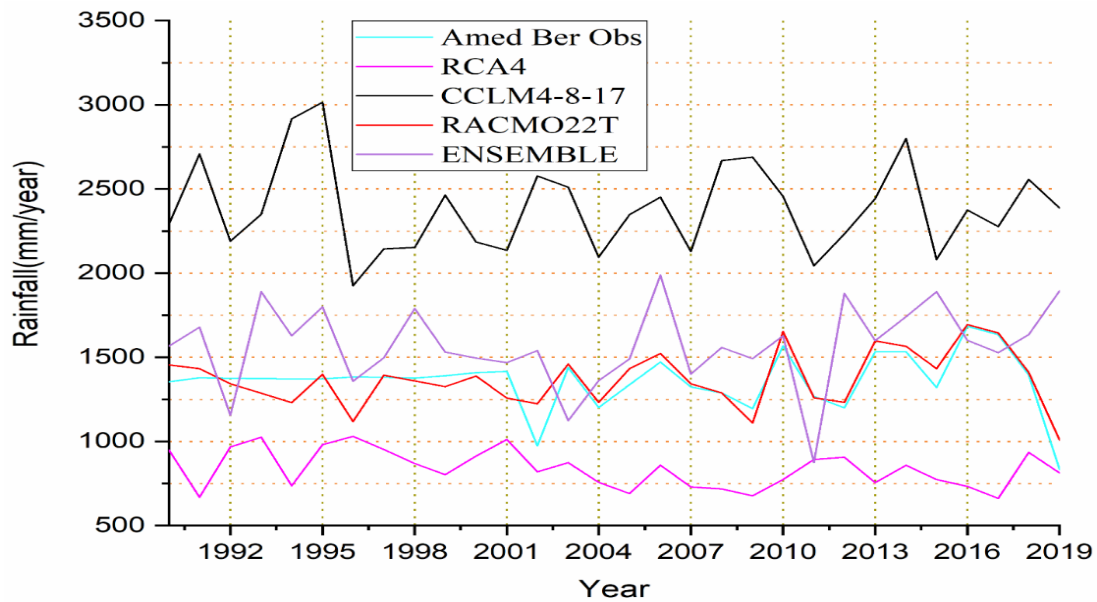

Figure 4.6 Annual observed and simulated Rainfall at Amed Ber station for Performance evaluation of different RCMs and their ENSEMBLE
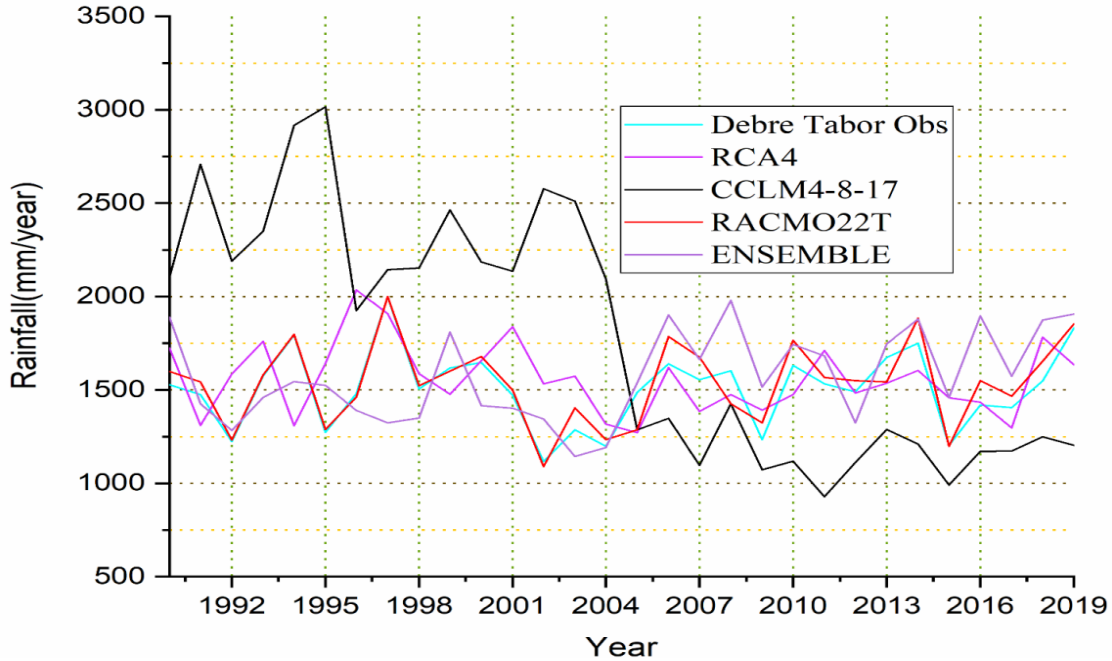
Figure 4.7 Annual observed and simulated Rainfall at Debre Tabor station for Performance evaluation of different RCMs and their ENSEMBLE

4.3 Trend analysis on Monthly, Seasonal and annual Rainfall and Temperature of Ribb watershed

Future rainfall and temperature (maximum and minimum) have analyzed over the time interval of 30 years for the near term (2025-2054) and long term (2055-2084). Non-parametric Mann-Kendall (M-K) detected monthly, seasonal, and annual precipitation and temperature trends. The purpose of the Mann-Kendall (M-K) test is for statistically assess if there is a monotonic upward or downward trend of the variable of interest over time and to get the magnitude of the trend Sen's slope is calculated. The near-term and long-term rainfall shows annually decreasing change while temperature shows increasing change for both RCP scenarios.

4.3.1 Trend analysis on mean Monthly Projected Rainfall

Figure 4. 8 Trend test on mean monthly scale for Observed and Projected (2025-2054) Rainfall

Table 4. 4 Parametric statistics values of trend test for mean monthly future rainfall (2025-2054) RCP4.5

Parameter	Jan	Feb	Mar	Apr	May	Jun	Jul	Aug	Sep	Oct	Nov	Dec
Kendall's tau	0.269	-0.103	0.062	0.398	-0.710	-0.182	-0.159	-0.448	-0.356	-0.457	-0.549	0.655
S	117.000	-45.000	27.000	173.000	-309.000	-79.000	-69.000	-195.000	-155.000	-199.000	-239.000	285.000
Var(S)	3141.667	3141.667	3141.667	3141.667	3141.667	3141.667	3141.667	3141.667	3141.667	3141.667	3141.667	3141.667
p	0.038	0.432	0.643	0.002	< 0.0001	0.164	0.225	0.001	0.006	0.000	< 0.0001	< 0.0001
α	0.05	0.05	0.05	0.05	0.05	0.05	0.05	0.05	0.05	0.05	0.05	0.05
Sens's slope	0.273	-0.051	0.581	7.867	-14.539	-3.390	-3.726	-8.158	-1.699	-1.352	-1.547	3.761

Table 4. 5 Parametric statistics values of trend test for Mean Monthly future rainfall (2025-2054) RCP8.5

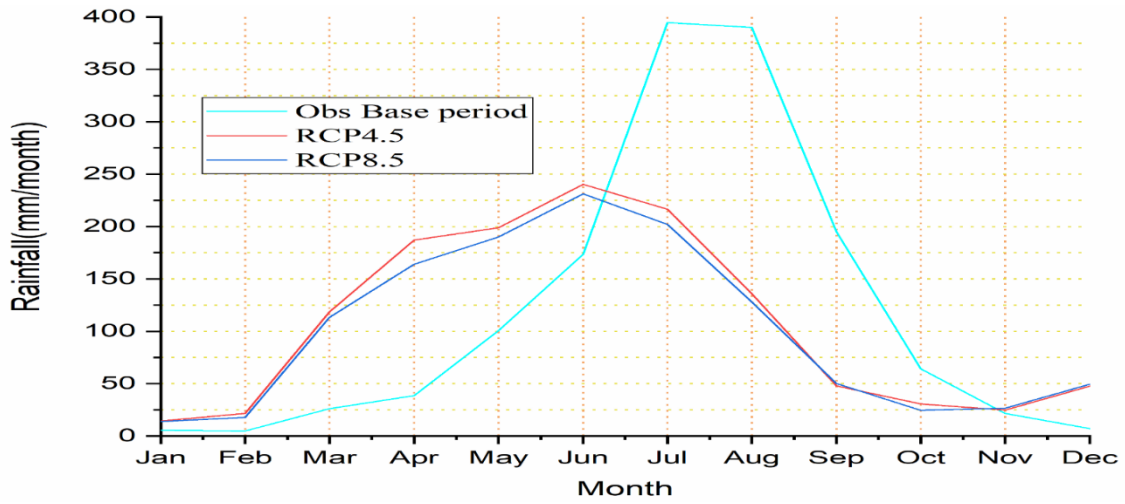| Parameter	Jan	Feb	Mar	Apr	May	Jun	Jul	Aug	Sep	Oct	Nov	Dec
Kendall's tau	0.310	-0.057	0.205	0.306	0.513	-0.108	-0.154	-0.430	-0.246	-0.411	-0.508	0.632
S	135.000	-25.000	89.000	133.000	223.000	-47.000	-67.000	-187.000	-107.000	-179.000	-221.000	275.000
Var(S)	3141.667	3141.667	3141.667	3141.667	3141.667	3141.667	3141.667	3141.667	3141.667	3141.667	3141.667	3141.667
p	0.017	0.669	0.116	0.019	< 0.0001	0.412	0.239	0.001	0.059	0.001	< 0.0001	< 0.0001
α	0.05	0.05	0.05	0.05	0.05	0.05	0.05	0.05	0.05	0.05	0.05	0.05
Sen's slope	0.334	-0.104	2.731	5.949	10.749	-1.861	-4.478	-7.492	-1.109	-0.769	-1.864	3.058

Figure 4. 9 Trend test on Seasonal scale for Observed and Projected (2025-2055) Rainfall

Table 4. 6 Parametric statistics values of trend test for Seasonal observed (1990-2019) and future Rainfall (2025-2054) RCP4.5 and RCP8.5

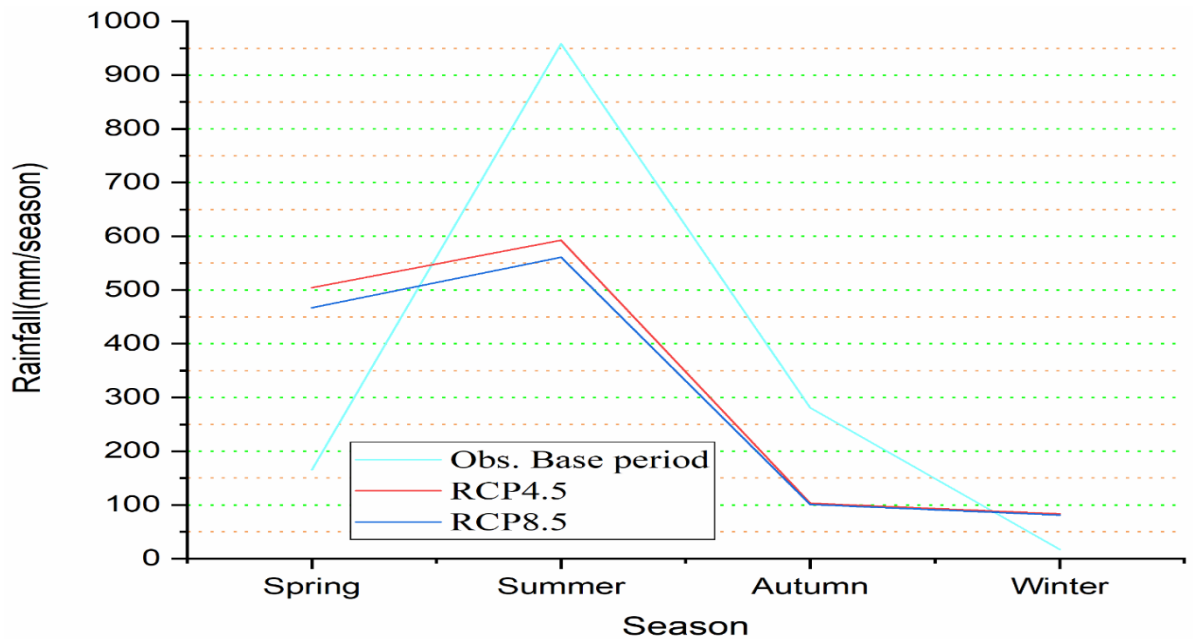| Obs. Base period						
	Kendall's tau	S	Var(S)	p	α	Sen's slope
Spring	0.122	53	3141.667	0.354	0.05	0.597
Summer	0.08	35	3141.667	0.544	0.05	0.61
Autumn	0.094	41	3141.667	0.475	0.05	0.409
Winter	0.08	35	3141.667	0.544	0.05	0.071
RCP4.5						
Spring	0.586	255	3141.667	< 0.0001	0.05	8.237
Summer	-0.297	-129	3141.667	0.022	0.05	-4.848
Autumn	-0.724	-315	3141.667	< 0.0001	0.05	-2.743
Winter	0.021	9	3141.667	0.887	0.05	0.158
RCP8.5						
Spring	0.232	101	3141.667	0.074	0.05	3.386
Summer	-0.411	-179	3141.667	0.001	0.05	-3.444
Autumn	-0.586	-255	3141.667	< 0.0001	0.05	-2.372
Winter	0.048	21	3141.667	0.721	0.05	0.729

Figure 4. 10 Trend test on Annual scale for Observed and Projected Rainfall

Table 4. 7 Parametric statistics values of trend test for annual observed (1990-2019) and future rainfall of RCP4.5 and RCP8.5 (2025-2054)

	Kendall's tau	S	Var(S)	p	α	Sen's slope
Obs. Base period	0.145	63	3141.667	0.269	0.05	3.042
RCP4.5	-0.016	-7	3141.667	0.015	0.05	-1.077
RCP8.5	-0.255	-111	3141.667	0.045	0.05	-7.704

RCP4.5 for mean monthly rainfall indicates a declining tendency in the near term (2025–2054) for February, May, and June-November. A significant declining trend has shown in the months of August-November. The months reflect a rising trend, with December, January, and April growing significantly (Table 4.4, Figure 4.8). RCP8.5 indicates the declining trend for February, May, and June-November. It shows a significant declining tendency August-November. Other months for RCP8.5 show a rising trend, with December, January, April, and May show a significant increase (Table 4.5, Figure 4.8). Seasonally, on RCP4.5, spring and winter show significant rising and declining trends over the summer and autumn (Table

4.6, Figure 4.9). RCP8.5 reveals a significant seasonal lowering trend in summer and autumn and a rising trend in spring and winter (Table 4.6, Figure 4.9). The near-term annual rainfall show a significant declining trend on both RCPs (Table 4.7, Figure 4.10). Overall, in this study, the near-term mean monthly rainfall indicate increasing and decreasing changes for the future, although the rise is less than the observed and the decline is greater for both RCPs in the short-term time horizon. (Setegn *et al*., 2011) reveal that the precipitation pattern is not constant, and the GCMs used in this study show a decrease in precipitation. (Dile *et al.,* 2013) in the Lake Tana watershed also indicated that annual mean precipitation may have been reduced in the first 30 years. According to their result, the drop in mean monthly precipitation might be as high as 30% between 2010 and 2040.
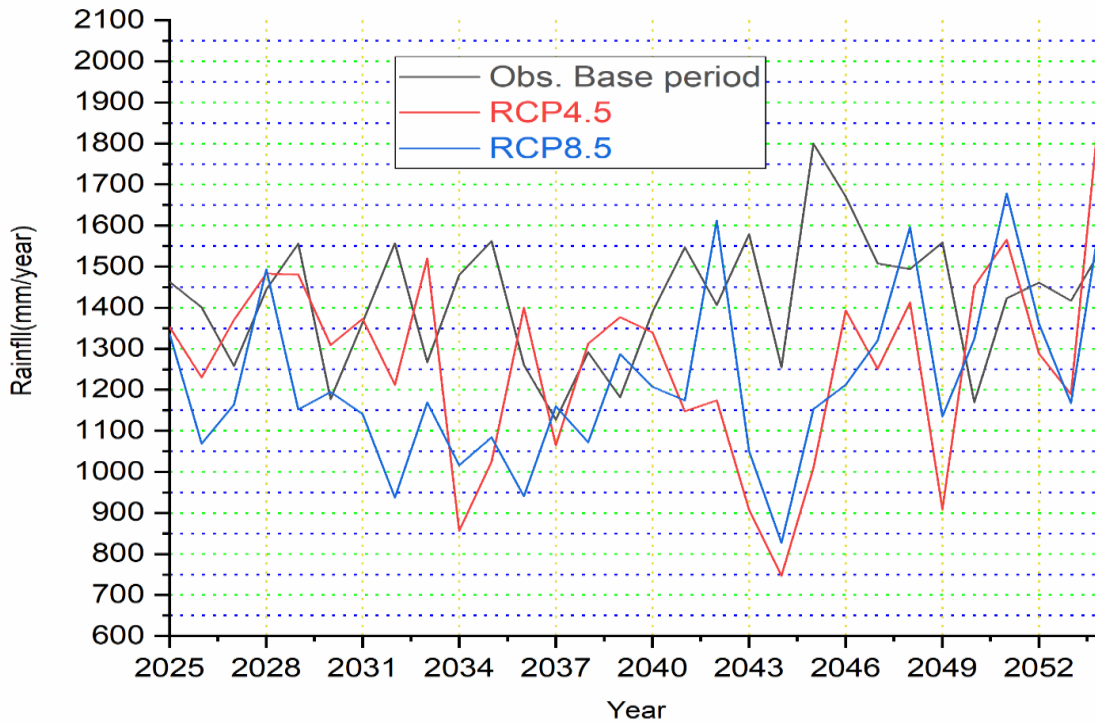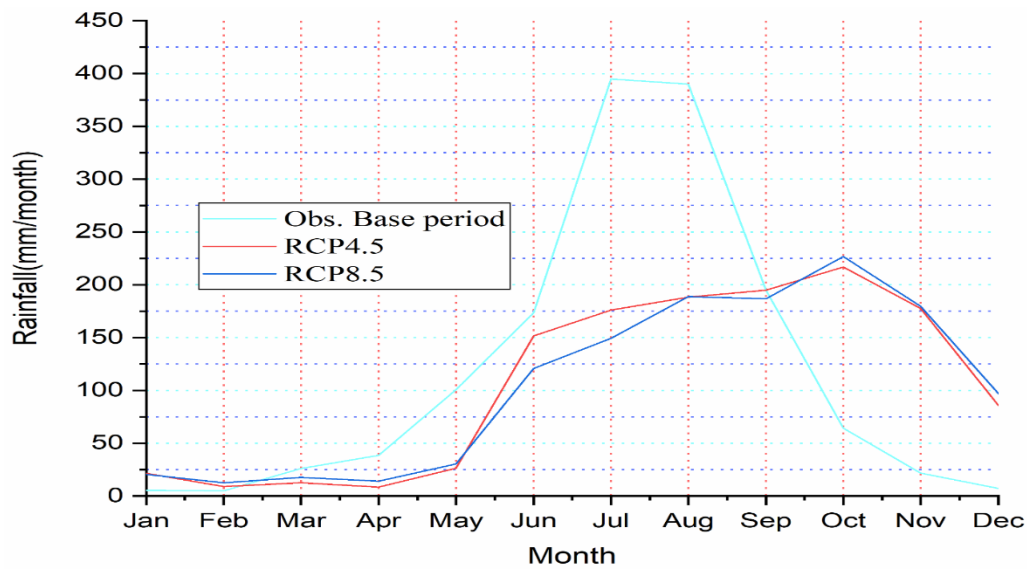

Figure 4. 11 Trend test on Mean monthly scale for Observed and Projected (2055-2084) Rainfall

Table 4. 8 Parametric statistics values of trend test for mean monthly future Rainfall RCP4.5 (2055-2084)

	Jan	Feb	Mar	Apr	May	Jun	Jul	Aug	Sep	Oct	Nov	Dec
Kendall's tau	0.163	0.297	-0.384	-0.080	-0.356	-0.434	-0.186	-0.375	-0.720	0.172	0.306	0.375
S	71.000	129.000	-167.000	-35.000	-155.000	-189.000	-81.000	-163.000	-313.000	75.000	133.000	163.000
Var(S)	3141.667	3141.667	3141.667	3141.667	3141.667	3141.667	3141.667	3141.667	3141.667	3141.667	3141.667	3141.667
p	0.212	0.022	0.003	0.544	0.006	0.001	0.153	0.004	<0.0001	0.187	0.019	0.004
α	0.05	0.05	0.05	0.05	0.05	0.05	0.05	0.05	0.05	0.05	0.05	0.05
Sen's slope	0.464	0.162	-0.319	-0.051	-1.377	-11.081	-3.897	-6.733	-14.090	4.243	5.977	3.766

Table 4. 9 Parametric statistics values of trend test for mean monthly future Rainfall RCP8.5 (2055-2084)

	Jan	Feb	Mar	Apr	May	Jun	Jul	Aug	Sep	Oct	Nov	Dec
Kendall's tau	0.329	0.439	-0.292	0.122	-0.039	-0.448	-0.140	-0.476	-0.678	0.352	0.287	-0.251
S	143.000	191.000	-127.000	53.000	-17.000	-195.000	-61.000	-207.000	-295.000	153.000	125.000	-109.000
Var(S)	3141.667	3141.667	3141.667	3141.667	3141.667	3141.667	3141.667	3141.667	3141.667	3141.667	3141.667	3141.667

p	0.011	0.001	0.025	0.354	0.775	0.001	0.284	0.000	<0.0001	0.007	0.027	0.054
α	0.05	0.05	0.05	0.05	0.05	0.05	0.05	0.05	0.05	0.05	0.05	0.05
Sen's slope	0.422	0.325	-0.373	0.127	-0.173	-9.207	-3.573	-8.454	-13.668	7.632	5.053	-2.505

Figure 4. 12 Trend analysis on Seasonal scale for observed and projected (2055-2084) long time horizon Rainfall

Table 4. 10 Parametric statistics values of trend test for seasonal future Rainfall RCP4.5 and RCP8.5 (2055-2084)

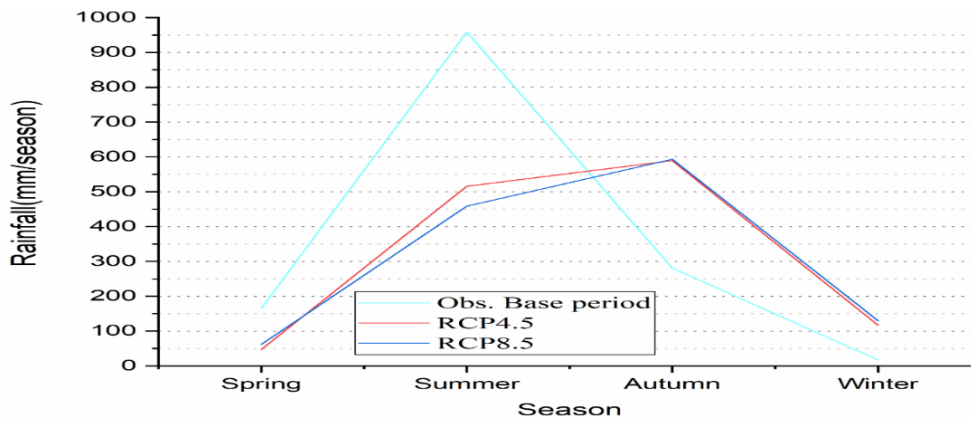| RCP4.5						
	Kendall's tau	S	Var(S)	p	α	Sen's slope
Spring	-0.352	-153	3141.667	0.007	0.05	-0.859
Summer	-0.136	-59	3141.667	0.301	0.05	-2.259
Autumn	0.306	133	3141.667	0.019	0.05	4.406
Winter	0.379	165	3141.667	0.003	0.05	2.18
RCP8.5						
Spring	-0.067	-29	3141.667	0.617	0.05	-0.139
Summer	-0.053	-23	3141.667	0.695	0.05	-0.976
Autumn	0.352	153	3141.667	0.007	0.05	5.684
Winter	0.379	165	3141.667	0.003	0.05	1.985
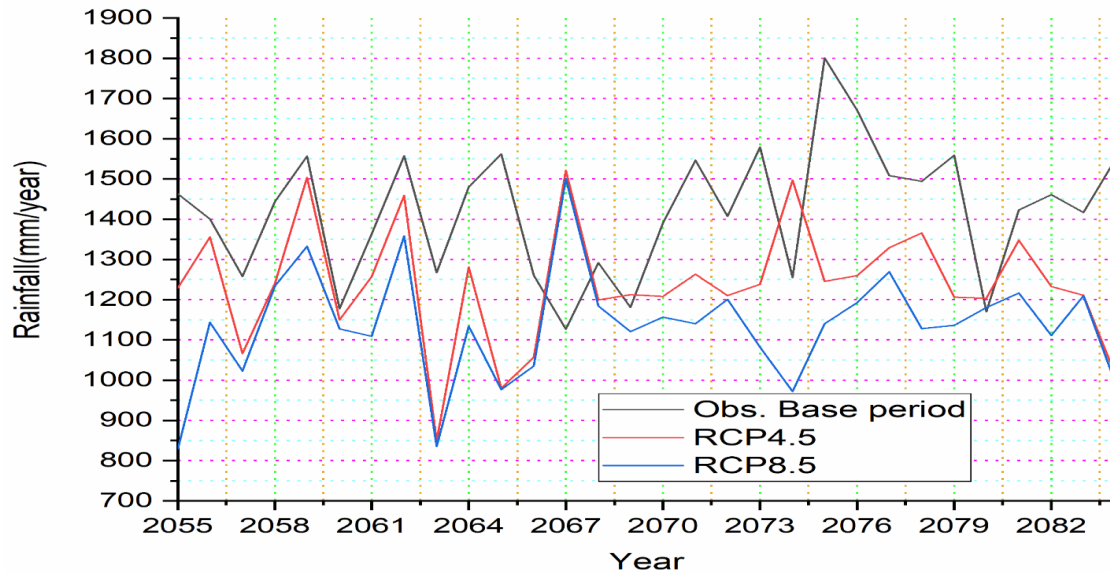
Figure 4. 13 Trend analysis on Annual scale for observed and projected (2055-2084) time horizon Rainfall

Table 4. 11 Parametric statistics values of trend test for future Annual Rainfall (2055-2084)

	Kendall's tau	S	Var(S)	p	α	Sen's slope
RCP4.5	-0.126	-55	3141.667	0.035	0.05	-4.33
RCP8.5	-0.205	-89	3141.667	0.016	0.05	-6.26

For the long-term time step (2055-2084), RCP4.5 for months, March-September, rainfall shows decreasing and increasing trends from October-February (Table 4.8, Figure 4.11). RCP8.5 shows decreasing trend for months March-September and an increasing trend from October-February (Table 4.9, Figure 4.11). RCP4.5 shows a significant increasing trend for season's autumn and winter, a significant decreasing trend shown in spring and summer. RCP8.5 shows a significant decreasing trend for season's spring and summer, a significant increasing trend shown in winter and autumn (Table 4.10, Figure 4.12). Long-term annual RCP4.5 and RCP8.5 rainfall show decreasing trend annually (Table 4.11, Figure 4. 13). (Tabari *et al.*, 2015) shows the amount of yearly rainfall is decreasing. (Adem *et al*., 2014) also studied the average daily rainfall drops as the rainy season progresses.

4.3.2 Trend analysis on Mean monthly, Seasonal and Annual Maximum and Minimum Temperature
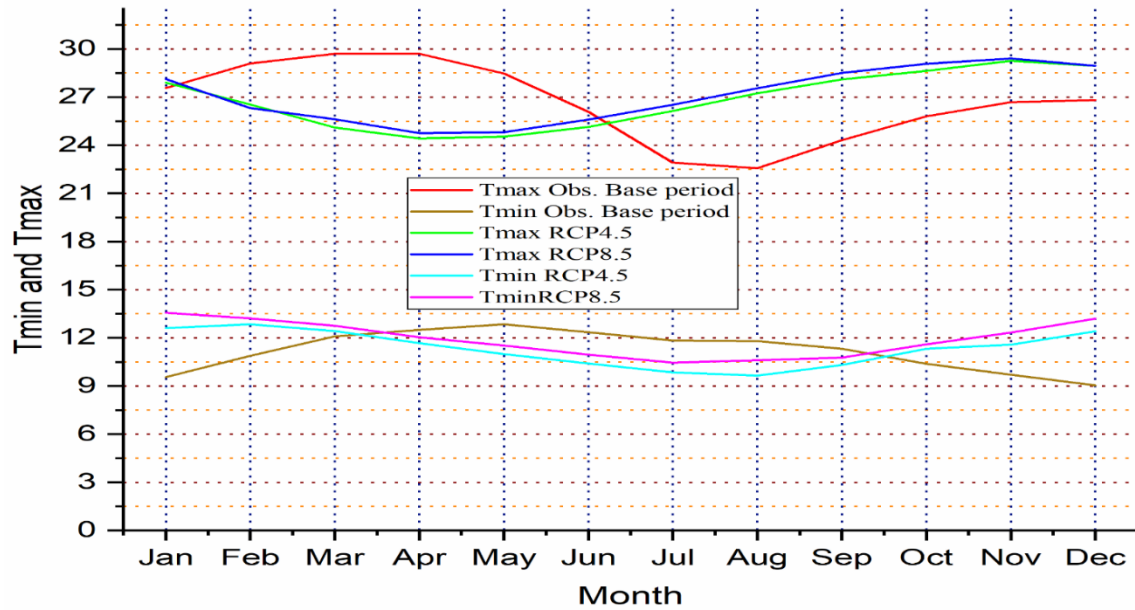
Figure 4. 14 Trend analysis on Mean monthly scale for observed and Projected (2025-2054) Maximum and Minimum Temperature

Table 4. 12 Parametric statistical values for trend test of Monthly Projected (2025-2054) Maximum Temperature RCP4.5 and RCP8.5

RCP4.5												
	Jan	Feb	Mar	Apr	May	Jun	Jul	Aug	Sep	Oct	Nov	Dec
Kendall's tau	-0.591	-0.761	-0.430	0.186	0.710	0.784	0.766	0.724	0.674	0.664	0.361	-0.218
S	-257.000	-331.000	-187.000	81.000	309.000	341.000	333.000	315.000	293.000	289.000	157.000	-95.000
Var(S)	3141.667	3141.667	3141.667	3141.667	3141.667	3141.667	3141.667	3141.667	3141.667	3141.667	3141.667	3141.667
p	< 0.0001	< 0.0001	0.001	0.153	< 0.0001	< 0.0001	< 0.0001	< 0.0001	< 0.0001	< 0.0001	0.005	0.094
α	0.05	0.05	0.05	0.05	0.05	0.05	0.05	0.05	0.05	0.05	0.05	0.05

Sen's slope	-0.261	-0.351	-0.210	0.064	0.209	0.227	0.175	0.165	0.188	0.175	0.105	-0.101
RCP8.5												
Kendall's tau	-0.586	-0.747	-0.490	0.145	0.692	0.798	0.793	0.761	0.834	0.747	0.375	-0.182
S	-255.000	-325.000	-213.000	63.000	301.000	347.000	345.000	331.000	363.000	325.000	163.000	-79.000
Var(S)	3141.667	3141.667	3141.667	3141.667	3141.667	3141.667	3141.667	3141.667	3141.667	3141.667	3141.667	3141.667
p	< 0.0001	< 0.0001	0.000	0.269	< 0.0001	< 0.0001	< 0.0001	< 0.0001	< 0.0001	< 0.0001	0.004	0.164
α	0.05	0.05	0.05	0.05	0.05	0.05	0.05	0.05	0.05	0.05	0.05	0.05
Sen's slope	-0.269	-0.295	-0.245	0.068	0.202	0.245	0.192	0.163	0.219	0.210	0.119	-0.097

Table 4. 13 Parametric statistical values for trend test of Monthly Projected (2025-2054) Minimum Temperature RCP4.5 and RCP8.5

	RCP4.5											
	Jan	Feb	Mar	Apr	May	Jun	Jul	Aug	Sep	Oct	Nov	Dec
Kendall's tau	0.149	-0.172	-0.182	-0.457	-0.485	-0.545	-0.310	0.241	0.614	0.687	0.646	0.439
S	65.000	-75.000	-79.000	-199.000	-211.000	-237.000	-135.000	105.000	267.000	299.000	281.000	191.000
Var(S)	3141.667	3141.667	3141.667	3141.667	3141.667	3141.667	3141.667	3141.667	3141.667	3141.667	3141.667	3141.667

p	0.254	0.187	0.164	0.000	0.000	<0.0001	0.017	0.064	<0.0001	<0.0001	<0.0001	0.001
α	0.05	0.05	0.05	0.05	0.05	0.05	0.05	0.05	0.05	0.05	0.05	0.05
Sen's slope	0.025	-0.018	-0.013	-0.069	-0.078	-0.077	-0.061	0.056	0.158	0.209	0.224	0.124
RCP8.5												
Kendall's tau	0.117	-0.186	-0.034	-0.508	-0.439	-0.508	-0.145	0.402	0.591	0.683	0.724	0.434
S	51.000	-81.000	-15.000	-221.000	-191.000	-221.000	-63.000	175.000	257.000	297.000	315.000	189.000
Var(S)	3141.667	3141.667	3141.667	3141.667	3141.667	3141.667	3141.667	3141.667	3141.667	3141.667	3141.667	3141.667
p	0.372	0.153	0.803	<0.0001	0.001	<0.0001	0.269	0.002	<0.0001	<0.0001	<0.0001	0.001
α	0.05	0.05	0.05	0.05	0.05	0.05	0.05	0.05	0.05	0.05	0.05	0.05
Sen's slope	0.019	-0.020	-0.003	-0.049	-0.077	-0.084	-0.029	0.074	0.177	0.229	0.222	0.096

Figure 4. 15Trend analysis on Seasonal scale for observed and projected (2025-2054) Temperature

Table 4. 14 Parametric statistical values for trend test of Seasonal Observed and Projected (2025-2054) Maximum and Minimum Temperature

Maximum Temperature						
	Kendall's tau	S	Var(S)	p	α	Sen's slope
Spring	0.085	37	3141.667	0.521	0.05	0.013
Summer	0.343	149	3141.667	0.008	0.05	0.04
Autumn	0.251	109	3141.667	0.054	0.05	0.027
Winter	-0.039	-17	3141.667	0.775	0.05	-0.005
Minimum Temperature						
Spring	0.168	73	3141.667	0.199	0.05	0.024
Summer	0.071	31	3141.667	0.592	0.05	0.008
Autumn	0.057	25	3141.667	0.669	0.05	0.006
Winter	-0.108	-47	3141.667	0.412	0.05	-0.01
Maximum Temperature RCP4.5						
Spring	0.117	51	3141.667	0.372	0.05	0.032
Summer	0.867	377	3141.667	< 0.0001	0.05	0.188

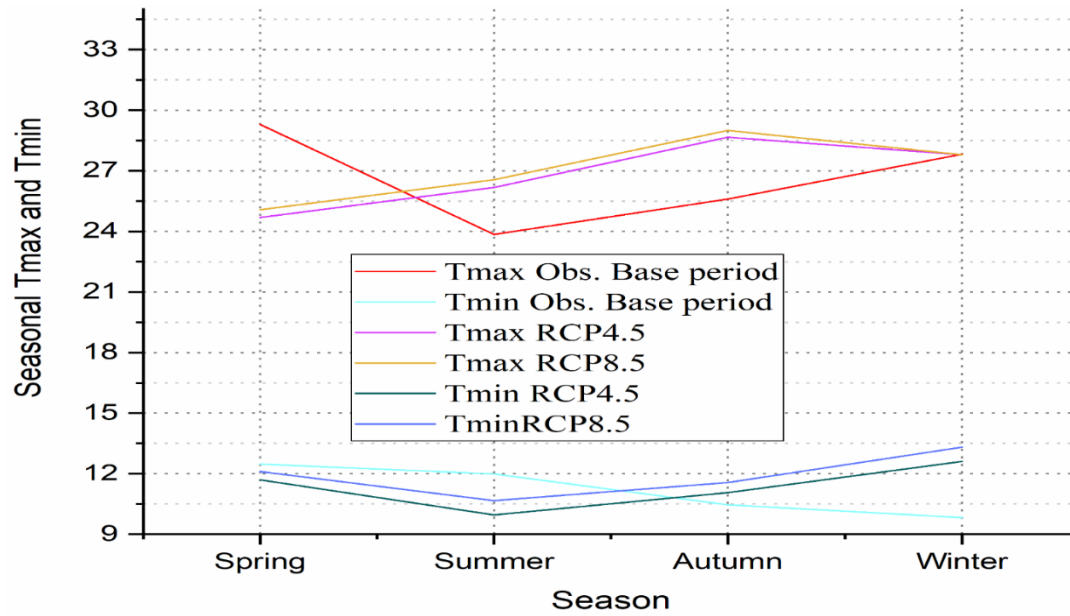|						
Autumn	0.752	327	3141.667	< 0.0001	0.05	0.147
Winter	-0.747	-325	3141.667	< 0.0001	0.05	-0.262
Maximum Temperature RCP8.5						
Spring	0.03	13	3141.667	0.83	0.05	0.009
Summer	0.839	365	3141.667	< 0.0001	0.05	0.201
Autumn	0.779	339	3141.667	< 0.0001	0.05	0.18
Winter	-0.733	-319	3141.667	< 0.0001	0.05	-0.23
Minimum Temperature RCP4.5						
Spring	-0.536	-233	3141.667	< 0.0001	0.05	-0.049
Summer	-0.251	-109	3141.667	0.054	0.05	-0.036
Autumn	0.793	345	3141.667	< 0.0001	0.05	0.203
Winter	0.301	131	3141.667	0.02	0.05	0.038
Minimum Temperature RCP8.5						
Spring	-0.6	-261	3141.667	< 0.0001	0.05	-0.051
Summer	-0.108	-47	3141.667	0.412	0.05	-0.012
Autumn	0.844	367	3141.667	< 0.0001	0.05	0.21
Winter	0.246	107	3141.667	0.059	0.05	0.035
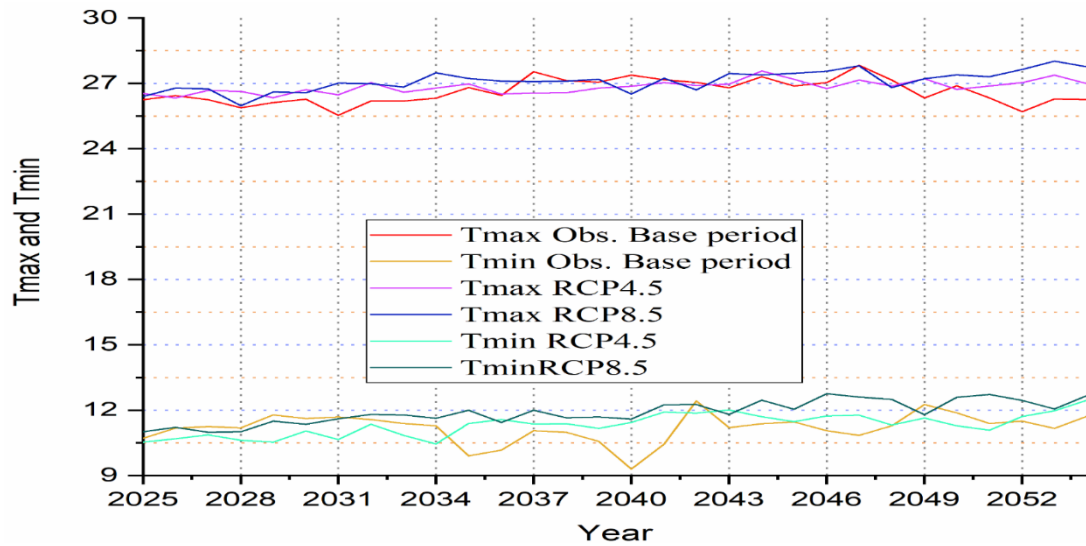
Figure 4. 16 Trend analysis on Seasonal scale for observed and projected (2025-2054) Temperature

Table 4. 15 Parametric statistical values for trend test of Annual Projected (2025-2054) Maximum and Minimum Temperature

	Kendall's tau	S	Var(S)	p	α	Sen's slope
Tmax Obs.	0.214	93	3141.67	0.101	0.05	0.019
Tmin Obs.	0.122	53	3141.67	0.354	0.05	0.01
Max.T RCP4.5	0.503	219	3141.67	0.00	0.05	0.023
Max.T RCP8.5	0.577	251	3141.67	< 0.0001	0.05	0.039
Min.T RCP4.5	0.526	229.000	3141.667	< 0.0001	0.05	0.046
Min.T RCP8.5	0.547	231	3141.667	< 0.0001	0.05	0.053

Temperatures in the near future (2025–2054) examined for RCP4.5 and RCP8.5 on a monthly, yearly, and seasonal basis. RCP4.5 on a monthly time scale, the maximum temperature indicates a significant rising trend from May to October (Table 4.12, Figure 4.14). Others show declining trend in January, February and March, while April and December show an insignificant growing and falling tendency, respectively. RCP8.5 indicates a considerable growing trend for May, June, July, August, September, October, and November. There is a significant increasing tendency for January, February, and March, whereas April and December exhibit small growing and falling trends (Table 4.13, Figure 4.14). RCP4.5 indicates a substantial rising trend for the maximum seasonal temperature for summer and autumn. Spring and winter exhibit minor growing and falling tendencies. RCP8.5 demonstrates a significant growing tendency for summer and autumn. Spring and winter exhibit negligible growing and falling trends, respectively (Table 14, Figure 4.15). The annual maximum temperature for both RCP4.5 and RCP8.5 indicates growing trend (Table 15, Figure 4.16). On RCP4.5, the minimum temperature on a monthly basis indicates a considerable growing tendency for September, October, November, and December, but an insignificant increasing trend for January. A significant declining trend realized in April, May, June, and July. A minor declining trend seen in February and March. RCP4,5 has a significant rising tendency in the autumn and winter. There was a falling trend in spring, and in summer, there was an insignificant decreasing trend (Table 4.14, Figure 4.15). RCP4.5 has a significant growing trend magnitude of on an annual basis, while RCP8.5 has a significant increasing trend (Mengistu *et al*., 2021), Worku *et al*., 2020), indicated that the maximum temperature across the Abay basin would rise in the future. This study also supports the rise

in Maximum and Lowest Temperatures since Ribb is one of the watersheds located in the Abay basin, and according to (Tekleab *et al.*, 2013), the minimum temperature exhibits the most significant growth trend.
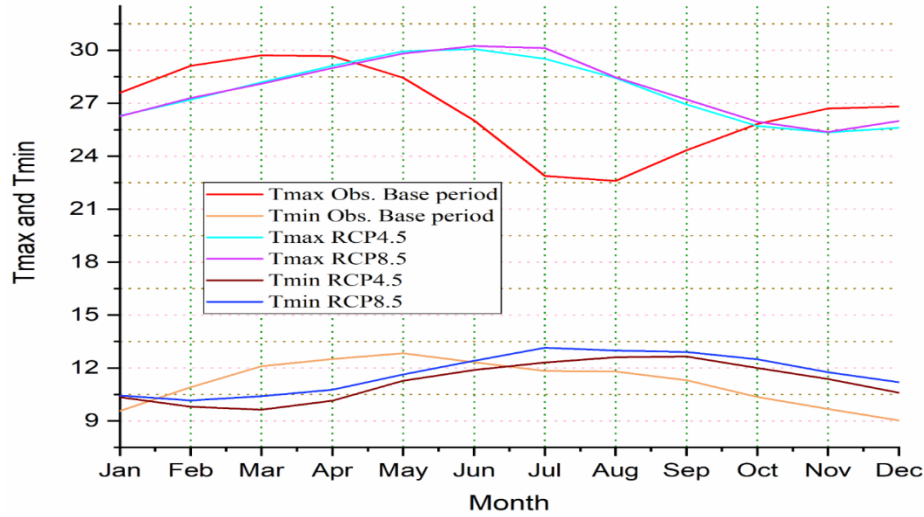
Figure 4. 17 Trend analysis on Mean monthly scale for observed and Projected (2055-2084) maximum and minimum temperature

Table 4. 16 Parametric statistical values for trend test of monthly Projected (2055-2084) Maximum temperature RCP4.5 and RCP8.5

	RCP4.5											
	Jan	Feb	Mar	Apr	May	Jun	Jul	Aug	Sep	Oct	Nov	Dec
Kendall's tau	0.669	0.724	0.752	0.784	0.761	0.297	-0.356	-0.697	-0.706	-0.278	0.393	0.637
S	291.000	315.000	327.000	341.000	331.000	129.000	-155.000	-303.000	-307.000	-121.000	171.000	277.000
Var(S)	3141.667	3141.667	3141.667	3141.667	3141.667	3141.667	3141.667	3141.667	3141.667	3141.667	3141.667	3141.667
p	< 0.0001	< 0.0001	< 0.0001	< 0.0001	< 0.0001	0.022	0.006	< 0.0001	< 0.0001	0.032	0.002	< 0.0001

	0.05	0.05	0.05	0.05	0.05	0.05	0.05	0.05	0.05	0.05	0.05	0.05
α												
Sen's slope	0.197	0.167	0.144	0.197	0.216	0.099	-0.162	-0.351	-0.337	-0.125	0.132	0.191
RCP8.5												
Kendall's tau	0.807	0.811	0.733	0.807	0.669	0.467	-0.094	-0.614	-0.632	-0.274	0.407	0.770
S	351.000	353.000	319.000	351.000	291.000	203.000	-41.000	-267.000	-275.000	-119.000	177.000	335.000
Var(S)	3141.667	3141.667	3141.667	3141.667	3141.667	3141.667	3141.667	3141.667	3141.667	3141.667	3141.667	3141.667
p	< 0.0001	< 0.0001	< 0.0001	< 0.0001	< 0.0001	0.000	0.475	< 0.0001	< 0.0001	0.035	0.002	< 0.0001
α	0.05	0.05	0.05	0.05	0.05	0.05	0.05	0.05	0.05	0.05	0.05	0.05
Sen's slope	0.230	0.202	0.174	0.206	0.196	0.163	-0.044	-0.288	-0.259	-0.128	0.120	0.240

Table 4. 17 Parametric statistical values for trend test of monthly Projected (2055-2084) Minimum temperature RCP4.5 and RCP8.5

RCP4.5												
	Jan	Feb	Mar	Apr	May	Jun	Jul	Aug	Sep	Oct	Nov	Dec
Kendall's tau	-0.522	-0.283	0.347	0.614	0.752	0.669	0.398	-0.200	-0.549	-0.540	-0.651	-0.582
S	-227.000	-123.000	151.000	267.000	327.000	291.000	173.000	-87.000	-239.000	-235.000	-283.000	-253.000
Var(S)	3141.667	3141.667	3141.667	3141.667	3141.667	3141.667	3141.667	3141.667	3141.667	3141.667	3141.667	3141.667
p	< 0.0001	0.030	0.007	< 0.0001	< 0.0001	< 0.0001	0.002	0.125	< 0.0001	< 0.0001	< 0.0001	< 0.0001
α	0.05	0.05	0.05	0.05	0.05	0.05	0.05	0.05	0.05	0.05	0.05	0.05
Sen's slope	-0.091	-0.059	0.082	0.177	0.228	0.247	0.105	-0.019	-0.051	-0.065	-0.092	-0.081
RCP8.5												
Kendall's tau	-0.352	0.048	0.600	0.752	0.743	0.697	0.545	0.126	0.011	-0.126	-0.338	-0.347
S	-153.000	21.000	261.000	327.000	323.000	303.000	237.000	55.000	5.000	-55.000	-147.000	-151.000
Var(S)	3141.667	3141.667	3141.667	3141.667	3141.667	3141.667	3141.667	3141.667	3141.667	3141.667	3141.667	3141.667
p	0.007	0.721	< 0.0001	< 0.0001	< 0.0001	< 0.0001	< 0.0001	0.335	0.943	0.335	0.009	0.007

α	0.05	0.05	0.05	0.05	0.05	0.05	0.05	0.05	0.05	0.05	0.05	0.05
Sen's slope	-0.062	0.020	0.150	0.247	0.277	0.230	0.118	0.033	0.001	-0.010	-0.050	-0.050
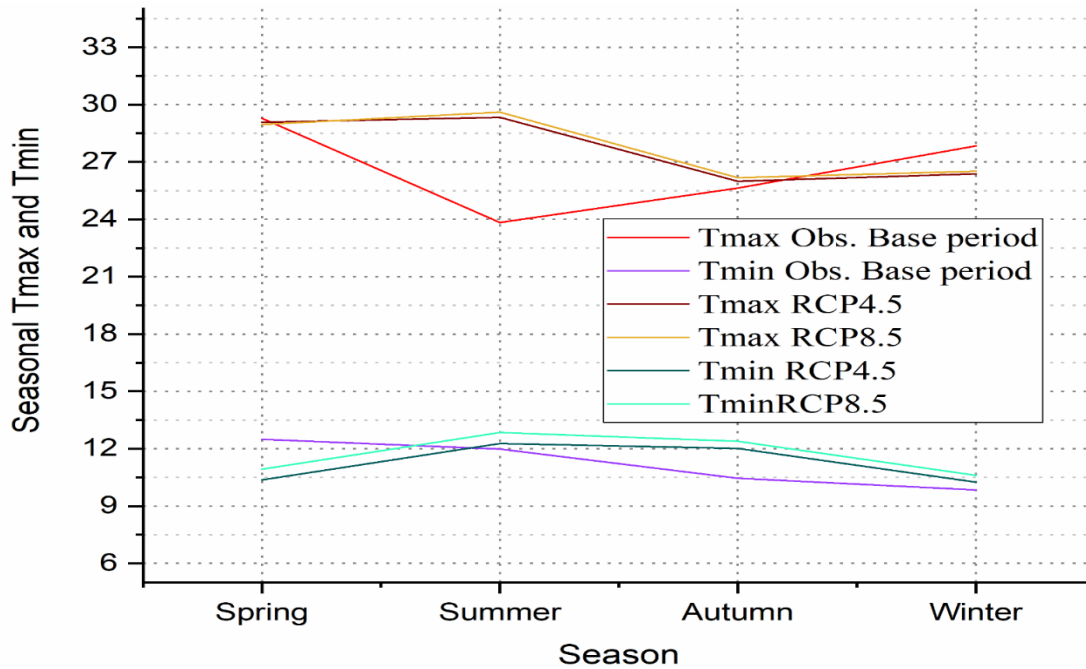
Figure 4. 18 Trend analysis on Seasonal scale for observed and Projected (2055-2084) maximum and minimum temperature

Table 4. 18 Parametric statistical values for trend test of Seasonal Projected (2055-2084) Maximum and Minimum temperature RCP4.5 and RCP8.5

	Kendall's tau	S	Var(S)	p	α	Sen's slope
RCP4.5						
Spring	0.890	387.000	3141.667	< 0.0001	0.05	0.180
Summer	-0.370	-161.000	3141.667	0.004	0.05	-0.150
Autumn	-0.352	-153.000	3141.667	0.007	0.05	-0.124
Winter	0.710	309.000	3141.667	< 0.0001	0.05	0.181
RCP8.5						
Spring	0.821	357.000	3141.667	< 0.0001	0.05	0.197
Summer	-0.251	-109.000	3141.667	0.054	0.05	-0.069

|						
Autumn	-0.329	-143.000	3141.667	0.011	0.05	-0.093
Winter	0.844	367.000	3141.667	< 0.0001	0.05	0.207
RCP4.5						
Spring	0.687	299.000	3141.667	< 0.0001	0.05	0.164
Summer	0.490	213.000	3141.667	0.000	0.05	0.109
Autumn	-0.715	-311.000	3141.667	< 0.0001	0.05	-0.071
Winter	-0.605	-263.000	3141.667	< 0.0001	0.05	-0.078
RCP8.5						
Spring	0.761	331.000	3141.667	< 0.0001	0.05	0.195
Summer	0.614	267.000	3141.667	< 0.0001	0.05	0.136
Autumn	-0.384	-167.000	3141.667	0.003	0.05	-0.023
Winter	-0.333	-145.000	3141.667	0.010	0.05	-0.038
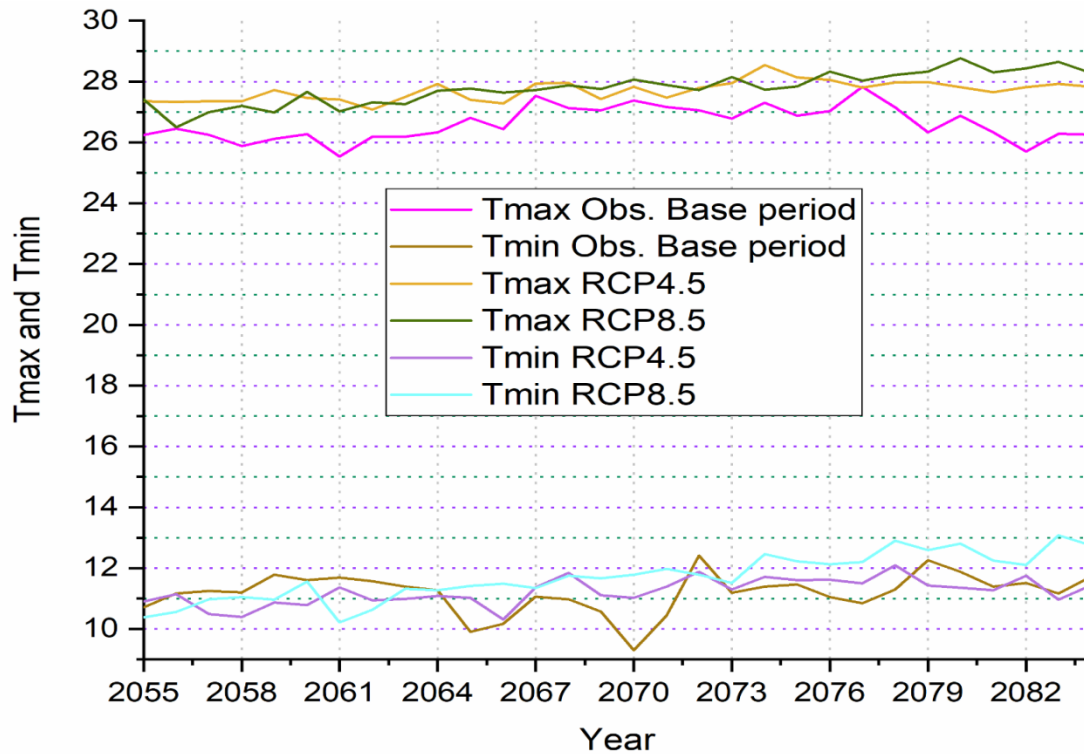
Figure 4. 19 Trend analysis on Annual scale for observed and Projected (2055-2084) maximum and minimum temperature

Table 4. 19 Parametric statistical values for trend test of Projected (2055-2084) Annual Maximum and Minimum temperature RCP4.5 and RCP8.5

	Kendall's tau	S	Var(S)	p	α	Sen's slope
Max.T RCP4.5	0.448	195.000	3141.667	0.001	0.05	0.020
Max.T RCP8.5	0.761	331.000	3141.667	< 0.0001	0.05	0.053
Min.T RCP4.5	0.434	189.000	3141.667	0.001	0.05	0.028
Min.T RCP8.5	0.766	333.000	3141.667	< 0.0001	0.05	0.078

RCP4.5 indicates increasing tendency for the long-term (2055–2084) maximum temperature in the months of January, February, March, April, May, November, December. A significant declining trend observed in July, August, September, and October. RCP8.5 indicates a considerable increase for the months of January, February, March, April, May, June, November, and December. August, September, and October showed significant declining trend, whereas July showed an insignificant change (Table 4.16, Figure 4.17). RCP4.5 indicates a significant rising trend in minimum temperatures for March, April, May, June. The other months show a substantial declining tendency. From March to July, RCP8.5 indicates increasing trend. In May, there is upward tendency. For the next months, there is a falling tendency in January, November, and December (Table 4.17, Figure 4.17). Seasonally, RCP4.5 shows a significant increasing trend for spring and winter, whereas summer and autumn show a significant decreasing trend on maximum temperature. Minimum temperature tends to increase significantly on seasons spring and autumn. Season's autumn and winter decrease significantly. RCP8.5 on maximum temperature shows a significant increasing trend in spring and winter. Summer shows an insignificant decreasing trend and autumn significant decreasing trend. RCP8.5 on minimum temperature shows a significant increasing trend for spring and summer. Autumn and winter show a significant decreasing trend (Table 4.18, Figure 4.18). RCP4.5 and RCP8.5 show a t increasing trend for both maximum Temperature and minimum Temperature annually (Table 4.19, Figure 4.19). (Getachew and Manjunatha, 2021 and Mengistu et al., 2021) also found that long-term temperature will tend to increase over the upper Blue Nile basin.

4.4 Impact of climate change on future Mean Monthly, Seasonal and Annual stream flow

The impact of climate change on Ribb River has assessed by forecasting the future two-time horizons near term (2025-2054) and long-term (2055-2084) using bias-corrected RCP4.5 and RCP8.5 precipitation and temperature from the RCM KNMI-RACMO22T model, which performs best for the Ribb watershed. It is extremely useful to know the magnitude of a watershed's streamflow to reach and carry out many Engineering judgments on the river. The climate change on streamflow is visible on the Ribb watershed. It has studied on Mean Month, Annually, and Seasonal time steps. As noted over section 4.2, Precipitation decreases and Temperature increases for both RCP4.5 and RCP8.5 Mean Monthly, Seasonally, and annually compared to the observed historical period, which has related to the reduction in streamflow of the future.

4.4.1 Impact of climate change on simulated Mean Monthly stream flow

The simulated mean monthly streamflow in the near term (2025-2054) shows increasing change on both RCP4.5 and RCP8.5 in mean monthly streamflow for the months from December-June in which the highest increase is shown in April ($26.16m^3$/s), May ($25.29m^3$/s) for RCP4.5 and April ($24.39m^3$/s), May ($23.08m^3$/s) for RCP8.5. The decreasing change was shown in the months from July-October, and in the months August (-$46.52m^3$/s), September (-$32.47m^3$/s) for RCP4.5 and September (-$49.43m^3$/s), October (-31.61) for RCP8.5, the highest decreasing change was recorded. On the long-term time step (2055-2084), the months from Dec-Mar show an increase in the mean monthly stream for RCP4.5, with Oct ($25.11m^3$/s) and November ($27.80m^3$/s) having the highest streamflow increment. Months from April to September show decreasing streamflow, with July ($24.25m^3$/s) and August ($42.85m3$/s) having the highest decrease on RCP4.5. RCP8.5 shows increased streamflow change months from December to April, with October ($25.79m^3$/s) and November (m^3/s) having the highest magnitude increase. Months from May-September show decreasing streamflow, in which July ($30.40m^3$/s) and August ($43.86m^3$/s) show the highest decrease (Figure 4.20). In this study, some months show increasing streamflow which agrees with the investigations of (Dile *et al*., 2013); for the mid-and long-term of the twenty-first century, the monthly mean volume of runoff in the Gilgelabay catchment appears to be growing considerably (up to 135%). In contrast to (Dile *et al*., 2013), (Abdo *et al*., 2009) reported

reductions in monthly mean runoff in the same watershed, and this inquiry is accepted in this study for certain months.

Figure 4. 20 The change in Mean Monthly stream flow (2025-2084)

4.4.2 Impact of climate change on simulated Seasonal stream flow

The impact of climate change has assessed on simulated seasonal streamflow. The near term (2025–2054) shows increasing streamflow during spring on RCP4.5 and small decreasing streamflow on RCP8.5. Summer shows decreasing streamflow for both RCPs in the near and long term. Autumn shows decreasing streamflow for RCP4.5 and an increase for RCP8.5. Season winter shows increasing streamflow for both RCP4.5 and RCP8.5's two-time horizons (Figure 4.21). Here, the increasing and decreasing of seasonal streamflow has directly related to the seasonal rainfall pattern (section 4.2.1).
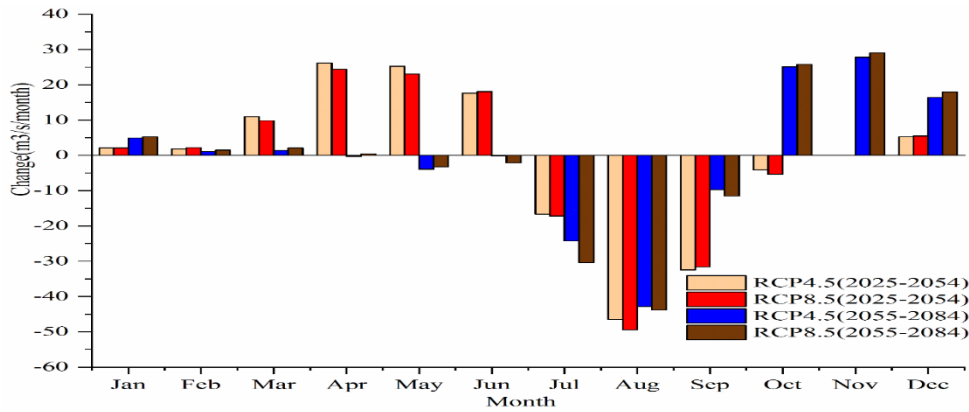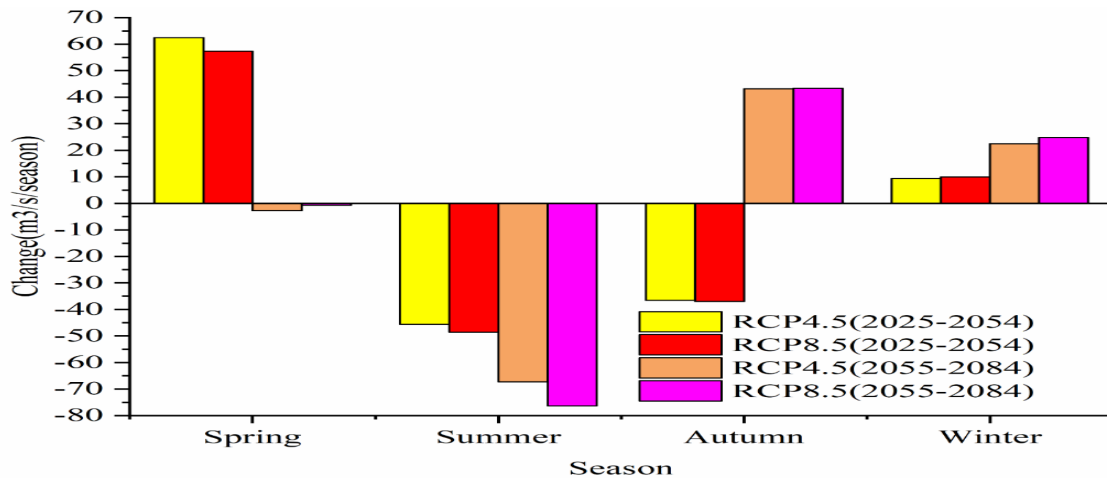

Figure 4. 21 The change in Seasonal stream flow (2025-2084)

4.4.3 Impact of climate change on simulated Annual stream flow

On the two-time horizons, annual simulated streamflow reveals declining streamflow for RCP4.5 and RCP8.5. The graph below shows that the decreasing change in the comparable period (2025-2054) is around 4.93 percent for RCP4.5 and 8.48 percent for RCP8.5. For the long-term time step (2055-2084), RCP4.5 decreased by 2.27 percent, and RCP8.5 decreased by 4.32 percent (Figure 4.22). According to (Koch and Cherie, 2013), the flow of the Upper Blue Nile is anticipated to reduce by 10 to 61 percent between the 2050s and 2090s compared to the average flow of the twentieth century (Taye *et al.,* 2011). In addition, the researchers looked at the future development of streamflow in the Lake Tana watershed in the context of climate change. According to this study, streamflow increases and decreases (-75 to 81 percent) are expected in numerous Upper Blue Nile Basin catchments during the 2050s. The study's findings support one of the catchments where streamflow has expected to decline in the future. (Worqlul *et al.,* 2018) found a decrease in the annual flow of the upper Abay Basin. The impact of climate change hydrology of the Ribb watershed was studied by (Ayalew, D.W., 2019) using SWAT simulated stream flow, and the results revealed that the Ribb streamflow will decrease in the future and it is supportive investigation for this specific research except the decreasing in magnitude.
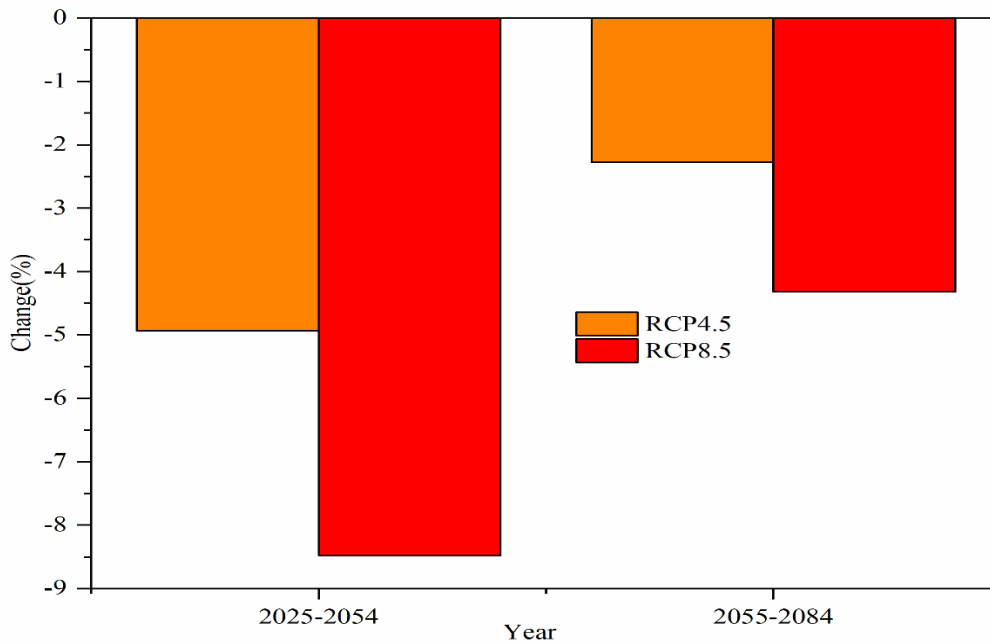

Figure 4. 22 The Annual change of stream flow (2025-2084)

4.5 Impact of climate change on extreme flows on the future time horizon

Flow duration curve estimates are frequently used to quantify hydrologic regimes(Kim and Kaluarachchi, 2009). The stream's discharge is shown against the percentage of the time the flow was equaled or surpassed on a flow-duration curve. If the number of individual values is quite big, the streamflow data is sorted in descending order of discharges using class intervals. For example, daily, weekly, ten daily or monthly values might be employed. If this listing has N data points, the plotting location of any discharge (or category value) Q is:

$$Pp = \frac{m}{N+1} * 100\%$$

Pp = percentage likelihood of the flow magnitude being equaled or surpassed, where m is the discharge's order number (or class value). For this study, 90% and 10% flow exceedance probabilities have used to describe low and high flow circumstances, respectively.

For both RCPs, the climate change impact has considered on Q10 and Q90 probability exceedance. Under these climate scenarios, there is a clear decrease in high flows (Q10) and an increase in low flows (Q90) (Figure 4.18 and Table 4.19). (Meresa and Gatachew, 2019) investigated that low flow rates are expected to rise the greatest, and this study is related. (Dile *et al*., 2013) also investigated that these extremes have been steadily growing in recent years. Changes in high flow (Q10) range from -36.20 to -34.07 and -36.06 to -34.85 in the near and long futures for RCP4.5 and RCP8.5, respectively, whereas changes in low flow (Q90) range from 2.37 to 1.09 and 2.40 to 1.39 in the near and long futures for RCP4.5 and RCP8.5, respectively (Figure 4.23 and Figure 4.24, Table 4.20).

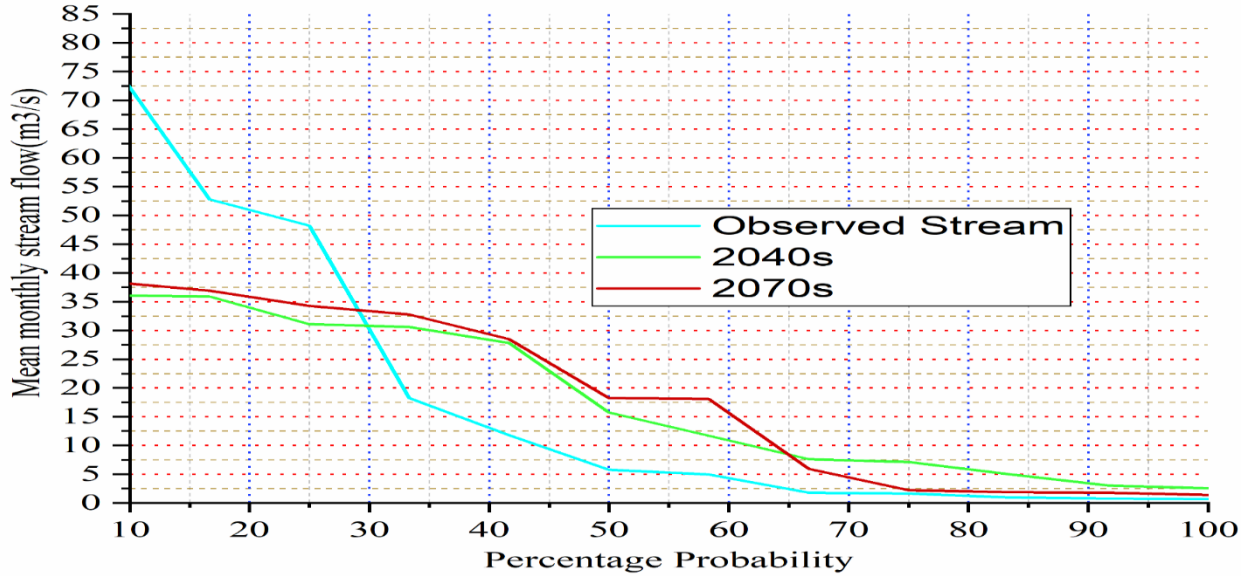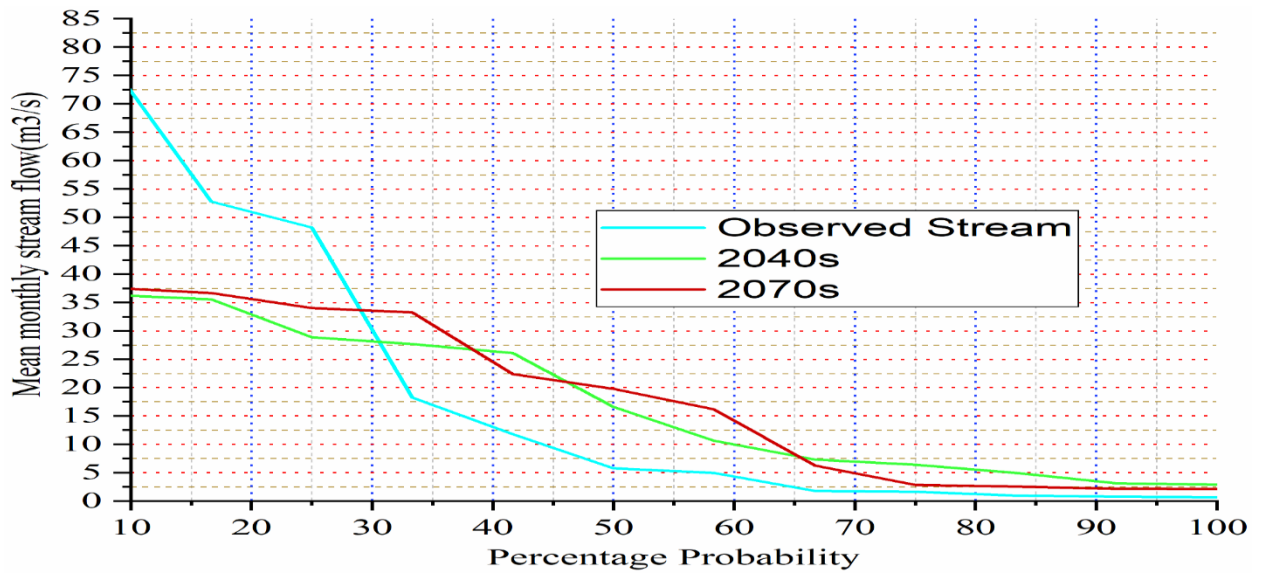Figure 4. 23 Flow Duration Curve to Analyze High Flow and Low Flow under RCP4.5

Figure 4. 24 Flow Duration Curve to Analyze High Flow and Low Flow under RCP8.5

Table 4. 20 Changes on Extreme flows under Climate change impact

	2025-2054		2055-2084	
	Q_{10}	Q_{90}	Q_{10}	Q_{90}
RCP4.5	-36.20	2.37	-34.07	1.09
RCP8.5	-36.06	2.40	-34.85	1.39

5. CONCLUSION AND RECOMMENDATIONS

5.1 CONCLUSION

This investigation employs bias-corrected climate data (precipitation and temperature) and HEC-HMS 4.7.1 based hydrological simulation to measure streamflow change in the Ribb watershed under climate change. The HEC-HMS 4.7.1 calibration and validation results showed that the model accurately predicted future Ribb watershed streamflow. The coefficient of determination (R^2) and Nash Sutcliffe (NSE) values for calibration were 0.89, 0.86, and for validation 0.86, and 0.84, respectively, which are considered satisfactory. Mean monthly, seasonal, and annual time scales analyzed precipitation and temperature trends, and they show decreasing and increasing trends for both the RCP4.5 and RCP8.5 scenarios in near-term and long-term time steps, but when compared to observed historical data, the magnitude of the decrease is high. However, on a near-term time scale, RCP4.5 shows a significant maximum mean monthly increase and decrease in precipitation for December and May, respectively, while RCP8.5 shows maximum increases and decreases for August and May, correspondingly. Summer and spring show decreasing trends for RCP4.5 and RCP8.5, respectively. Annually, the near-term time horizon shows a decreasing trend for RCP4.5 and RCP8.5. For the long-term time step, the months of September and June show the highest mean monthly increase and decrease, respectively, for RCP4.5 and RCP8.5. Autumn and summer show a high increase and a decrease, respectively, for both scenarios, whereas RCP4.5 shows a decrease, but RCP8.5 shows an increasing change annually.

Maximum and minimum temperatures show an increase in magnitude for both RCP4.5 and RCP8.5 compared to the observed data. The near-term maximum temperature shows increasing and decreasing changes in June and February for RCP4.5 and RCP8.4, respectively, whereas the minimum temperature shows November and June for RCP4.5 and October and June for RCP8.5. RCP4.5 and RCP8.5 show an increasing and decreasing trend in maximum temperatures in the summer and winter seasons, respectively. Long-term Maximum temperature increases and decreases in June and August for RCP4.5 and RCP8.5, respectively, while Minimum Temperature increases in June and November for both scenarios. Winter shows the increasing change for RCP4.5 and RCP8.5. However, summer shows decreasing change for RCP4.5 and autumn for RCP8.5. Long-term maximum and minimum temperatures show an overall increase in magnitude compared to the Ribb

watershed temperature. As the main objective, the streamflow change over the Ribb watershed under climate change was analyzed on a mean monthly, seasonally, and annual time scale. In this research, the change in streamflow was in line with precipitation and temperature. Overall, precipitation decreased, and temperature decreased compared to observed data. In the near-term time step, the mean monthly streamflow was greater in April than in August, the highest decreasing stream measured for RCP4.5 and RCP8.5. Summer and spring shows were decreasing and increasing flows for RCP4.5 and RCP8.5. For the long-time step, November and August show an increase and a decrease in flow, respectively, for both scenarios. Autumn and summer predict an increase and a decrease in both RCPs in the long term. Annually, the forecasted flow shows decreasing change for both RCPs in the near future and the far future. Extreme flows of Ribb were examined using the Flow duration (Discharge Frequency) Curve. The result from FDC shows increasing for low flows and decreasing high flows.

5.2 RECOMMENDATIONS

This research presupposes that the area's land use/land cover data is constant, whereas it is not. Therefore, future research should address the influence of land use/cover changes on streamflow. In addition to the impacts of land use/land cover, many factors will impact stream flows of a watershed in which this study does not explicitly include; examples include soil type, Evapotranspiration, and imperviousness.

Because the influence of silt on streamflow was not considered in this study, other researchers can enhance it by including it in future studies of climate change's impact on watershed hydrology.

Future streamflow decreased for two-time horizons: 2025-2054 and 2055-2084. As a result, populations of the Ribb watershed will need to put in more effort to preserve water during the rainy or summer seasons to continue using irrigation and other agricultural and water resource development throughout the stated future time horizons.

This study depicts the future streamflow magnitude for the Ribb watershed for the two scenarios, RCP4.5 and RCP8.5, but does not consider the socioeconomic activity and its effects on the flow. As a result, the findings of this study should be interpreted with caution and regarded as a guideline for further research rather than precise forecast.

REFERENCES

Aawar, T. And D. Khare (2020). "Assessment of climate change impacts on streamflow through hydrological model using SWAT model: a case study of Afghanistan." Modeling Earth Systems and Environment 6(3): 1427-1437.

Addor, N. And L. Melsen (2019). "Legacy, rather than adequacy, drives the selection of hydrological models." Water resources research 55(1): 378-390.

Adem, A. And W. Bewket (2011). A climate change country assessment report for Ethiopia. Forum for Environment (ECSNCC).

Adem A. et al. (2014) Climate Change Projections in the Upper Gilgel Abay River Catchment, Blue Nile Basin Ethiopia. In: Melesse A., Abtew W., Setegn S. (eds) Nile River Basin. Springer, Cham.

Aerts, J. And P. Droogers (2004). "Climate Change in contrasting river basins." Adaptation strategies for water for food and water for the environment, CABI, Wallingfort.

Ahmadi, H. And J. Azizzadeh (2020). "The impacts of climate change based on regional and global climate models (rcms and gcms) projections (case study: Ilam province)." Modeling Earth Systems and Environment 6(2): 685-696.

Aliye, M.A., Aga, A.O., Tadesse, T. and Yohannes, P., 2020. Evaluating the performance of HEC-HMS and SWAT hydrological models in simulating the rainfall-runoff process for data scarce region of Ethiopian Rift Valley Lake Basin. Open Journal of Modern Hydrology, 10(04), p.105.

Asitatikie, A. N. And E. Tabor (2020). "Land Use/Land Cover Dynamics in Upper Ribb Watershed, Lake Tana Sub Basin, Ethiopia."

Ayalew, D.W., 2019. Evaluating the Potential Impact of Climate Change on the Hydrology of Ribb Catchment, Blue Nile Basin, Ethiopia (Master's thesis).

Bartolini, S., Massai, R., Iacona, C., Guerriero, R. and Viti, R., 2019. Forty-year investigations on apricot

Behulu, F., Mutua, B.M., Gadissa, T. and Nyadawa, M., 2018. The effect of climate change on loss of lake volume: case of sedimentation in central rift valley basin, Ethiopia.

Berhanu, D. (2018). "Performance of bias correction methods for hydrological impact study in Lake Tana sub-basin."

Beyene, T., Lettenmaier, D.P. and Kabat, P., 2010. Hydrologic impacts of climate change on the Nile River Basin: implications of the 2007 IPCC scenarios. Climatic change, 100(3), pp.433-461.

Bjørnæs, C. 2013. "A guide to representative concentration pathways." CICERO. Center for International Climate and Environmental Research: 351-357.

Bürger, C.M., Kolditz, O., Fowler, H.J. and Blenkinsop, S., 2007. Future climate scenarios and rainfall–runoff modelling in the Upper Gallego catchment (Spain). Environmental Pollution, 148(3), pp.842-854.

Chakilu, G.G., Sándor, S. and Zoltán, T., 2020. Change in stream flow of gumara watershed, upper Blue Nile basin, Ethiopia under representative concentration pathway climate change scenarios. Water, 12(11), p.3046.

Conway, D. 2000. "The climate and hydrology of the Upper Blue Nile River." Geographical Journal 166(1): 49-62.

Council, N. R. 2011. Advancing the science of climate change, National Academies Press.

Cunderlik, J. And S. P. Simonovic 2004. Calibration, verification and sensitivity analysis of the HEC-HMS hydrologic model, Department of Civil and Environmental Engineering, The University of Western ….

Dariane, A.B., Bagheri, R., Karami, F. and Javadianzadeh, M.M., 2020. Developing heuristic multi-criteria auto calibration method for continuous HEC-HMS in snow-affected catchment. International Journal of River Basin Management, 18(1), pp.69-80.

Demissie, T. A. And C. H. Sime 2021. "Assessment of the performance of CORDEX regional climate models in simulating rainfall and air temperature over southwest Ethiopia." Heliyon 7(8): e07791.

Deressa, G., Guta, G. and Bushira, K.M., 2022. The Response of Streamflow to Climate Change in Gumera Watershed, Blue Nile River Basin, Ethiopia. CURRENT APPLIED SCIENCE AND TECHNOLOGY, pp.13-pages.

Dibaba, W.T., Miegel, K. and Demissie, T.A., 2019. Evaluation of the CORDEX regional climate models performance in simulating climate conditions of two catchments in Upper Blue Nile Basin. *Dynamics of Atmospheres and Oceans*, *87*, p.101104.

Dile, Y.T., Berndtsson, R. and Setegn, S.G., 2013. Hydrological response to climate change for gilgel abay river, in the lake tana basin-upper blue Nile basin of Ethiopia. PloS one, 8(10), p.e79296.

Duque-Méndez, N.D., Orozco-Alzate, M. and Vélez, J.J., 2014. Hydro-meteorological data analysis using OLAP techniques. Dyna, 81(185), pp.160-167.

Ehret, U., Zehe, E., Wulfmeyer, V., Warrach-Sagi, K. and Liebert, J., 2012. HESS Opinions" Should we apply bias correction to global and regional climate model data?". Hydrology and Earth System Sciences, 16(9), pp.3391-3404.

Ekeu-wei, I.T., Blackburn, G.A. and Pedruco, P., 2018. Infilling missing data in hydrology: Solutions using satellite radar altimetry and multiple imputation for data-sparse regions. Water, 10(10), p.1483.

Elsanabary, M. H. And T. Y. Gan 2015. "Evaluation of climate anomalies impacts on the Upper Blue Nile Basin in Ethiopia using a distributed and a lumped hydrologic model." Journal of Hydrology 530: 225-240.

Endris, H.S., Omondi, P., Jain, S., Lennard, C., Hewitson, B., Chang'a, L., Awange, J.L., Dosio, A., Ketiem, P., Nikulin, G. and Panitz, H.J., 2013. Assessment of the performance of CORDEX regional climate models in simulating East African rainfall. Journal of Climate, 26(21), pp.8453-8475.

Enyew, B.D., Van Lanen, H.A.J. and Van Loon, A.F., 2014. Assessment of the impact of climate change on hydrological drought in Lake Tana catchment, Blue Nile basin, Ethiopia. J. Geol. Geosci, 3, p.174.

Ertuğrul, M., 2019. Future forest fire danger projections using global circulation models (GCM) in Turkey. Fresenius Environmental Bulletin, 28(4), pp.3261-3269.

Evans, J. 2011. CORDEX–An international climate downscaling initiative. 19th international congress on modelling and simulation, Perth, Australia.

Fazzini, M., Bisci, C. and Billi, P., 2015. The climate of Ethiopia. In Landscapes and landforms of Ethiopia (pp. 65-87). Springer, Dordrecht.

Fentaw, F., 2010. Assessment of Climate Change Impacts on the Hydrology of Upper Guder Catchment, Upper Blue Nile.

Fentaw, F., Mekuria, B. and Arega, A., 2018. Impacts of climate change on the water resources of guder catchment, Upper Blue Nile Ethiopia. Waters, 1(1), p.16.

Firat, M., Dikbas, F., Koç, A.C. and Gungor, M., 2010. Missing data analysis and homogeneity test for Turkish precipitation series. Sadhana, 35(6), pp.707-720.

Flato, G., Marotzke, J., Abiodun, B., Braconnot, P., Chou, S.C., Collins, W., Cox, P., Driouech, F., Emori, S., Eyring, V. and Forest, C., 2014. Evaluation of climate models. In Climate change 2013: the physical science basis. Contribution of Working Group I to the Fifth Assessment Report of the Intergovernmental Panel on Climate Change (pp. 741-866). Cambridge University Press.

Fletcher, S. E. M. And H. Schaefer 2019. "Rising methane: A new climate challenge." Science 364(6444): 932-933.

Gao, Y., Merz, C., Lischeid, G. and Schneider, M., 2018. A review on missing hydrological data processing. Environmental earth sciences, 77(2), pp.1-12.

Gebre, S. L. And F. Ludwig 2015. "Hydrological response to climate change of the upper blue Nile River Basin: based on IPCC fifth assessment report (AR5)." Journal of Climatology & Weather Forecasting 3(01): 1-15.

Gebre, S.L., 2015. Application of the HEC-HMS model for runoff simulation of Upper Blue Nile River Basin. *Hydrology: Current Research*, *6*(2), p.1.

Getachew, B. And B. Manjunatha 2021. "Future climate change projection and trends under CMIP5 in Lake Tana basin, Upper Blue Nile River Basin, Ethiopia." Environmental Challenges: 100385.

Gizaw, M.S., Biftu, G.F., Gan, T.Y., Moges, S.A. and Koivusalo, H., 2017. Potential impact of climate change on streamflow of major Ethiopian rivers. Climatic Change, 143(3), pp.371-383.

Gyawali, R. And D. W. Watkins 2013. "Continuous hydrologic modeling of snow-affected watersheds in the Great Lakes basin using HEC-HMS." Journal of Hydrologic Engineering 18(1): 29-39.

Ismail, H., Kamal, M.R., Hin, L.S. and Abdullah, A.F., 2020. Performance of HEC-HMS and ArcSWAT Models for Assessing Climate Change Impacts on Streamflow at Bernam River Basin in Malaysia. Pertanika Journal of Science & Technology, 28(3).

Hewitson, B., Lennard, C., Nikulin, G. and Jones, C., 2012. CORDEX-Africa: a unique opportunity for science and capacity building. CLIVAR Exchanges, 17(3), pp.6-7.

Houghton, D. D. And W. M. Organization 2002. Introduction to climate change: Lecture notes for meteorologists, Secretariat of the World Meteorological Organization Geneva, Switzerland.

Houghton, J.T., Ding, Y.D.J.G., Griggs, D.J., Noguer, M., van der Linden, P.J., Dai, X., Maskell, K. and Johnson, C.A., 2001. Climate change 2001: the scientific basis. The Press Syndicate of the University of Cambridge.

Iturbide, M., Gutiérrez, J.M., Alves, L.M., Bedia, J., Cerezo-Mota, R., Cimadevilla, E., Cofiño, A.S., Di Luca, A., Faria, S.H., Gorodetskaya, I.V. and Hauser, M., 2020. An update of IPCC climate reference regions for subcontinental analysis of climate model data: definition and aggregated datasets. Earth System Science Data, 12(4), pp.2959-2970.

IPCC. 2013. Climate Change 2013, the physical science basis. Cambridge and New York, Cambridge university press

IPCC, 2014. In: Core Writing Team, Pachauri, R.K., Meyer, L.A.(Eds), Climate Change 2014: Synthesis Report. Contribution of Working Groups I, II and III to the Fifth Assessment Report of the Intergovernmental Pannel on Climate Change. IPCC, Geneva, Switzerland

Jiang, Q., Qi, Z., Tang, F., Xue, L. and Bukovsky, M., 2020. Modeling climate change impact on streamflow as affected by snowmelt in Nicolet River Watershed, Quebec. Computers and Electronics in Agriculture, 178, p.105756.

Kaffas, K. And V. Hrissanthou 2014. "Application of a continuous rainfall-runoff model to the basin of Kosynthos river using the hydrologic software HEC-HMS." Glob. NEST J 16(1): 188-203.

Kashani, M. H. And Y. Dinpashoh 2012. "Evaluation of efficiency of different estimation methods for missing climatological data." Stochastic Environmental Research and Risk Assessment 26(1): 59-71.

Kebede, S., Travi, Y., Alemayehu, T. and Marc, V., 2006. Water balance of Lake Tana and its sensitivity to fluctuations in rainfall, Blue Nile basin, Ethiopia. Journal of hydrology, 316(1-4), pp.233-247.

Kim, U. And J. J. Kaluarachchi 2009. "Climate change impacts on water resources in the upper blue Nile River Basin, Ethiopia 1." JAWRA Journal of the American Water Resources Association 45(6): 1361-1378.

Koch, M. And N. Cherie 2013. SWAT modeling of the impact of future climate change on the hydrology and the water resources in the upper Blue Nile River basin, Ethiopia. Proceedings of the 6th International Conference on Water Resources and Environment Research, ICWRER.

Leander, R., Buishand, T.A., van den Hurk, B.J. and de Wit, M.J., 2008. Estimated changes in flood quantiles of the river Meuse from resampling of regional climate model output. Journal of Hydrology, 351(3-4), pp.331-343.

Gebre, S.L., Tadele, K. and Mariam, B.G., 2015. Potential impacts of climate change on the hydrology and water resources availability of Didessa Catchment, Blue Nile River Basin, Ethiopia. J. Geol. Geosci, 4, p.193.

Lenhart, T., Fohrer, N. and Frede, H.G., 2003. Effects of land use changes on the nutrient balance in mesoscale catchments. Physics and Chemistry of the Earth, Parts A/B/C, 28(33-36), pp.1301-1309.

MelkamuTeshomeAyana, N. and Mohammed, A.K., 2018. Assessment of the Impacts of Climate Change on Gibe-III Reservoir Using Reliability, Resilience and Vulnerability (RRV) Indices.

Mengistu, D., Bewket, W., Dosio, A. and Panitz, H.J., 2021. Climate change impacts on water resources in the Upper Blue Nile (Abay) River Basin, Ethiopia. Journal of Hydrology, 592, p.125614.

Meresa, H. K. And M. T. Gatachew 2019. "Climate change impact on river flow extremes in the Upper Blue Nile River basin." Journal of Water and Climate Change 10(4): 759-781.

Negewo, T. F. And A. K. Sarma 2021. "Evaluation of Climate Change-Induced Impact on Streamflow and Sediment Yield of Genale Watershed, Ethiopia."

Negi, J.D.S., Chauhan, P.S. and Negi, M., 2003. Evidences of climate change and its impact on structure and function of forest ecosystems in and around Doon valley. Indian forester, 129(6), pp.757-769.

Khoi, D.N., 2016. Comparision of the HEC-HMS and SWAT hydrological models in simulating the stream flow. Journal of Science and Technology, 53(5A), pp.189-195.

K. S. Abdo; B. M. Fiseha; T. H. M. Rientjes; A. S. M. Gieske; A. T. Haile (2009). Assessment of climate change impacts on the hydrology of Gilgel Abay catchment in Lake Tana basin, Ethiopia. , 23(26), 0–0. doi:10.1002/hyp.7363

Nigatu, Z.M., Rientjes, T. and Haile, A.T., 2016. Hydrological impact assessment of climate change on Lake Tana's water balance, Ethiopia. American journal of climate change, 5(1), pp.27-37.

Nurelegn, M. G. And S. M. Amare 2014. "Land use/cover dynamics in Ribb Watershed, North Western Ethiopia." Journal of Natural Sciences Research 4(16): 9-16.

Ramirez-Villegas, J., Challinor, A.J., Thornton, P.K. and Jarvis, A., 2013. Implications of regional improvement in global climate models for agricultural impact research. Environmental Research Letters, 8(2), p.024018.

Randall, D.A., Wood, R.A., Bony, S., Colman, R., Fichefet, T., Fyfe, J., Kattsov, V., Pitman, A., Shukla, J., Srinivasan, J. and Stouffer, R.J., 2007. Climate models and their evaluation. In Climate change 2007: The physical science basis. Contribution of Working Group I to the Fourth Assessment Report of the IPCC (FAR) (pp. 589-662). Cambridge University Press.

Reshmidevi, T.V., Kumar, D.N., Mehrotra, R. and Sharma, A., 2018. Estimation of the climate change impact on a catchment water balance using an ensemble of GCMs. Journal of Hydrology, 556, pp.1192-1204.

Salih Duri Abdulahi; Brook Abate; Arus Edo Harka; Sead Burhan Husen (2021). "Response of climate change impact on streamflow: the case of the Upper Awash sub-basin, Ethiopia." Journal of Water and Climate Change. https://doi.org/10.2166/wcc.2021.251

Schneider, S.H. and Dickinson, R.E., 1974. Climate modeling. Reviews of Geophysics, 12(3), pp.447-493.

Scott, D., Hall, C.M. and Gössling, S., 2016. A review of the IPCC Fifth Assessment and implications for tourism sector climate resilience and decarbonization. Journal of Sustainable Tourism, 24(1), pp.8-30.

Setegn, S.G., Rayner, D., Melesse, A.M., Dargahi, B. and Srinivasan, R., 2011. Impact of climate change on the hydroclimatology of Lake Tana Basin, Ethiopia. Water Resources Research, 47(4).

Soliman, E.S., Sayed, M.A. and Jeuland, M., 2009. Impact assessment of future climate change for the Blue Nile basin using a RCM nested in a GCM. Nile Basin Water Engineering Scientific Magazine, 2, pp.15-30.

Song, X., Zhang, J., Zhan, C., Xuan, Y., Ye, M. and Xu, C., 2015. Global sensitivity analysis in hydrological modeling: Review of concepts, methods, theoretical framework, and applications. Journal of hydrology, 523, pp.739-757.

Solomon, S., Manning, M., Marquis, M. and Qin, D., 2007. Climate change 2007-the physical science basis: Working group I contribution to the fourth assessment report of the IPCC (Vol. 4). Cambridge university press.

Soriano, E., Mediero, L. and Garijo, C., 2019. Selection of bias correction methods to assess the impact of climate change on flood frequency curves. Water, 11(11), p.2266.

Steffen, W., Richardson, K., Rockström, J., Schellnhuber, H.J., Dube, O.P., Dutreuil, S., Lenton, T.M. and Lubchenco, J., 2020. The emergence and evolution of Earth System Science. Nature Reviews Earth & Environment, 1(1), pp.54-63.

Stocker, T. 2014. Climate change 2013: the physical science basis: Working Group I contribution to the Fifth assessment report of the Intergovernmental Panel on Climate Change, Cambridge university press.

Subramanya, K. 2013. Engineering hydrology, 4e, Tata mcgraw-Hill Education.

Tabari, H., Taye, M.T. and Willems, P., 2015. Statistical assessment of precipitation trends in the upper Blue Nile River basin. Stochastic environmental research and risk assessment, 29(7), pp.1751-1761.

Tarekegn, D. And A. Tadege 2006. "Assessing the impact of climate change on the water resources of the Lake Tana sub-basin using the WATBAL model." Discuss. Pap 30.

Tassew, B.G., Belete, M.A. and Miegel, K., 2019. Application of HEC-HMS model for flow simulation in the Lake Tana basin: The case of Gilgel Abay catchment, upper Blue Nile basin, Ethiopia. Hydrology, 6(1), p.21.

Taye, M.T., Ntegeka, V., Ogiramoi, N.P. and Willems, P., 2011. Assessment of climate change impact on hydrological extremes in two source regions of the Nile River Basin. Hydrology and Earth System Sciences, 15(1), pp.209-222.

Teutschbein, C. and Seibert, J., 2012. Is bias correction of Regional Climate Model (RCM) simulations possible for non-stationary conditions?. Hydrology & Earth System Sciences Discussions, 9(11).

Tekleab, S., Mohamed, Y. and Uhlenbrook, S., 2013. Hydro-climatic trends in the Abay/upper Blue Nile basin, Ethiopia. Physics and Chemistry of the Earth, Parts A/B/C, 61, pp.32-42.

Tigabu, T. B., et al. (2020). "Statistical analysis of rainfall and streamflow time series in the Lake Tana Basin, Ethiopia." Journal of Water and Climate Change 11(1): 258-273.

Timmermans, B., Wehner, M., Cooley, D., O'Brien, T. and Krishnan, H., 2019. An evaluation of the consistency of extremes in gridded precipitation data sets. Climate dynamics, 52(11), pp.6651-6670.

Van Vuuren, D.P., Edmonds, J., Kainuma, M., Riahi, K., Thomson, A., Hibbard, K., Hurtt, G.C., Kram, T., Krey, V., Lamarque, J.F. and Masui, T., 2011. The representative concentration pathways: an overview. Climatic change, 109(1), pp.5-31.

Wang, H., Stephenson, S.R. and Qu, S., 2020. Quantifying the relationship between streamflow and climate change in a small basin under future scenarios. Ecological Indicators, 113, p.106251.

Woldeselassie, T., 2015. CLIMATE CHANGE IMPACT ASSESSMENT ON RUNOFF POTENTIAL IN UPPER AWASH BASIN: A CASE STUDY OF LEGEDADI-DIRE CATCHMENT.

Worku, G., Teferi, E., Bantider, A. and Dile, Y.T., 2020. Statistical bias correction of regional climate model simulations for climate change projection in the Jemma sub-basin, upper Blue Nile Basin of Ethiopia. Theoretical and Applied Climatology, 139(3), pp.1569-1588.

Worqlul, A.W., Dile, Y.T., Ayana, E.K., Jeong, J., Adem, A.A. and Gerik, T., 2018. Impact of climate change on streamflow hydrology in headwater catchments of the Upper Blue Nile Basin, Ethiopia. Water, 10(2), p.120.

Yadav, R., Tripathi, S.K., Pranuthi, G. and Dubey, S.K., 2014. Trend analysis by Mann-Kendall test for precipitation and temperature for thirteen districts of Uttarakhand. Journal of Agrometeorology, 16(2), p.164.

Yokoo, Y. and Sivapalan, M., 2011. Towards reconstruction of the flow duration curve: development of a conceptual framework with a physical basis. *Hydrology and Earth System Sciences*, *15*(9), pp.2805-2819.

Zegeye, H., 2018. Climate change in Ethiopia: impacts, mitigation and adaptation. International Journal of Research in Environmental Studies, 5(1), pp.18-35.

Zhang, Y., You, Q., Chen, C. and Ge, J., 2016. Impacts of climate change on streamflows under RCP scenarios: A case study in Xin River Basin, China. Atmospheric Research, 178, pp.521-534.

Zhou, Q., Liu, G. and Zhang, Z., 2009, August. Improvement and optimization of thiessen polygon method boundary treatment program. In 2009 17th International Conference on Geoinformatics (pp. 1-5). IEEE.
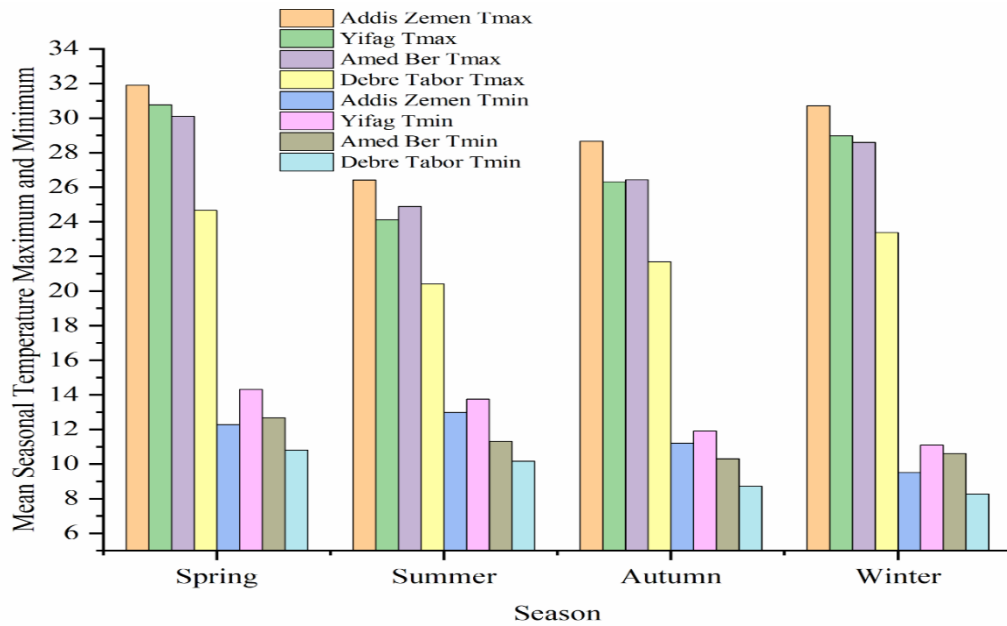
APPENDIXES

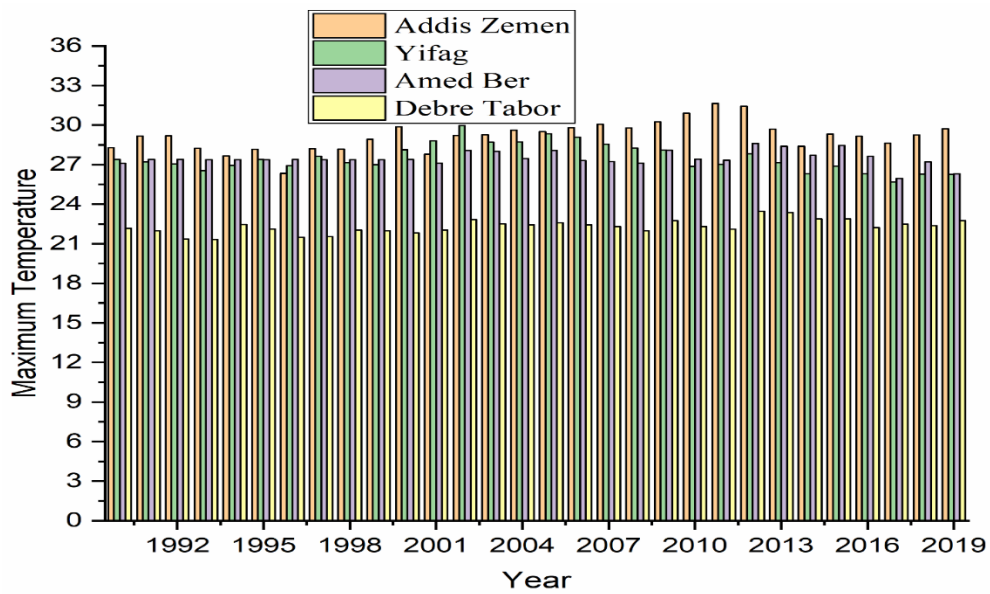Appendix A 1 Seasonal observed Rainfall distribution
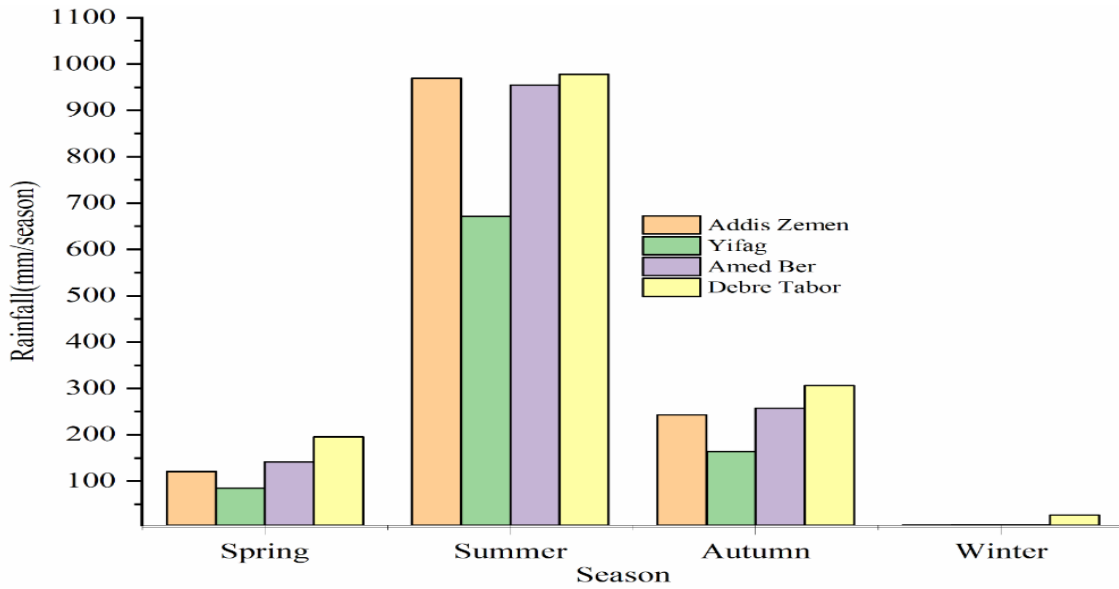
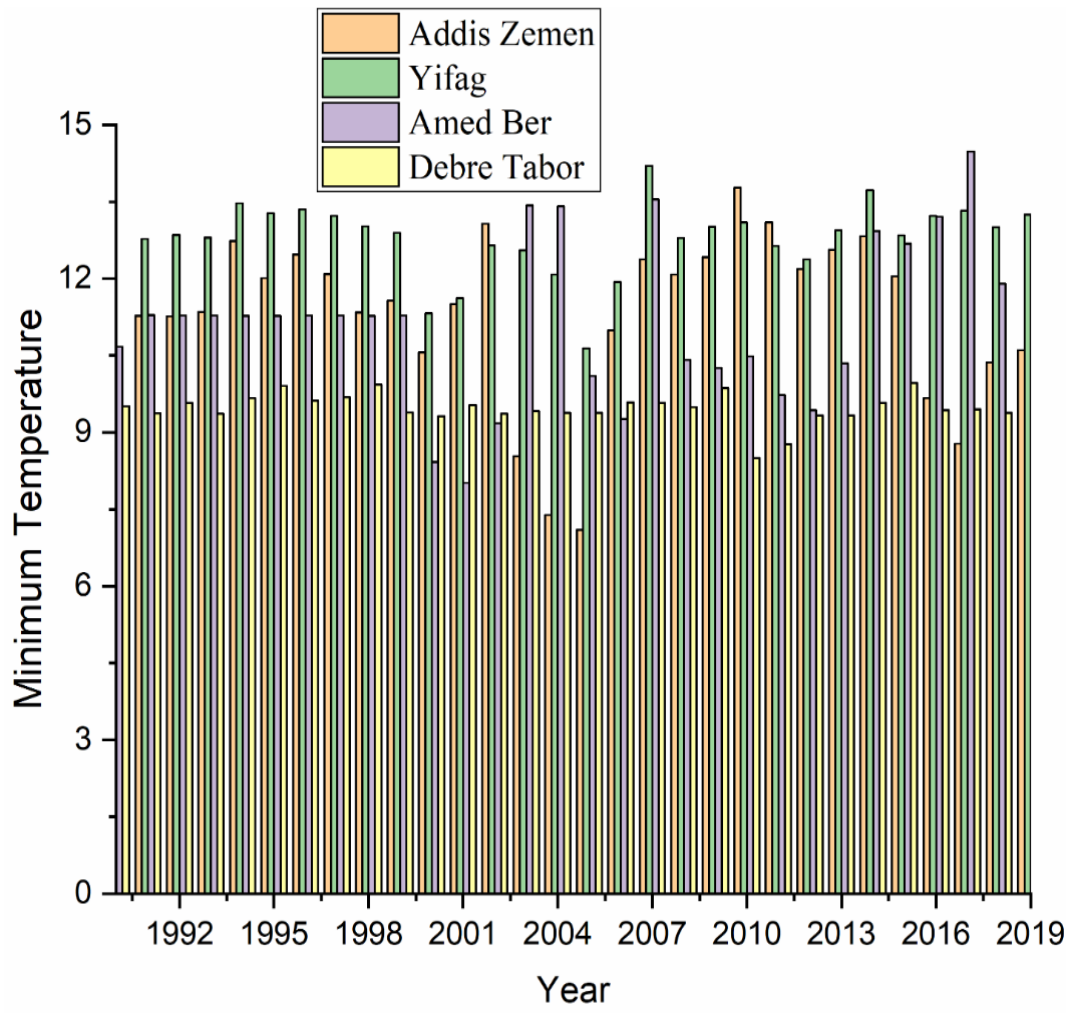Appendix A 2 Annual observed Rainfall distribution
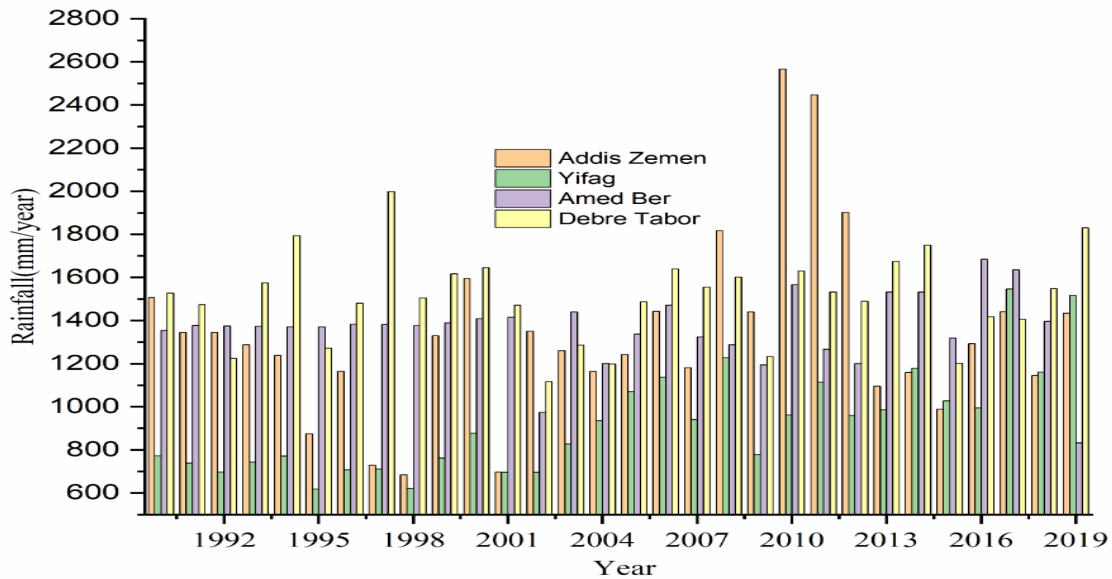
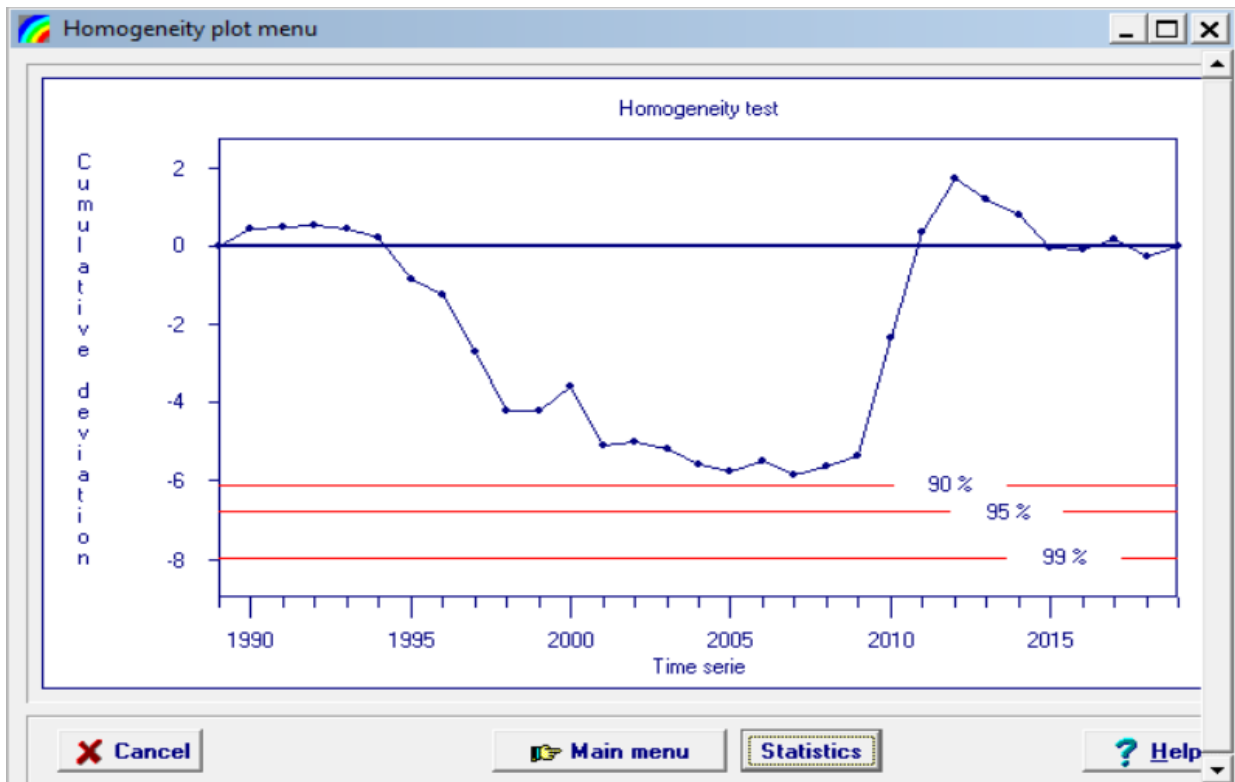Appendix A 3 Seasonal observed maximum and minimum temperature

Appendix A 4 Annual observed maximum temperature

Appendix A 5 Annual observed minimum temperature

Appendix B 1 Homogeneity test for Addis Zemen

Appendix B 2 Homogeneity test for Amed Ber
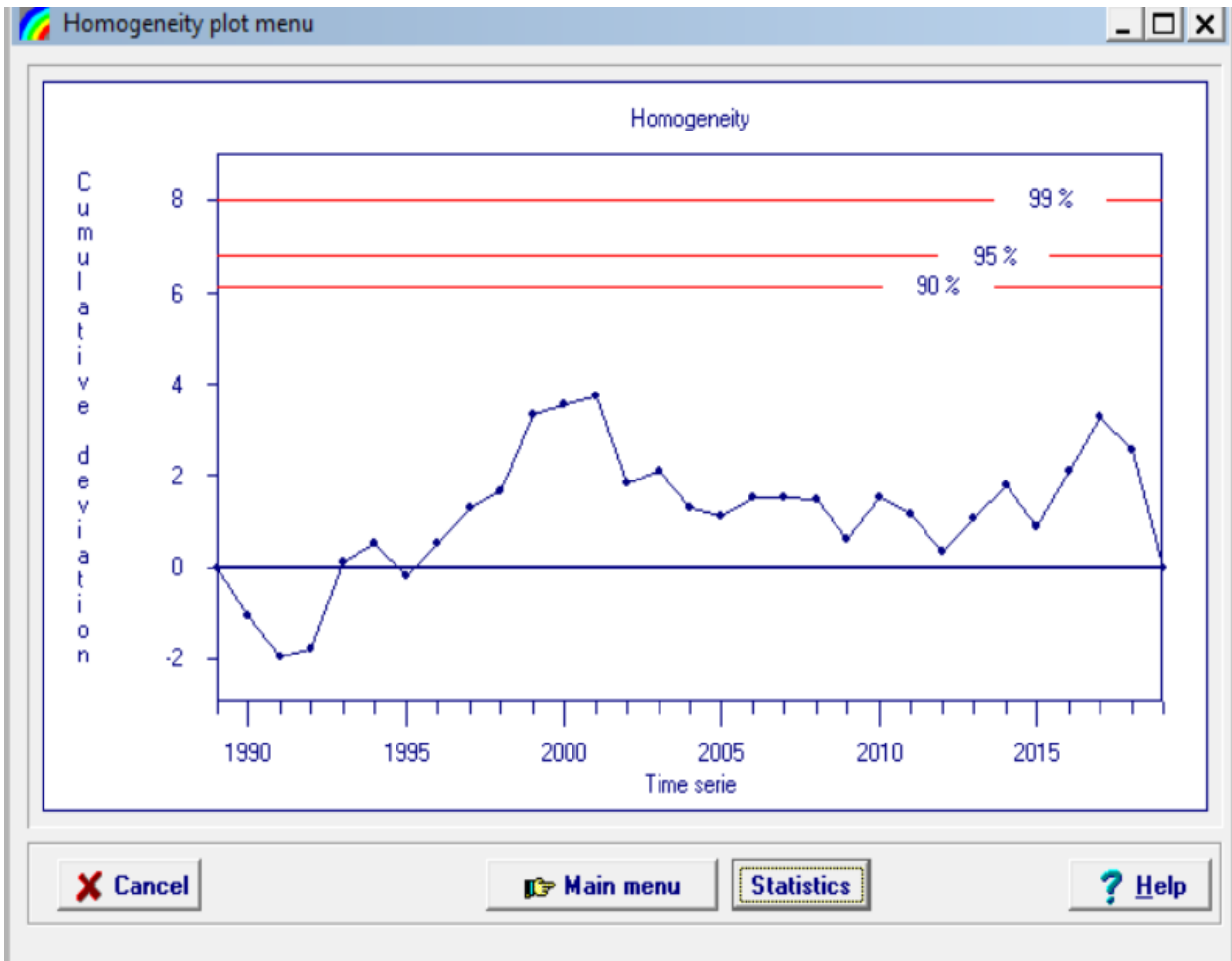
Appendix B 3 Homogeneity test for Debre Tabor
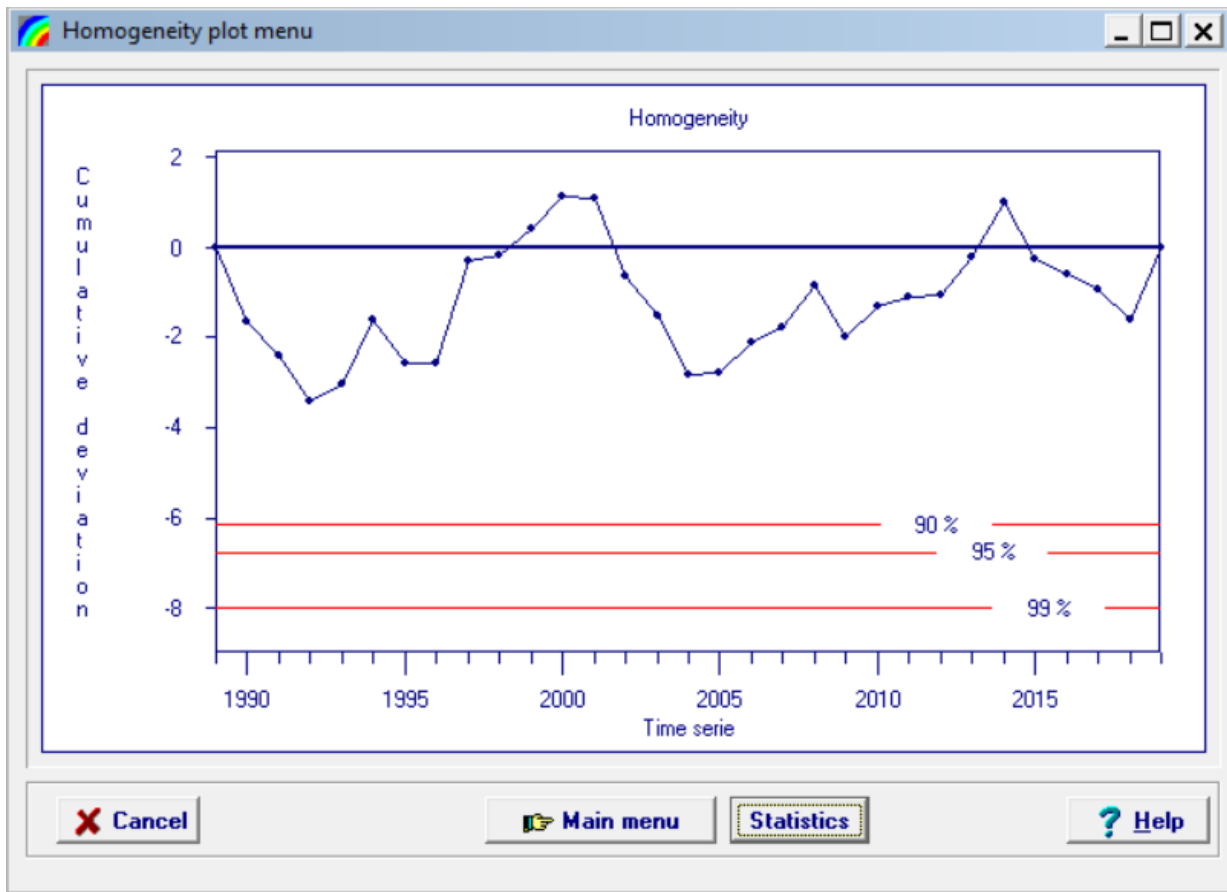
Appendix C 1 Parametric statistics values of trend test for mean monthly observed rainfall

Parameter	Jan	Feb	Mar	Apr	May	Jun	Jul	Aug	Sep	Oct	Nov	Dec
Kendall's tau	-0.278	0.021	0.090	-0.039	0.145	0.030	-0.011	0.053	0.131	-0.039	0.039	-0.201
S	-118.000	9.000	39.000	-17.000	63.000	13.000	-5.000	23.000	57.000	-17.000	17.000	-86.000
Var(S)	3097.333	3125.000	3141.667	3141.667	3141.667	3141.667	3141.667	3141.667	3141.667	3141.667	3141.667	3113.333
p	0.036	0.886	0.498	0.775	0.269	0.830	0.943	0.695	0.318	0.775	0.775	0.128
α	0.05	0.05	0.05	0.05	0.05	0.05	0.05	0.05	0.05	0.05	0.05	0.05
Sen's slope	-0.071	0.000	0.313	-0.206	1.446	0.396	-0.041	0.734	1.028	-0.251	0.063	-0.119

Appendix C 2 Parametric statistical values of trend test for Observed Maximum and Minimum Temperature

Maximum Temperature												
	Jan	Feb	Mar	Apr	May	Jun	Jul	Aug	Sep	Oct	Nov	Dec
Kendall's tau	0.136	0.113	0.067	0.195	-0.048	0.016	0.421	0.269	0.149	0.232	0.034	-0.011
S	59.0	49.0	29.0	85.0	-21.0	7.0	183.0	117.0	65.0	101.0	15.0	-5.0
Var(S)	3141.667	3141.667	3141.667	3141.667	3141.667	3141.667	3141.667	3141.667	3141.667	3141.667	3141.667	3141.667

p-value	alpha	Sen's slope	Minimum Temperature					
			Kendall's tau	S	Var(S)	p-value	alpha	Sen's slope
0.301	0.05	0.017	-0.053	-23.000	3141.667	0.695	0.05	-0.007
0.392	0.05	0.015	0.131	57.000	3141.667	0.318	0.05	0.012
0.617	0.05	0.014	0.200	87.000	3141.667	0.125	0.05	0.034
0.134	0.05	0.030	0.168	73.000	3141.667	0.199	0.05	0.024
0.721	0.05	-0.009	0.099	43.000	3141.667	0.454	0.05	0.019
0.915	0.05	0.004	0.044	19.000	3141.667	0.748	0.05	0.002
0.001	0.05	0.068	0.062	27.000	3141.667	0.643	0.05	0.007
0.038	0.05	0.038	0.062	27.000	3141.667	0.643	0.05	0.009
0.254	0.05	0.022	0.177	77.000	3141.667	0.175	0.05	0.018
0.074	0.05	0.037	0.071	31.000	3141.667	0.592	0.05	0.008
0.803	0.05	0.003	-0.085	-37.000	3141.667	0.521	0.05	-0.012
0.943	0.05	-0.001	-0.117	-51.000	3141.667	0.372	0.05	-0.018

Appendix D 1 Mean monthly and seasonally observed and Simulated Stream flow

| Month | Observed | 2025-2054 | | 2055-2084 | | Season | Observed | 2025-2054 | | 2055-2084 | |
		RCP4.5	RCP8.5	RCP4.5	RCP8.5			RCP4.5	RCP8.5	RCP4.5	RCP8.5
Jan	0.97	3.06	3.14	5.93	6.25	Spring	8.24	70.65	65.59	5.47	7.54
Feb	0.68	2.56	2.89	1.80	2.17	Summer	148.16	102.61	99.61	80.89	71.82
Mar	0.77	11.72	10.65	2.20	2.87	Autumn	64.98	28.38	27.96	108.13	108.30
Apr	1.67	27.83	26.06	1.39	2.14	Winter	3.46	12.75	13.35	25.96	28.21
May	5.80	31.10	28.88	1.88	2.54						
Jun	18.26	35.91	36.34	18.10	16.19						
Jul	52.76	36.09	35.57	28.51	22.36						
Aug	77.13	30.61	27.70	34.27	33.27						
Sep	48.20	15.73	16.60	38.46	36.68						
Oct	11.79	7.63	6.39	36.90	37.58						
Nov	4.98	5.01	4.97	32.78	34.04						
Dec	1.81	7.13	7.32	18.23	19.80						

Appendix D 2 Mean Annual observed and simulated stream flow

Year	Observed	Year	RCP4.5	RCP8.5	Year	RCP4.5	RCP8.5
1990	15.95	2025	18.18	17.99	2055	17.25	11.29
1991	17.95	2026	17.51	15.43	2056	16.73	19.22
1992	18.16	2027	19.01	16.70	2057	18.88	15.51
1993	17.39	2028	20.23	19.88	2058	20.51	17.75
1994	21.97	2029	20.47	16.55	2059	19.06	21.23
1995	16.47	2030	19.11	17.10	2060	20.90	16.33

1996	20.75	2031	19.44	16.44	2061	15.69	18.17
1997	12.23	2032	16.86	13.59	2062	25.22	20.48
1998	17.02	2033	21.34	16.80	2063	17.22	12.75
1999	25.57	2034	12.65	14.86	2064	22.69	18.07
2000	21.17	2035	14.63	15.55	2065	14.54	14.59
2001	19.11	2036	19.75	13.49	2066	18.81	14.99
2002	21.00	2037	15.57	17.00	2067	21.80	21.40
2003	24.67	2038	18.61	15.54	2068	18.37	17.10
2004	18.65	2039	19.10	18.14	2069	16.54	17.70
2005	23.47	2040	19.03	17.28	2070	16.83	16.98
2006	15.81	2041	16.30	16.85	2071	20.14	19.10
2007	22.74	2042	16.98	22.70	2072	18.25	18.25
2008	21.63	2043	13.08	15.24	2073	16.59	17.53
2009	21.33	2044	11.53	12.34	2074	14.19	23.19
2010	26.88	2045	14.89	16.36	2075	16.25	21.49
2011	19.89	2046	19.77	17.91	2076	17.22	18.36
2012	17.81	2047	17.47	18.48	2077	18.30	18.95
2013	16.71	2048	20.37	22.79	2078	20.50	19.45
2014	15.17	2049	13.40	15.87	2079	22.44	17.46
2015	13.37	2050	20.64	19.41	2080	19.00	17.22
2016	15.70	2051	21.64	22.97	2081	17.73	19.32
2017	14.97	2052	18.01	18.68	2082	17.67	20.01
		2053	17.38	16.07	2083	18.40	18.28
		2054	25.42	20.31	2084	15.73	19.69

Appendix D 3 Change of stream flow in Mean monthly, seasonally and annually time steps

Month	2025-2054		2055-2084		Season	2025-2054		2055-2084	
	RCP4.5	RCP8.5	RCP4.5	RCP8.5		RCP4.5	RCP8.5	RCP4.5	RCP8.5
Month	2.09	2.17	4.96	5.28	Spring	62.41	57.35	-2.77	-0.69
Jan	1.88	2.21	1.12	1.49	Summer	-45.55	-48.54	-67.27	-76.33
Feb	10.96	9.88	1.43	2.10	Autumn	-36.60	-37.02	43.16	43.33
Mar	26.16	24.39	-0.28	0.47	Winter	9.29	9.89	22.50	24.75
Apr	25.29	23.08	-3.92	-3.26	Annually				
May	17.65	18.08	-0.16	-2.07	2025-2054		2055-2084		
Jun	-16.67	-17.19	-24.25	-30.40	RCP4.5	RCP8.5	RCP4.5	RCP8.5	
Jul	-46.52	-49.43	-42.85	-43.86	-4.93	-8.48	-2.27	-4.32	
Aug	-32.47	-31.61	-9.75	-11.52					
Sep	-4.16	-5.40	25.11	25.79					
Oct	0.03	-0.01	27.80	29.06					
Nov	5.31	5.50	16.42	17.99					
Dec	2.09	2.17	4.96	5.28					